Scuola Internazionale Superiore di Studi Avanzati - Trieste

Area of Physics
Ph.D. in Astrophysics

# The nature of Dark Matter from properties of galaxies

Advisor:
**Prof. P. Salucci**

Candidate:
**E. V. Karukes**

Thesis submitted in partial fulfillment of the requirements
for the degree of Doctor Philosophiae

Academic Year 2015/2016

SISSA - Via Bonomea 265 - 34136 TRIESTE - ITALY

# Acknowledgements

I would like to express my special appreciation and thanks to my advisor Paolo Salucci. I appreciate all his contributions of time, ideas and discussions during these 3 years of my PhD. His advices on both research as well as on my career have been invaluable. I am thankful also to SISSA for useful lectures and to all professors of the Astrophysical sector, in particular to Alessandro Bressan, Luigi Danese and Andrea Lapi for fruitful discussions.

I also thank all my friends and colleagues at SISSA Alessio, Mauro, Elena, Guillaume, Bruno, Xiao, Federico, Marco, Andrei and Lasma, who made more enjoyable the long working days and the short weekends. Then, I would like to thank Gor, Elias and Francesca for their strong and tasty coffee, that many times helped me to be productive until late. A special thank goes to my two supportive officemates Claudia and Serena for the infinite discussions about everything. I cannot forget about my friends from Rostov Polina, Roma, Vanya, Ilya and many others for all the enjoyable time we had spend together and I hope we will spend in the future. A special acknowledgement goes to my best mate of many years Nastya with whom we should write a book about all our adventures together.

Finally, I would express my gratitude to my big family and to Джованни who has already become a part of my family in these years. In particular I would like to thank my mother and my father for their love, support and sacrifices. This thesis is dedicated to them.

# Published papers

## Citations to Published and Submitted Works

The work presented in this thesis has been partially published in scientific papers.

- *Modeling the Mass Distribution in the Spiral Galaxy NGC 3198*, E. V. Karukes & P. Salucci, proceedings of Young Researcher Meeting, 2014, Journal of Physics Conference Series, 566, 012008

- *$R^n$ gravity is kicking and alive: The cases of Orion and NGC 3198*, P. Salucci, C. Frigerio Martins & E. Karukes, 2014, International Journal of Modern Physics D, 23, 1442005

  This essay received an Honorable Mention in the 2014 Essay Competition of the Gravity Research Foundation.

- *The dark matter distribution in the spiral NGC 3198 out to 0.22 $R_{vir}$*, E.V. Karukes, P. Salucci & G. Gentile, 2015, A&A, 578, A13

- *The universal rotation curve of dwarf disk galaxies*, E.V. Karukes & P. Salucci., submitted to MNRAS, arXiv:1609.06903

# Abstract

($\Lambda$) cold dark matter (CDM) has become the standard theory of cosmological structure formation, within which cosmological measurements are confronted and interpreted. Although its predictions appear to be in good agreement with data on large scale structure, a number of discrepancies with data emerges on the galactic and sub-galactic scales.

In this Thesis we investigate the distribution of dark matter in late Hubble type galaxies and we address the key challenges of galaxy formation and evolution in the ($\Lambda$)CDM scenario by means of the kinematics of a sample of dwarf disk galaxies.

We develop tests based on the mass modelling of rotation curves for the validation of dark matter halo models on galactic scales. These tests have been applied in order to investigate the core-cusp controversy, and to analyze galactic rotation curves in the framework of modified Newtonian dynamics. We also derived the universal rotation curve of dwarf disk galaxies, the latter are crucial objects in testing the ($\Lambda$)CDM scenario.

# Preface

During the last few decades, it has been discovered that only 15.5 % of the total matter in the Universe is in form of ordinary baryonic matter. While, the other 84.5 % is provided by dark matter (DM), which is detectable only through its gravitational influence on luminous matter. The widely accepted hypothesis on the form of DM is that it is composed of cold, neutral, weakly interacting particles, which are not present in the Standard Model of particle physics and not yet observed at any existing experiments. This standard cold dark matter (CDM) scenario has been very successful in reproducing most properties of the local and high-redshift Universe.

However, despite these great achievements, at the galactic and sub-galactic scales the predictions made by the ($\Lambda$)CDM model diverge from observational data that probe the innermost regions of DM halos and the properties of the Milky Way's dwarf galaxy satellites.

Essentially, these small-scale controversies of the standard collisionless particle paradigm can be solved by evolving the baryonic physics effects (see, e.g., Binney et al., 2001; Governato et al., 2010; Pontzen and Governato, 2012). However, in the lowest mass galaxies this solution seems very unappealing, because it is difficult to explain how baryons in a galaxy with stellar mass similar to that of globular clusters can change the inner structure of a dark halo. Alternatively, the small-scale conflicts could be the evidence of more complex physics in the dark sector itself, such as self-interacting dark matter (SIDM) and warm dark matter (WDM) (see, e.g. Lovell et al., 2014; de Vega et al., 2014a; Spergel and Steinhardt, 2000). Otherwise, modified gravity theories, like MOND (Milgrom, 1983), f(R) (Capozziello et al., 2007) and many other similar theories may help in solving these issues.

The goals of my research are to try to understand the nature of the previously described small-scale problems and to address some of the key challenges of galaxy formation in low-mass local dwarf disk galaxies.

In this Thesis a study of the RCs and the inferred DM properties of late Hubble type galaxies is presented. The outline of this Thesis is then as follows. In the introduction Chapter we give a brief overview of the history of DM discovery, then we summarize the basis of the possible nature of DM along with popular alternatives to DM.

In Chapter 2 we develop a test for analyzing galactic RCs in the framework of f(R) theories of gravity. This work shows that in some cases the modified gravity theories can fit the available kinematical data much better than ($\Lambda$)CDM halo models.

In Chapter 3 we use high-quality very extended kinematics of the spiral galaxy NGC 3198 in order to derive its distribution of DM out to $\sim$0.22 $R_{vir}$ and test it against

three different DM density profiles. First, we use a typical mass-modelling technique to show that "flat" RCs can be well fitted by either a cored DM or a cuspy DM halo, just by adjusting the amount of the stellar matter content. Second, we use the new model-independent local density method proposed by Salucci et al. (2010) and we find that the derived density profile strongly supports a cored distribution of DM, adding independent evidence to the idea of cored DM distribution in this galaxy.

Chapter 4 is devoted to the kinematical investigation of the sample of 36 dwarf disk dominated galaxies, which are members of the Local Volume ($\sim$ 11 Mpc, see for details Karachentsev et al., 2013), in the framework of the Universal Rotation Curve (Persic et al., 1996). We find that in these low-mass galaxies the structural properties of the luminous and dark components emerge very well correlated. We also find no evidence for the sharp decline in the baryonic to halo mass relation. This can be considered as a key challenge for the ($\Lambda$)CDM model of galaxy formation and specially to the abundance matching techniques.

Finally, the conclusions and future perspectives of this thesis are presented in Chapter 5.

# Contents

# Chapter 1

# Introduction

## 1.1 History of DM discovery

The first indication for the possible existence of dark matter (DM) came from the dynamical study of the Milky Way. It started with Öpik (1915) who was probably the first one to estimate the dynamical density of matter near the Sun by analysing vertical motions of stars near the plane of the Galaxy. A similar analysis was done later by the Dutch astronomer Jacobus Kapteyn. In his work Kapteyn (1922) established the relation between the motion of stars and their velocity dispersion. Both astronomers found that the summed contribution of all known stellar populations (and interstellar gas) is sufficient to explain the vertical oscillations of stars - in other words, there was no evidence for hypothetical matter. Then the British astronomer Jeans (1922) reanalysed the vertical motions of stars near the plane of the Galaxy, and found that some dark matter probably existed near the Sun.

Ten years after, in 1932 a student of Jacobus Kapteyn, Jan Hendric Oort, improved Kapteyn's analysis and determined quantitatively the difference between the dynamical density of matter and the density due to the visible stars in the Solar vicinity (Oort, 1932). Although this difference was often considered as an indication for the presence of dark matter, later this measurement was determined to be incorrect (Kuijken and Gilmore, 1989).

The second indication of the possible DM existence came from the measurements of radial velocities of galaxies in the Coma cluster, carried out by Zwicky (1933). He found that the velocities of the individual galaxies with respect to the cluster mean velocity are much larger than those expected from the estimated total mass of the cluster, calculated from masses of individual galaxies. This means that the cluster should contain a huge

amount of some invisible matter in order to hold all the galaxies together. According to his estimate the amount of dark matter in this cluster should be about 160 times greater than expected from their luminosity (a value revised today). A similar conclusion was made by Smith (1936) for galaxies in the Virgo cluster. Furthermore, a certain discrepancy was detected also between masses of individual galaxies and masses of pairs and groups of galaxies (Holmberg, 1937; Page, 1952, 1959, 1960). The method used for the mass determination of pairs and groups of galaxies is based on the virial theorem and is almost identical to the procedure used to calculate masses of clusters of galaxies.

The third, "classical" indication of the DM existence comes from the rotation curves (RC) of galaxies. In 1939 Babcock obtained long-slit spectra of the Andromeda galaxy M31, which showed no evidence for the Kaplerian decline, i.e. the outer regions of M31 were rotating with higher velocities than expected from the stellar mass. He interpreted this result either as a high mass-to-light ratio in the periphery or as a strong dust absorption. Later on, after the second world war, the technological advances allowed astronomers to routinely detect the RCs of tens of galaxies. In particular, in 1951 the 21 cm line, predicted by van de Hulst in 1944, was detected for the first time. Then, six years later, in 1957, van de Hulst, Jean Jacques Raimond, and Hugo van Woerden published the first radio rotation curve of M31, where they found that the neutral hydrogen emitting the 21-cm line extends much farther than the optical image. They were able to measure the rotation curve of M31 up to about 30 kpc from the center. About ten years later Roberts (1966) performed similar observations for the atomic hydrogen clouds of M31, but with much higher resolution. His flat radio M31 RC was later confirmed by optical data presented by Rubin and Ford (1970). In Fig.1.1 we compare the measurements by Roberts (1966) (yellow and red curves) and Rubin and Ford (1970) (blue curve), showing their fair agreement.

Although Roberts was among the first to recognize the implications of the observed flatness of galactic RCs (Roberts and Rots, 1973), only with the work of Rubin et al. (1980) it was clear that *"the conclusion is inescapable that non-luminous matter exists beyond the optical galaxy"*. This work opened the so called "dark matter problem" in galaxies. At the same time, Bosma (1978, 1981a,b) carried out the HI measurements of 25 spiral galaxies, which confirmed and extended the work by Rubin.

Furthermore, the conclusion that a significant amount of non-luminous matter must exist beyond the optical galaxy was also consistent with the theoretical idea of the existence of a massive and more or less spherical component that surrounds the visible part of a spiral galaxy (i.e. the DM halo), proposed by Ostriker and Peebles (1973). A parametrization, from the simulations outcome, of the dark halo mass distribution was proposed, almost twenty years after, by Navarro et al. (1996a). It is based on the

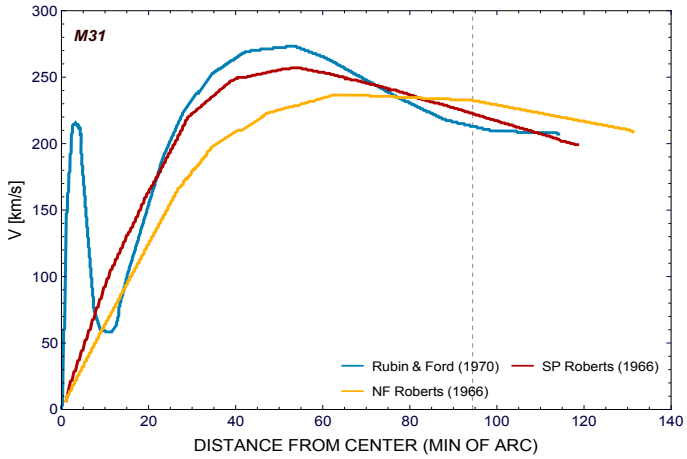


**Figure 1.1:** Comparison of RCs of M31. Yellow and red lines are RCs derived from each side (approaching and receding) by Roberts (1966). Blue line reproduces one of the fit models of M31 RC as described in Rubin and Ford (1970). The dashed vertical line shows the value of the optical radius.

paradigm that DM is made by massive gravitationally interacting elementary particles with extremely weak, if not null, interaction via other forces (e.g. White and Negroponte, 1982; Jungman et al., 1996). At the same time, the study of more than a thousand of normal spiral RCs showed that the best way to represent and model their RCs comes from the concept of a universal rotation curve (URC), i.e. a single function of the total galaxy luminosity and of a characteristic radius of the luminous matter distribution which represents the RCs of all spirals[1].

This concept, implicit in Rubin et al. (1985), pioneered in Persic and Salucci (1991), set by Persic et al. (1996) (PSS, Paper I) and extended to large galactocentric radii by Salucci et al. (2007) has provided us with the mass distribution of (normal) disk galaxies in the magnitude range $-23.5 \lesssim M_I \lesssim -17$.[2]

## 1.2 New matter or modified gravity?

The systematic progress in studying the data from weak (Refregier, 2003) and strong (Tyson et al., 1998) lensing, studies of the large scale structure (Allen et al., 2003), Big Bang nucleosynthesis (Fields and Sarkar, 2006), distant supernovae (Riess et al., 1998;

[1] i.e. $R_{opt}$ defined as the radius encompassing 83 % of the total luminosity.

[2] Extensions of the URC to other Hubble types are investigated in Salucci and Persic (1997); Noordermeer et al. (2007).

Perlmutter et al., 1999) and the Cosmic Microwave Background (Komatsu et al., 2011) showed us that the Universe contains much more DM than baryonic matter. In addition to DM, recent observations report that in order to fill the matter/energy between unity and observed matter density gap we should assume that some sort of vacuum energy exists. All in all, we have that the Universe consists of 4 % baryons, 22 % DM which is detectable, up to now, only through its gravitational influence on luminous matter and 74 % of dark energy.

There are many different theories about the nature of dark matter. These theories can actually be slotted into three general groups: Hot DM, Cold DM and Warm DM.

An alternative to DM (as well as to dark energy) is to consider that the evidences observed by astronomers are not due to an unseen mass component, but it is instead the signature of the failure of Newtonian gravity. This idea was proposed by Milgrom in 1983 (Milgrom, 1983) and was called the modified Newtonian dynamics (MOND). Another recently suggested class of theories, that modify the usual Newtonian gravitational potential are the f(R) theories (see Capozziello et al., 2007).

We are going to discuss in more details the above mentioned and some other theories below.

### 1.2.1 Modified gravity

#### MOND

MOND is an empirically motivated modification of Newtonian gravity or inertia proposed by Milgrom as an alternative to DM and it is certainly the most studied model (see for a review Sanders and McGaugh, 2002). According to MOND, below a certain acceleration threshold $a_0$ the Newtonian gravity is no longer valid and the effective gravitational acceleration approaches $\sqrt{a_0 g_n}$ where $g_n$ is the usual Newtonian acceleration. This modification consists of two observational systematics of galaxies:

- the observed galactic RCs of different Hubble type (e.g. Gentile et al., 2007a,b; Sanders and Noordermeer, 2007; Milgrom and Sanders, 2003)
- the tight scaling relation of a luminosity-rotation velocity (the Tully-Fisher relation): $M \propto V^{\alpha}$, with $\alpha \sim 4$ (McGaugh, 2004, 2005).

If one wants to explain the observed asymptotically flat galactic RCs by means of MOND, a natural first choice is to propose that gravitational attraction becomes more

like $1/r$ beyond some length scale which is comparable to the scale of galaxies. Then the modified law of attraction about a point mass $M$ is:

$$F = \frac{GM}{r^2} f(r/r_0), \tag{1.1}$$

where $r_0$ is a new constant of length of the order of a few kpc, and $f(x)$ is a function with the asymptotic behaviour: $f(x) = 1$, where $x \ll 1$ and $f(x) = x$, where $x \gg 1$.

Instead of Newton's second law as $\mathbf{F} = \mathbf{a}m$, Milgrom (1983) modified $\mathbf{F}$ with the function $\mu(a)$, where $a$ is the acceleration. Then Newton's second law in MOND reads:

$$\mathbf{F} = m\mathbf{a}\mu\left(\frac{a}{a_0}\right), \tag{1.2}$$

where $a_0 \simeq 10^{-8} cm/s^2$ is a new physical parameter with units of acceleration and $\mu(x)$ is an interpolation function whose asymptotic values are $\mu(x) = x$ for $x \ll 1$ (smal values of the acceleration, called Mondian regime) and $\mu(x) = 1$ for $x \gg 1$ (high values of the acceleration, called Newtonian regime).

The analytical form of $\mu(a/a_0)$ in MOND remains free to be determined from observations. RCs fitting lead to $\mu(x) = x/\sqrt{(1+x^2)}$, while the so called interpolation function reads $\mu(x) = x/(1+x)$.

In both forms, $a \gg a_0$ recovers Newton's second law, while the case $a \ll a_0$ yields a force $F$ proportional to the velocity squared:

$$F = ma\left(\frac{a}{a_0}\right) = m\frac{a^2}{a_0} = \frac{GmM}{r^2}, \tag{1.3}$$

such that

$$a = \frac{\sqrt{GMa_0}}{r}. \tag{1.4}$$

For a point mass $M$, setting $a$ to the centripetal acceleration around the galactic centre, leads to

$$a = \frac{V^2}{r} = \frac{\sqrt{GMa_0}}{r}. \tag{1.5}$$

Therefore, the circular velocity reaches a plateau $V_{flat} = \sqrt[4]{GMa_0}$ that allows to successfully fit flat rotation curves.

Although at the galactic scales MOND is successful in reproducing many galactic phenomena, at cluster scales, nonetheless, MOND proves much less successful. In particular, the observations of a pair of merging clusters known as the "bullet cluster", clearly show

that the gravitational potential does not trace the distribution of baryons (Clowe et al., 2006). In Fig. 1.2 the combination of the weak lensing and X-ray maps of the Bullet cluster shows that the dominant population of baryonic mass, detected by the X-ray image, is well separated from the distribution of mass. Therefore, when the two clusters are colliding, the regular matter interact, while the DM interact weakly. The largest part of the mass of the two galaxies remain in the centre of the source galaxies. Such a separation is possible only if there is a large amount of matter weakly interacting, such as a non-baryonic DM halo. Therefore, the spatial offset of the centre of the total mass from the centre of the baryonic mass peak cannot be explained with an alteration of the gravitational force law. However, MOND has received a renewed interest after the proposal of a possible fully covariant relativistic formulation referred to as Tensor-Vector-Scalar gravity (TeVeS) (Skordis, 2008).

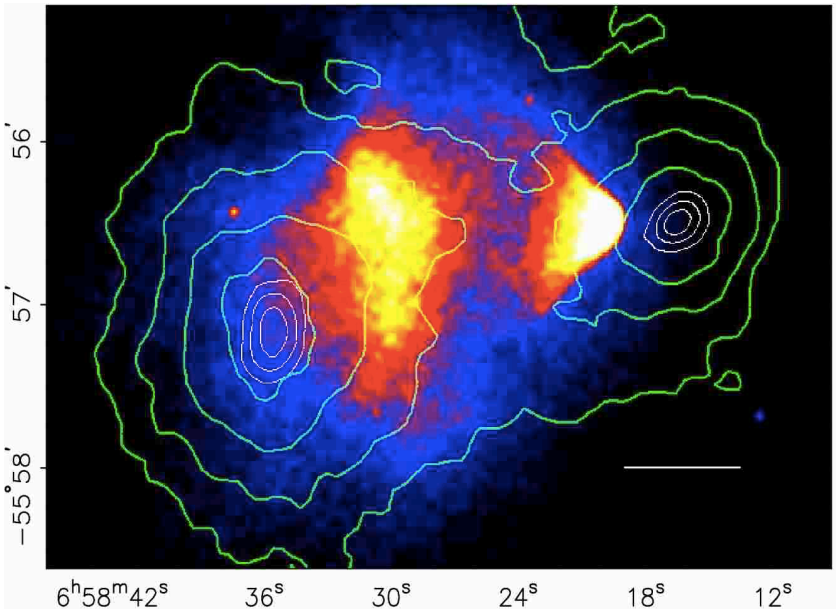


**Figure 1.2:** Convergence map of the bullet cluster. The coloured map represents the X-ray image of this system of merging clusters, obtained in a 500 second exposure with Chandra. The white bar is shown for scale, and represents a distance of 200 kpc at the location of the cluster. The green contours denote the reconstructed lensing signal, proportional to the projected mass in the system. From Clowe et al. (2006).

### $f(R)$ theories

Another theory of gravity modification, which plays a major role at astrophysical scales is f(R) theory. This theory, recently proposed by Capozziello et al. (2007), modifies the usual Newtonian gravitational potential generated by (baryonic) matter as an effect of power-law fourth order theories of gravity that replace in the gravity action the Ricci scalar $R$ with a function $f(R) \propto R^n$, where $n$ is a slope parameter.

In $f(R)$ theories of gravity the gravitational action is defined to be:

$$\mathcal{S} = \int d^4x \sqrt{-g}\,[f(R) + \mathcal{L}_m], \tag{1.6}$$

where $g$ is the metric determinant, $R$ is the Ricci scalar and $\mathcal{L}_m$ is the matter Lagrangian. Nojiri and Oodintsiv (2007); Capozziello and de Laurentis (2011) consider $f(R) = f_0 R^n$, where $f_0$ is a constant to give correct dimensions to the action and $n$ is the slope parameter. The modified Einstein equation is obtained by varying the action with respect to the metric components.

Solving the vacuum field equations for a Schwarzschild-like metric in the Newtonian limit of weak gravitational fields and low velocities, the modified gravitational potential for the case of a point-like source of mass $m$, is given by

$$\phi(r) = -\frac{Gm}{r}\left\{1 + \frac{1}{2}[(r/r_c)^\beta - 1]\right\}, \tag{1.7}$$

where the relation between the slope parameter $n$ and $\beta$ is given by:

$$\beta = \frac{12n^2 - 7n - 1 - \sqrt{36n^4 + 12n^3 - 83n^2 + 50n + 1}}{6n^2 - 4n + 2}. \tag{1.8}$$

Note that for $n = 1$ the usual Newtonian potential is recovered. The large and small scale behaviour of the total potential constrain the parameter $\beta$ to be $0 < \beta < 1$.

The solution Eq. (1.7) can be generalized to extended systems with a given density distribution $\rho(r)$ by simply writing:

$$\begin{aligned} \phi(r) &= -G \int d^3r' \, \frac{\rho(\mathbf{r'})}{|\mathbf{r} - \mathbf{r'}|} \, \{1 + \frac{1}{2}[\frac{|\mathbf{r} - \mathbf{r'}|^\beta}{r_c^\beta} - 1]\} \\ &= \phi_N(r) + \phi_C(r), \end{aligned} \tag{1.9}$$

where $\phi_N(r)$ represents the usual Newtonian potential and $\phi_C(r)$ the additional correction. In this way, the Newtonian potential can be re-obtained when $\beta = 0$. Once the gravitational potential has been computed, one may evaluate the rotation curve $V_c^2(r)$ and compare it with the data.

In Chapter 2 we will show that $f(R) = f_0 R^n$ is able to recover the observed kinematics of galaxies (see also Frigerio Martins and Salucci, 2007; Capozziello et al., 2006). Nevertheless, similarly to MOND, on bigger scales, for example from the point of view of gravitational lensing, f(R)-gravity still needs a non negligible amount of DM in order to reproduce the observations (note that the role of DM, in this case, might play the missing baryons) (see Lubini et al., 2011).

### 1.2.2 If particle: Hot, Cold, Warm or Self-interacting?

Already in 80's particle physicists started to propose that some sort of non-baryonic hypothetical elementary particles, such as axions, neutrinos, photinos, etc., may serve as candidates for DM particles. There were several reasons to search for this kind of particles. First of all, no baryonic candidate did fit the observational data. Second, the Big Bang nucleosynthesis implies baryon density to be a few percent ($\sim 0.04$) of the critical density, while the total budget of DM is of the order $\sim 0.3$ of the critical density. Therefore, we are forced to consider that not all of the DM is baryonic.

At the beginning of 80's the favoured particle candidates were neutrinos, later this model was called Hot DM (Doroshkevich et al., 1980; Zeldovich et al., 1980). Thanks to numerical simulations, we know today that neutrinos in their standard form move with too high velocities (very close to speed of light and with masses 10s of few eV) such that they can escape from small density fluctuations and not being able to form small structures as galaxies. However, these particles provided an important template for the class of hypothetical species that would later be known as weakly interacting massive particles (WIMPs).

WIMPs are the most famous class of the DM candidates (in particular the most promising in supersymmetric theories are neutralinos) and along with non thermally produced axions, they represent the most studied candidates for the Cold DM model. The mass of neutralinos usually vary from ∼100 GeV to few TeV and they couple to other particles with strengths characteristic of the weak interactions. Axions are much lighter than neutralinos (often $\lesssim 0.01\, eV$) and furthermore, they are expected to be extremely weakly interacting with ordinary matter (weaker than neutralinos). Contrary to Hot DM, in the Cold DM scenario the structure formation in the Universe starts at an early epoch, and superclusters consist of a network of small galaxy filaments, similar to the observed distribution of galaxies. Thus, Cold DM simulations reproduce quite well the large scale structure of the Universe (Blumenthal et al., 1984). Nonetheless, there are significant problems at galactic scales (discussed extensively later in this Thesis).

Warm DM consists in DM species with velocities intermediate between those of Hot DM and Cold DM (see e.g. Bode et al., 2001). Warm DM candidates have a mass around $\sim 1\, keV$. The most common Warm DM candidates are sterile neutrinos and gravitinos. Although the suppression of the growth of structures on small scales is the main feature of Warm DM, which can help to solve many small scale problems arising in Cold DM scenario (see e.g Lovell et al., 2014; de Vega et al., 2014a), the "classic" N-body Warm DM simulations show that Warm DM models exhibit cusps or small cores with sizes smaller than the observed cores (see e.g. Colín et al., 2008; Kuzio de Naray et al., 2010; Viñas et al., 2012; Macciò et al., 2012). However, other simulations show that once the quantum nature of Warm DM is taken into account, it is possible to reconstruct the correct structure for small scales (below kpc) (see e.g Destri et al., 2013; de Vega et al., 2014a). Furthermore, the current Lyman $\alpha$ forest measurements on the DM power spectrum provides tight constrains on the mass of Warm DM particles. The suggested mass is too large to maintain solutions to the small-scale problems of CDM. However, the recent analysis of these observed bounds, done by Garzilli et al. (2015), relaxes the constraints significantly (see for more discussion Bringmann et al., 2016). This upgraded the interest to Warm DM models.

The last, but not least, relatively new DM model, which we are going to discuss is Self-interacting DM, proposed by Spergel and Steinhardt (2000) in order to solve the small scale problems of Cold DM without discarding the latter. In this picture, the microscopic interaction between DM particles is non-negligible and can affect the dynamics of halo formation by suppressing small-scale density fluctuations (Bœhm et al., 2001, 2002; Boehm et al., 2005; van den Aarssen et al., 2012; Dvorkin et al., 2014). Furthermore, Bœhm et al. (2014); Schewtschenko et al. (2016) showed that in the framework of interacting DM it is also possible to solve other small-scale problems and even to put constrains on the simplest models for DM self-interaction such that they may no longer be sufficient to reduce the tension at small scales (see e.g. Rocha et al., 2013; Peter et al., 2013; Vogelsberger et al., 2012; Zavala et al., 2013). Interestingly, systems of particular importance for self-interacting DM are colliding galaxy clusters (see for more details e.g. Kahlhoefer et al., 2014), such as the Bullet Cluster (see Fig. 1.2 and previous Section for details), Abel 520 (Mahdavi et al., 2007; Jee et al., 2012) or the recently discovered Musket Ball Cluster (Dawson et al., 2012), as it can put robust constrains on DM candidates (or it can even rule out candidates such as supersymmetric neutralinos and axions) (Robertson et al., 2016).

We would like to stress that all these different alternatives to the Cold DM paradigm are not only motivated by the arising small scale problems, but also by the fact that the

most simple Cold DM candidates (WIMPs) have not been detected so far, despite the large number of experiments to detect it.

There are three different kinds of DM searches, that use different assumptions and approaches to detect DM. They can be shortly summarised in Fig. 1.3.

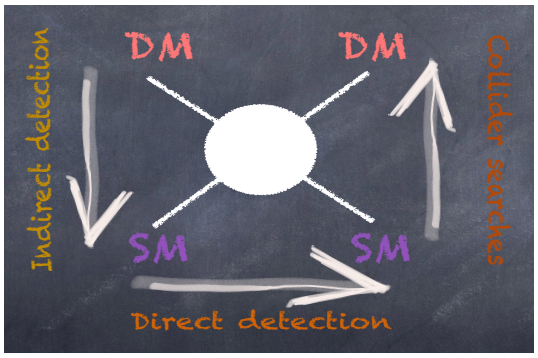


**Figure 1.3:** Cartoon resembling a Feynman diagram which illustrates different ideas for DM particle detection. Depending on the direction of the time axis, different types of searches can be recognised. SM stands for the Standard Model particle, DM for the dark matter particle.

Direct detection experiments are designed to observe interactions of DM particles which are expected to scatter off nuclei in underground detectors (Goodman and Witten, 1985). The established kinetic energy of a recoiling nucleus due to a WIMP interaction is expected to be in a range from several keV to several hundreds of keV depending on the mass of the DM particle and the type of target nuclei. So far only hints from two DM experiments DAMA (DArk MAtter) (Bernabei et al., 2013) and the Si detectors in CDMS-II (Agnese et al., 2013) are reporting DM detection. These hints, however, are in tension with null results of many other experiments, e.g. LUX (Large Underground Xenon) (Akerib et al., 2014) and SuperCDMS (Agnese et al., 2014). Nonetheless, one should not exclude the possibility that these discrepancies are due to the case that different experiments are sensitive to different physics of WIMP interactions which is poorly predicted by theoretical models and some effects regarding their interactions are not taken into account while comparing different results.

Indirect DM experiments are based on searching for the annihilation products of the DM particles. Promising sources for the indirect DM searches are usually considered to be either the most dense regions of the Milky Way, such as the galactic center (see e.g Daylan et al., 2016), the inner halo of our galaxy (see e.g. Ackermann et al., 2012), the center of the Sun or extragalactic sources, such as satellite dwarf spheroidal galaxies of the Milky Way (see e.g. Drlica-Wagner et al., 2015). Furthermore, recently, dwarf spiral Milky Way satellite galaxies became, as well, potential candidates for the indirect DM searches (see e.g. Buckley et al., 2015; Caputo et al., 2016). However, in some of these regions it is usually very complicated to understand the underlying astrophysics, i.e. to correctly estimate the astrophysical background. Therefore, one should look for the regions with the best signal to background ratio.

Additionally, in both direct and indirect searches there are large systematics in the interpretation of the data from experiments due to the uncertainties in the DM density distribution in the Milky Way. There are several works based on the investigation of the influence of such systematics on the interpretation of data (see e.g. Calore et al., 2015; Bozorgnia et al., 2016).

Finally, searches for DM particles are also performed at accelerators, in particular at the Large Hadron Collider (LHC). The main advantage of collider searches is that they do not suffer from astrophysical uncertainties and that there is no lower limit to their sensitivity on DM masses. However, collider searches can detect DM only "indirectly" through the measurement of missing energy, being the DM particle electrically and colour neutral. Colliders are superior to direct searches if DM is very light ($< 10$GeV) or if interactions are spin dependent. So far no LHC run showed any evidence of DM particles.

In conclusion to this paragraph we would like to say that the null detection of a DM particle with current experiments indicates the following:

- DM is most likely not fully made of the WIMP candidates;
- and it is likely that DM lies outside of the standard mass range.

## 1.3 Discussion on Standard Cold DM

Despite its uncertain nature, DM is the key driver of structure formation in the Universe. In previous paragraphs our discussion was concentrated on the potential alternatives to the standard DM model along with the discussion about various candidates for a DM particle and its possible detections. On the other hand, in this paragraph we are

going to concentrate on the standard Cold DM (CDM) model and its possible baryonic modifications.

Let us recall, that the current paradigm of CDM assumes that DM is cold and collisionless. This model is extremely successful in describing the Universe at large scales. However, at the galactic and sub-galactic scales this scenario has significant challenges, which we are going to introduce below (e.g. Salucci, 2001; de Blok and Bosma, 2002a; Gentile et al., 2005; Weinberg et al., 2013).

### The core-cusp problem

High-resolution cosmological N-body simulations have shown that CDM halos always exhibit steep power-law mass density distribution at their centres (Dubinski and Carlberg, 1991; Navarro et al., 1996b, 1997). The latter can be fairly well described according to the well known Navarro-Frenk-White (NFW) fitting formula, which predicts an asymptotic behaviour of $\rho \sim r^{\alpha}$, where the inner density power index is $\alpha = -1$. However, the kinematical observations of galactic RCs prefer shallower central regions or "cores" ($\alpha = 0$).

The core-cusp problem is best documented in low-mass rotationally supported dwarf galaxies which are strongly DM dominated even at small radii and which therefore are ideal tracers of the inner DM density distribution. In 2001 de Blok et al. (2001) analysed a sample of high-resolution optical and 21 cm RCs of low surface brightness galaxies (LSB). The authors showed that halos of LSB galaxies are dominated by cores (see left panel of Fig. 1.4).

Furthermore, in the paper by McGaugh et al. (2001) was demonstrated that beam-smearing is not responsible for cores in LSB, as was suggested by others (see e.g van den Bosch et al., 2000; van den Bosch and Swaters, 2001). On the right panel of Fig. 1.4 we show the similar result for a larger sample (including galaxies from de Blok et al., 2001) of dwarf disk galaxies presented in Oh et al. (2015). Once more we can see that most of the galaxies tend to have cores and not cusps. As for dwarf spheroidal galaxies our current lack of knowledge about the anisotropy of stellar disk velocity makes their density profiles not uniquely constrained by the data (see e.g. Koch et al., 2007; Gilmore et al., 2007; Battaglia et al., 2008).

In contrast to dwarfs, in normal spiral galaxies the observed RCs are strongly degenerate due to uncertainties in the stellar mass-to-light ratio. Several ideas were proposed in order to solve this degeneracy. One of them is to use near-infrared surface photometry (K-band or 3.6 $\mu$m), which provides the closest proxy to the stellar mass (Verheijen, 2001, see e.g.). Another way is to investigate the contribution of the stellar disk to the observed

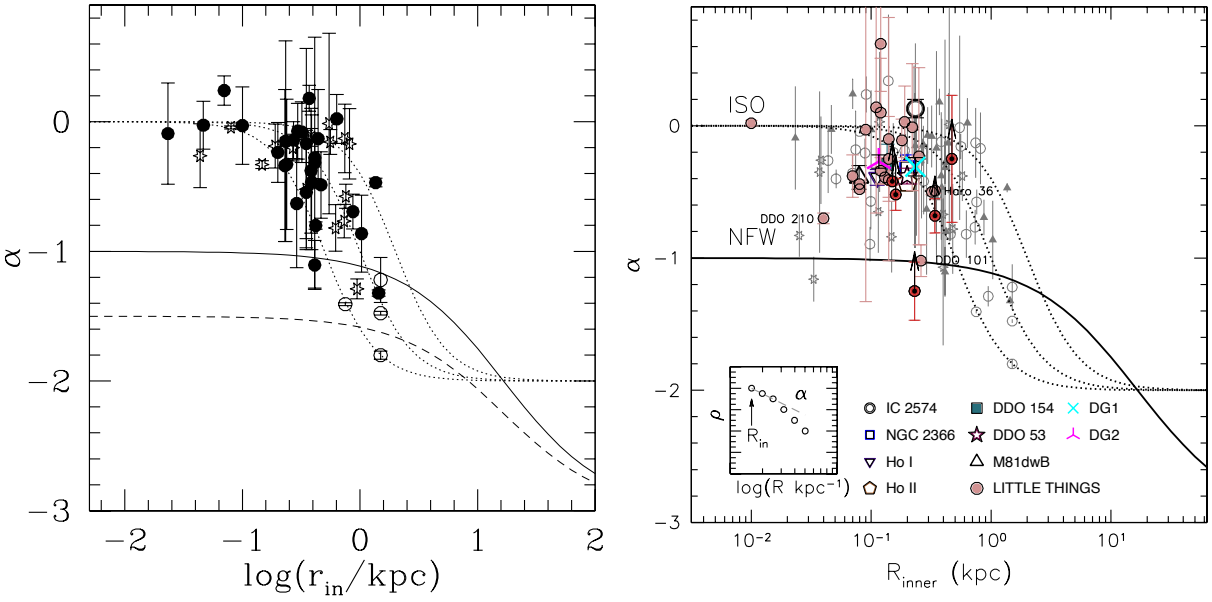


**Figure 1.4:** Inner slope of the DM density profile $\alpha$ vs the radius $R_{in}$ of the innermost point within which $\alpha$ is measured as described in the small figure (de Blok et al., 2001). The solid and dashed lines represents the theoretical prediction of NFW and ISO halos, respectively. Left panel: sample of LSB from de Blok et al. (2001). Right panel: sample of galaxies presented in this plot is described in Oh et al. (2015).

RCs in spirals systematically. For example, in Persic et al. (1996) the authors presented the concept of a universal rotation curve (URC), i.e. a single function of the total galaxy luminosity and of a characteristic radius of the luminous matter[1] which represents the RCs of all spirals (see Fig. 1.5) and can be very well fitted by empirically motivated (cored) DM density profile (Burkert profile, Burkert, 1995a). In Chapter 4 we will extend this concept down to dwarf disk galaxies.

In conclusion, in spirals it is not easy to derive the inner DM density slopes since in this region they are dominated by the stellar content. Therefore, usually, the velocity profiles of spiral galaxies are well fitted by either a cored or a cuspy DM halo, just by adjusting the amount of the stellar matter content. However, for the cuspy profiles the emerging fit parameters are not always physical. In more details, the derived mass-to-light ratio is unrealistically low and/or the derived concentration parameter tends to be lower than that predicted in numerical simulations performed in ($\Lambda$)CDM scenario (for more details see, e.g., Gentile et al., 2004). The latter will be also shown in Section 3 by

[1]i.e. $R_{opt}$ defined as the radius compressing 83 % of the total luminosity.

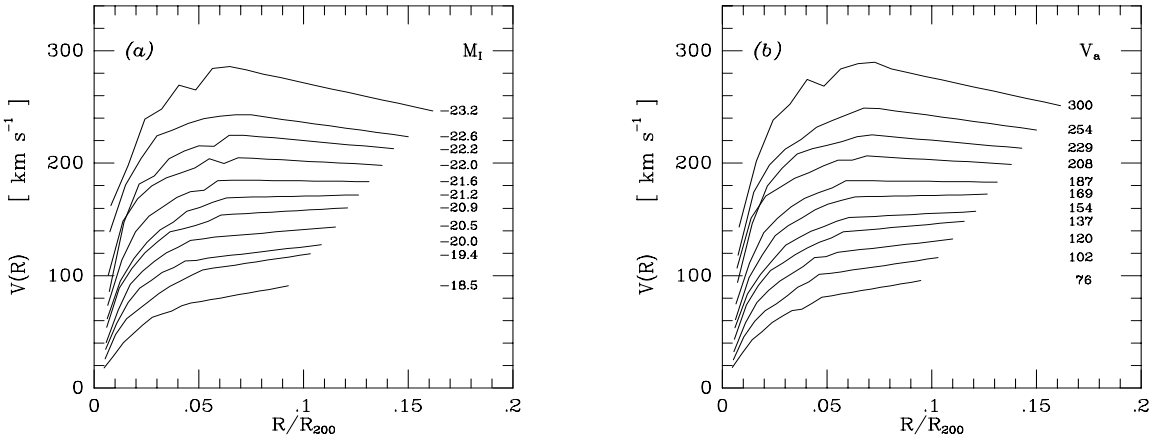


**Figure 1.5:** The universal rotation curve of spiral galaxies at different luminosities and velocities (panels (a) and (b),respectively). Radii are in units of $R_{200}$, the radius encompassing a mean halo overdensity of 200, which represents the characteristic scalelength of the DM distribution.

means of high-resolution optical and 21 cm observations of the spiral galaxy NGC 3198. Furthermore, in Section 3 we will also show that in addition to the core-cusp problem in the inner part of NGC 3198 ($R < 2R_D$), at the outer radii ($R > 4R_D$) the measured DM halo density is found to be higher than the corresponding ($\Lambda$)CDM once.

In addition the core-cusp problem has been also noticed at galaxy clusters scales. Kinematics and lensing constraints in cD galaxies (giant elliptical galaxy), which are located in the centre of relaxed clusters, showed that the clusters DM profiles is flatter than a NFW profile, but the total mass profile is in agreement with the NFW predictions (Sand et al., 2002, 2004; Newman et al., 2013b,a).

### Missing satellites + field galaxies

DM-only cosmological simulations of structure formation predict thousands of low-mass-halos which should orbit within a Milky Way-sized halos. However, only a few tens of such satellites have been observed to date (Klypin et al., 1999; Moore et al., 1999). Similar discrepancy also occurs in the field (isolated) galaxies (Zavala et al., 2009; Papastergis et al., 2011; Ferrero et al., 2012; Klypin et al., 2015). This discrepancy can be illustrated

by comparison of the observed and theoretical estimates of the circular velocity function[1] of galaxies. For example, in Fig. 1.6 [2] is shown the comparison of the observed velocity function of the Local Volume galaxies (inside the 10 Mpc sphere) (purple shaded area) with the theoretical prediction of the circular velocity function for halos in the (Λ)CDM model. In this plot is clearly evident that CDM over-predicts the number of galaxies with the circular velocities below $\sim$ 80 km/s.

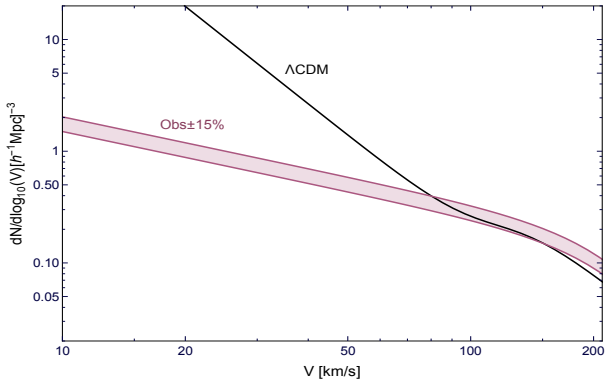


**Figure 1.6:** Comparison of the observed and theoretical estimates of the circular velocity function. The purple shaded area shows the regions of the observed velocity function (with 15 % of uncertantes) in the Local Volume (see eq. 12 of Klypin et al., 2015). The black solid curve shows the (Λ)CDM predictions corrected for the effect of baryons (see eq. 9,10 of Klypin et al., 2015).

### Too big to fail

Too big to fail (TBTF) was first identified by Boylan-Kolchin et al. (2011): DM-only (Aquarius simulation) simulations predict subhalos too massive and dense, by a factor $\simeq 5$, to host even the brightest satellites of the Milky Way (Springel et al., 2008). In Fig. 1.7 is shown the maximum rotation velocity $V_{max}$ as function of the visual magnitude in V-band $M_V$ (Boylan-Kolchin et al., 2012). This plot confirms that the simulations produce much more massive subhalos (magenta dots) than the observed dwarf spheroidal galaxies (square symbols with errors). Similar results were reported by Ferrero et al. (2012) in analysing the DM of faint dwarf irregular galaxies in the field. They argued

[1]The velocity function is defined as the abundance of galaxies with a given circular velocity. It is used as a substitution to the luminosity function due to the fact that the latter is much more difficult to predict theoretically.

[2]Reproduction of Fig. 11 in Klypin et al. (2015).

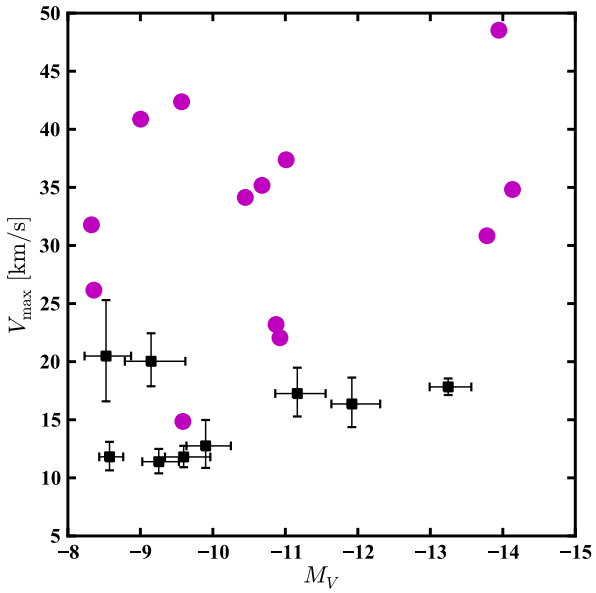


**Figure 1.7:** Values of $V_{max}$ ($V_{circ}(r_{max}) = V_{max}$) are computed in Section 4.1 of Boylan-Kolchin et al. (2012) for the nine luminous Milky Way dwarf spheroidals (square symbols with errors), along with $V_{max}$ values of the most massive subhalos with $M_V < -8$ (magnitudes are assigned by abundance matching) of the Aquarius simulations (magenta dots).

that many of these dwarfs have the total masses well beyond those predicted by different abundance matching models (Guo et al., 2010; Moster et al., 2013). The result of Ferrero et al. (2012) is also supported by recent works based on the analysis of the M31 satellites (Tollerud et al., 2014; Collins et al., 2014) and of the other sample of field galaxies (Kirby et al., 2014; Garrison-Kimmel et al., 2014b; Papastergis et al., 2015). Additionally, in our Chapter 4 we show analogous results for a sample of dwarf disk galaxies in the Local Volume ($\sim$ 11 Mpc).

## 1.4 Standard CDM with baryons

The above discrepancies, in principle, can be considered as a hint to physics beyond the ($\Lambda$)CDM, for example, modification of gravity, which we introduced in subsection 1.2.1, or exotic DM models, see the discussion in subsection 1.2.2. However, it is important to stress that all of these discrepancies arise from a comparison between the observed universe and the collisionless cosmological N-body simulations, that are needed to be modified taking into account baryonic processes.

In fact, DM cores can form due to the energetic feedback from supernovae by driving stellar winds (Navarro et al., 1996a; Gnedin and Zhao, 2002; Mo and Mao, 2004; Governato et al., 2010), driving the random bulk motion of the gas (Mashchenko et al., 2006), or by creating fast oscillations in the inner galaxy potential (Read and Gilmore, 2005; Pontzen and Governato, 2012). The central DM density can also be lowered by tidal stripping. However, the latter would not help to solve the issue raised by field dwarf irregular galaxies (Ferrero et al., 2012; Papastergis et al., 2015, see also our result in Chapter 4). In order to illustrate how baryonic outflows can affect the initial cuspy profile see Fig. 1.8 taken from Governato et al. (2012). In this paper the authors used cosmological hydrodynamical simulations in order to show that once baryonic processes are correctly taken into account, flat inner DM profiles (e.g. the solid black line of Fig. 1.8 for z=0) are a common property of field galaxies formed within ($\Lambda$)CDM model. Di Cintio et al. (2014b) in their simulations also obtained similar results. In their study they analysed the response of DM distribution to different feedback schemes within the set of simulated galaxies. Some of their resulting density profiles are shown on Fig. 1.9. This figure represents how the dark matter density profiles of the hydrodynamic simulations can vary depending on physics (MUGS in black compared to MaGICC fiducial simulations, that use early stellar feedback, in red), galaxy mass (solid line at high mass and dashed line at medium mass), and how the hydrodynamic simulations compare with the dark matter only run (solid grey line).

Additionally, several authors have noted that if DM halos are cored rather than cusped, this can naturally alleviate both the TBTF and the missing satellites problems (see e.g. Read et al., 2006; Madau et al., 2014; Di Cintio et al., 2014b; Ogiya and Burkert, 2015; Zolotov et al., 2012; Arraki et al., 2014).

In conclusion it is useful to note, that the precise scales and effects of these solutions are still under debate. Although many groups have used hydrodynamical simulations to study core-cusp transformation, there is still no a common agreement on where, if anywhere, the core-cusp transformation really occurs.

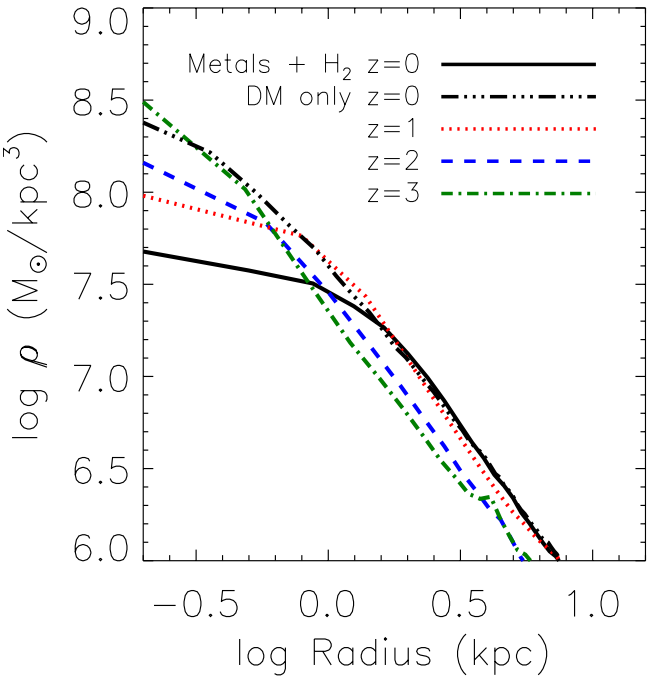


**Figure 1.8:** The DM density profile of a simulated dwarf galaxy in Governato et al. (2012), at z=0,1,2,3. The resulting shallow inner profile at z=0 is shown by the solid black line. For comparison, the density profile of the same galaxy, but simulated with DM only, is shown in the black dot-dashed line. In the DM only simulation, the DM maintains its cuspy density profile at all redshifts.

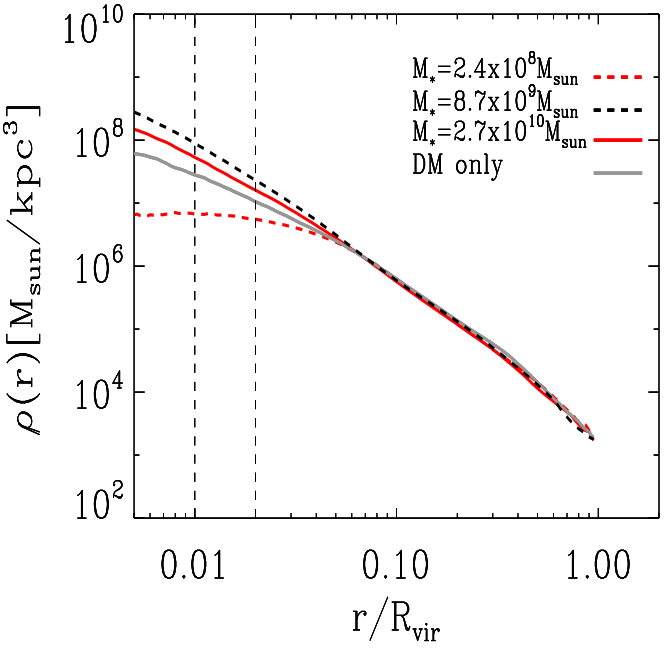


**Figure 1.9:** Density profiles of contracted (solid red and dashed black lines) and expanded (dashed red line) dark matter haloes, together with the corresponding DM only prediction (solid grey). The vertical dashed lines indicate 0.01 and 0.02 of the virial radius, our fiducial range to measure $\alpha$. From Di Cintio et al. (2014b).

# Chapter 2

# $R^n$ gravity is kicking and alive: The cases of Orion and NGC 3198

In this Chapter we analyzed the Rotation Curves of two crucial objects, the Dwarf galaxy Orion and the low luminosity Spiral NGC 3198, in the framework of $R^n$ gravity. We surprisingly found that the no DM power-law f(R) case fits them well, performing much better than ($\Lambda$)CDM Dark Matter halo models. The level of this unexpected success can be a boost for $R^n$ gravity.

## 2.1 Introduction to the problem

It was already introduced in Chapter 1 that the Rotation Curves (RCs) of spiral galaxies show a non-Keplerian circular velocity profile which cannot be explained by considering a Newtonian gravitational potential generated by the baryonic matter (Rubin, 1983). Current possible explanations include the postulate of a new yet not detected state of matter, the dark matter, e.g. (Rubin, 1983), a phenomenological modification of the Newtonian dynamics (Milgrom, 1983), and higher order Gravitational Theories, see e.g (Carroll et al., 2004; Capozziello and de Laurentis, 2011; Capozziello et al., 2004, 2006; Sotiriou and Faraoni, 2010; Nojiri and Odintsov, 2011).

In this Chapter we would like to test whether the recently proposed f(R)-gravity (see for more details on the f(R) theory in the Introduction) is able to reproduce the dynamical observations in galaxies. Previously, Frigerio Martins and Salucci (Frigerio Martins and Salucci, 2007) investigated the consistency and the universality of this theory by means of a sample of spirals, obtaining a quite good success that was encouraging for further

investigations. Recently, crucial information for two special objects has been available and we are now able to test the theory in unprecedented accurate way.

Orion is a dwarf galaxy of luminous mass $< \frac{1}{100}$ the Milky Way stellar disk mass with a baryonic distribution dominated by a HI disk, whose surface density is accurately measured and, noticeably, found to have some distinct feature. The stellar disk, on the other side, is a pure exponential disk. The available rotation curve (Frusciante et al., 2012) is extended and it is of very high resolution. Noticeably, this is one of the smallest galaxies for which we have a very accurate profile of the gravitating mass.

NGC3198 is a normal spiral about 2 times less luminous than the Milky Way. For a decade it held the record of the galaxy with the (HI) rotation curve showing the clearest evidence for Dark Matter (van Albada et al., 1985). Then, the record went to other galaxies with optical RCs, but recent radio measurements of a high-resolution (Gentile et al., 2013) has likely brought it back to this galaxy. Furthermore, in the next Chapter we are going to present the mass modelling of the same very extended HI RC of NGC3198 in order to investigate the DM distribution in this spiral galaxy.

The heart of this Chapter is that these two galaxies show without doubt a "Dark Matter Phenomenon" but, when we analyse the issue in detail, we realise that well physically motivated halos of dark particles fail to account for their Rotation Curves. Our idea is to use these them to constrain proposed modifications of gravity: in the framework of those, can the baryonic matter alone account for the observed RCs when, in Standard Newtonian Gravity, the baryonic + dark matter together badly fail?

## 2.2 Data and methodology of the test

Let us remind following that for these galaxies we have high quality RC and a very good knowledge of the distribution of the luminous matter (Gentile et al., 2013; Frusciante et al., 2012; Opik et al., 2015). Any result of the mass modelling could not be questioned on base of putative observational errors or biases. It is matter of fact that NFW halos + luminous matter model badly fits these very RCs (Frusciante et al., 2012; Opik et al., 2015) and many others (Donato et al., 2009a; Persic et al., 1996; Salucci and Persic, 1999).

We decompose the total circular velocity into stellar and gaseous contributions. Available photometry and radio observations show that the stars and gas in these spirals are distributed in an infinitesimal thin and circular symmetric disk; from the HI flux we directly measure $\Sigma_{gas}(r)$ its surface density distribution (multiplied by 1.33 to take into account also the He contribution). In these galaxies, the stars follow the usual Freeman

exponential thin disk:

$$\Sigma_D(r) = (M_D/2\pi R_D^2)\, e^{-r/R_D}. \tag{2.1}$$

$M_D$ is the disk mass and it is kept as a free parameter, $R_D$ is the scale length, measured directly from optical observations.

The distribution of the luminous matter has, to a good extent, a cylindrical symmetry and hence potential then Eq. (1.9), which was presented in the Introduction part, reads

$$\phi(r) = -G \int_0^\infty dr'\, r' \Sigma(r') \int_0^{2\pi} \frac{d\theta}{|\mathbf{r} - \mathbf{r'}|} \{1 + \frac{1}{2}[\underbrace{\frac{|\mathbf{r} - \mathbf{r'}|^\beta}{r_c^\beta}} - 1]\}. \tag{2.2}$$

$\Sigma(r')$ is the surface density of the stars, given by Eq. (2.1), or of the gas, given by an interpolation of the HI mesurements. $\beta$ and $r_c$ are, in principle, free parameters of the theory, with the latter perhaps galaxy dependent. We fix $\beta = 0.7$ to have agreement with previous results (see also Frigerio Martins and Salucci, 2007).

Defining $k^2 \equiv \frac{4r\,r'}{(r+r')^2}$, we can express the distance between two points in cylindrical coordinates as $|\mathbf{r} - \mathbf{r'}| = (r + r)^2(1 - k^2 cos^2(\theta/2))$. The derivation of the circular velocity due to the marked term of Eq. (2.2), that we call $\phi_\beta(r)$, is now direct:

$$r\, \frac{d}{dr}\, \phi_\beta(r) = -2^{\beta-3} r_c^{-\beta}\, \pi\, \alpha\, (\beta - 1)\, G\, I(r), \tag{2.3}$$

where the integral is defined as

$$\mathcal{I}(r) \equiv \int_0^\infty dr' r' \frac{\beta - 1}{2} k^{3-\beta}\, \Sigma(r')\, \mathcal{F}(r), \tag{2.4}$$

with $\mathcal{F}(r)$ written in terms of confluent hyper-geometric function: $\mathcal{F}(r) \equiv 2(r + r')\, {}_2F_1[\frac{1}{2}, \frac{1-\beta}{2}, 1, k^2] + [(k^2 - 2)r' + k^2 r]\, {}_2F_1[\frac{3}{2}, \frac{3-\beta}{2}, 2, k^2]$.

The total circular velocity is the sum of each squared contribution:

$$V_{CCT}^2(r) = V_{N,stars}^2 + V_{N,gas}^2 + V_{C,stars}^2 + V_{C,gas}^2, \tag{2.5}$$

where the $N$ and $C$ subscripts refer to the Newtonian and the additional modified potentials of the two different contributions (gas and stars) to the total potential Eq. (1.9).

In Fig. 2.1 the velocities are shown only in the ranges of $r$ where their square are positive.

The RCs are $\chi^2$ best-fitted with the free parameters: the scale length ($r_c$) of the theory and the gas mass fraction ($f_{gas}$) related to the disk mass simply by $M_D = M_{gas}(1 - f_{gas})/f_{gas}$ with the gas mass measured . The errors for the best fit values of the free parameters are calculated at one standard deviation.

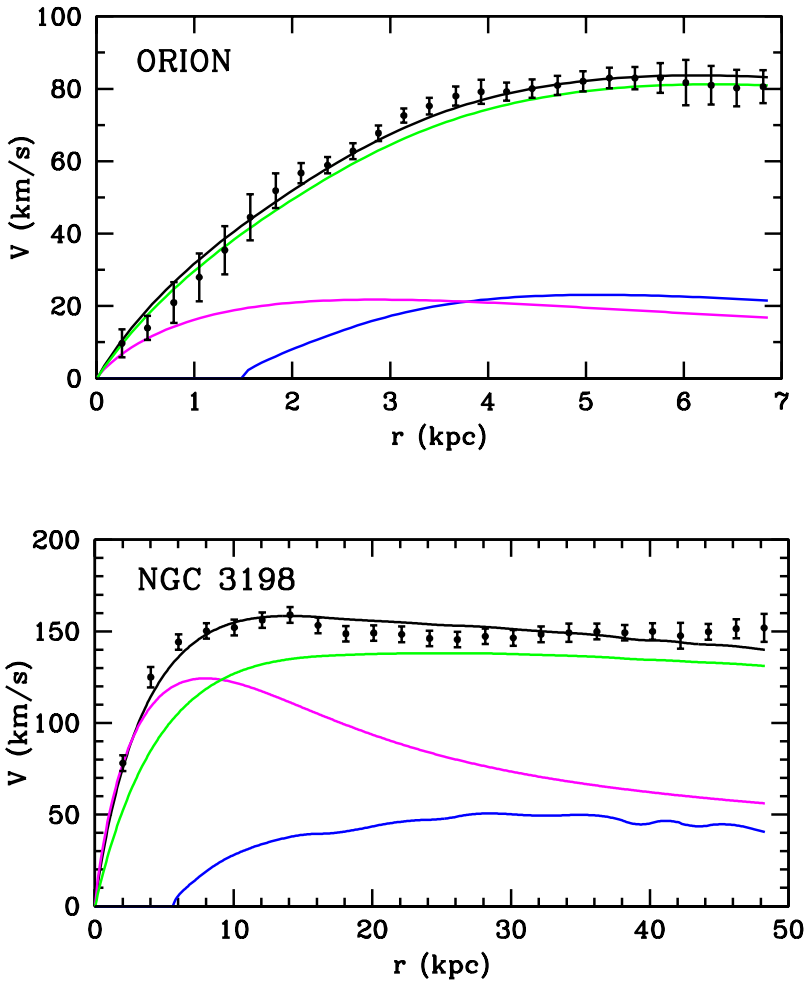


**Figure 2.1:** Black: best-fit total circular velocity $V_{CCT}$. Blue: Newtonian gaseous contribution. Magenta: Newtonian stars contribution. Green: non-Newtonian gaseous and stars contributions to the model.

Let us recall that we can write

$$V^2_{stars}(r) = (GM_D/2R_D)\, x^2 B(x/2), \tag{2.6}$$

where $x \equiv r/R_D$, $G$ is the gravitational constant and the quantity $B = I_0K_0 - I_1K_1$ is a combination of Bessel functions (Freeman, 1970).

## 2.3 Results

We summarize the results of our analysis in Fig. 2.1. We find that the velocity model $V_{CCT}$ is well fitting the RCs for very reasonable values of the stellar mass-to-light ratio. The resulting disk masses are $(3.7 \pm 0.8) \times 10^8 M_\odot$ and $(3.4 \pm 0.8) \times 10^{10} M_\odot$ respectively for Orion and NGC3198. The other parameters are: Orion $r_c = (0.013 \pm 0.002)$ $kpc$ and gas fraction=$(55 \pm 20)$%, NGC3198 $r_c = (0.4 \pm 0.05)$ $kpc$ and gas fraction=$(29 \pm 10)$%. The values of $\chi^2$ are $\simeq 1$ confirming the success of the fit.

The value for the scale-length parameter $r_c$ is found smaller for the less massive galaxy and larger for the more massive one, in line with previous results and with the idea of a scale dependent modification of gravity (Capozziello and De Laurentis, 2012).

## 2.4 Conclusions

Extended theories of gravity, created to tackle theoretical cosmological problems have something to say on another issue of Gravity, the Phenomenon of Dark Matter in galaxies. We have tested two objects with state of the art kinematical data that, in addition, are not accounted by the dark matter halo paradigm and we found that a scale dependent $R^n$ Gravity is instead able to account for them. Extended theories of Gravity candidate themselves to explain the phenomenon of dark matter with only the luminous matter present in galaxies.

## 2. $R^n$ gravity is kicking and alive: The cases of Orion and NGC 3198

# Chapter 3

# The Dark Matter Distribution in the Spiral NGC 3198 out to 0.22 $R_{vir}$

In the previous Chapter we used the kinematical data of two galaxies in order to test the alternative theories of gravity, in particular f(R) theories. We now turn the discussion to a more in depth analysis of DM halos in galaxies.

In this Chapter we use recent very extended (out to 48 kpc) HI kinematics alongside with previous H$\alpha$ kinematics of the spiral galaxy NGC 3198 in order to derive its distribution of dark matter (DM).

First, we used a chi-square method to model the Rotation Curve of this galaxy in terms of different profiles of its DM distribution: the universal rotation curve (URC) mass model (stellar disk + Burkert halo + gaseous disk), the NFW mass model (stellar disk + NFW halo + gaseous disk) and the Baryon$\Lambda$CDM mass model (stellar disk + NFW halo modified by baryonic physics + gaseous disk). Secondly, in order to derive the DM halo density distribution we apply a new method which does not require a global and often uncertain mass modelling.

We find that, while, according to the standard method, both URC and NFW mass models can account for the RC, the new method instead leads to a density profile which is sharp disagrees with the dark halo density distribution predicted within the Lambda cold dark matter ($\Lambda$CDM) scenario. We find that the effects of baryonic physics proposed by Di Cintio et al. (2014b) modify the original $\Lambda$CDM halo densities in such a way that the resulting profile is more compatible with the DM density of NGC 3198 derived using our new method. However, at large distances, r $\sim$ 25 kpc, also this modified Baryon$\Lambda$CDM halo profile appears to create a tension with the derived DM halo density.

## 3.1 Introduction

It has been known for several decades that the kinematics of disk galaxies leads to a mass discrepancy (e.g. Bosma, 1978; Bosma and van der Kruit, 1979; Rubin et al., 1980). While in their inner regions that range between one and three disk exponential scale lengths according to the galaxy luminosity (Salucci and Persic, 1999), the observed baryonic matter accounts for the rotation curves (RCs) (e.g. Athanassoula et al., 1987; Persic and Salucci, 1988; Palunas and Williams, 2000), we must add an extra mass component in the outer regions, namely a dark matter (DM) halo to account for that component. The kinematics of spirals is now routinely interpreted in the framework of a DM component. In the widely accepted Lambda cold dark matter ($\Lambda$CDM) scenario, the virialized structures are distributed according the well known NFW profile proposed by Navarro, Frenk, and White (Navarro et al., 1996b). Although, the $\Lambda$CDM scenario describes the large-scale structure of the Universe well (e.g. Springel, 2005), it seems to fail on the scales of galaxies (de Blok and Bosma, 2002b; Gentile et al., 2004, 2005). One of such failure that has already been presented in the introduction part of this Thesis, the "core-cusp problem": empirical profiles with a central core of constant density, such as the pseudo-isothermal (Begeman et al., 1991; Kent, 1986) and the Burkert (Salucci and Burkert, 2000a), fit the available RCs much better than the mass models based on NFW haloes.

In the present work, we derive the DM content and distribution in the spiral galaxy NGC 3198. This galaxy has been the subject of several investigations. It was studied by means of optical (Cheriguène, 1975; Hunter et al., 1986; Bottema, 1988; Wevers et al., 1986; Kent, 1987; Corradi et al., 1991; Daigle et al., 2006) and HI-21 cm radio observations (Bosma, 1981a; van Albada et al., 1985; Begeman, 1987, the latter established it as the object with the clearest evidence for DM), see also (de Blok et al., 2008; Gentile, 2008).

Our present analysis is mainly based on the HI observations by Gentile et al. (2013), part of the HALOGAS (Westerbork Hydrogen Accretion in LOcal GAlaxieS) survey. The main goal of HALOGAS is to investigate the amount and properties of extra-planar gas by using very deep HI observations. In fact, for this galaxy, they present a very extended RC out to 720 arcsec, corresponding to $\sim$ 48 kpc for a galaxy distance at 13.8 Mpc (Freedman et al., 2001). The previous HI observations by de Blok et al. (2008) were only extended out to $\sim$ 38 kpc, for the same galaxy distance. In Gentile et al. (2013) this extended RC was modelled in the framework of modified Newtonian dynamics (MOND) and in our previous Chapter this RC was tested in the framework of f(R) gravity. Here, we want to use such a uniquely extended kinematics to help resolving the DM core-cusp issue. To the very reliable kinematics available from 2 to 48 kpc we apply *two* different mass decomposition methods that will derive the DM halo structure. This is compared

with a) the empirically based halo profiles coming from the URC, b) the NFW haloes and c) the baryon ΛCDM haloes, the outcome of scenarios in which baryonic physics has shaped the DM halo density.

This Chapter is organized as follows. In Sect. 3.2 we present the HI and H$\alpha$ kinematics used in this study. In Sect. 3.3 we model the RC by using the quadrature sum of the contributions of the individual mass components (stellar disk + dark halo + gas disk) where the dark halo has a NFW or a Burkert density profile, respectively. In Sect. 3.4 we obtain the results of standard mass modelling of the NGC 3198 RC. In Sect. 3.5 we use a recent mass modelling technique to obtain a very robust and careful determination of the DM halo density of NGC 3198 and to show that it is at variance with the NFW density profile in an unprecedented way. We consider the mass dependent density profiles obtained by hydro-dynamical simulations of ΛCDM haloes in Sect. 3.6. Our conclusions are drawn in Sect. 3.7.

## 3.2 Kinematics data

### 3.2.1 HI data

The HI data of NGC 3198 were taken in the framework of the HALOGAS survey (Heald et al., 2011) and they were presented in Gentile et al. (2013). The data were obtained with the WSRT (Westerbork Synthesis Radio Telescope) for 10 × 12 hours, with a total bandwidth of 10 MHz subdivided into 1024 channels. The data cube used to derive the rotation curve has a beam size of 35.2 × 33.5 arcsec, and we were able to detect emission down to $\sim 10^{19}$ atoms cm$^{-2}$.

To construct the gas distribution and the rotation curve of this galaxy in a reliable way, we modelled the whole data cube by means of the TiRiFiC software (Józsa et al. 2007). We successfully modelled the HI observations of NGC 3198 with a thin and a thick neutral hydrogen disk, and, thanks to an increased sensitivity, we were able to trace the rotation curve out to a distance of $\sim$ 48 kpc (for the galaxy distance of 13.8 Mpc), i.e. to a larger radius than those reached in previous studies. More details about the data reduction analysis and modelling can be found in Gentile et al. (2013).

### 3.2.2 H$\alpha$ data

The H$\alpha$ rotation curves of NGC 3198 have been published by many authors (Cheriguène, 1975; Hunter et al., 1986; Bottema, 1988; Wevers et al., 1986; Kent, 1987; Corradi et al., 1991; Daigle et al., 2006). We notice that Corradi et al. (1991) and Daigle et al. (2006)

measurements are a good representation of these data. In Fig. 3.1, these RCs are plotted along with the HI RC used in this work. H$\alpha$ data provide us measurements of the circular velocity at five different new (inner) radii not mapped by the present HI RC and four more measurements at radii at which we can combine them with our HI data. The hybrid RC (HI+H$\alpha$ data) is listed in Table 3.1. All together, HI and H$\alpha$ RCs agree very well within the observational errors where they coexist. With respect to the HI RC of Gentile (2008), the present hybrid RC covers the innermost and the outermost regions significantly better; however, H$\alpha$ RCs give us no new useful information for $r < 2$ kpc, owing to its large observational uncertainties and because in this very inner region the kinematics is strongly influenced by non-axisymmetric motions (see Corradi et al., 1991).

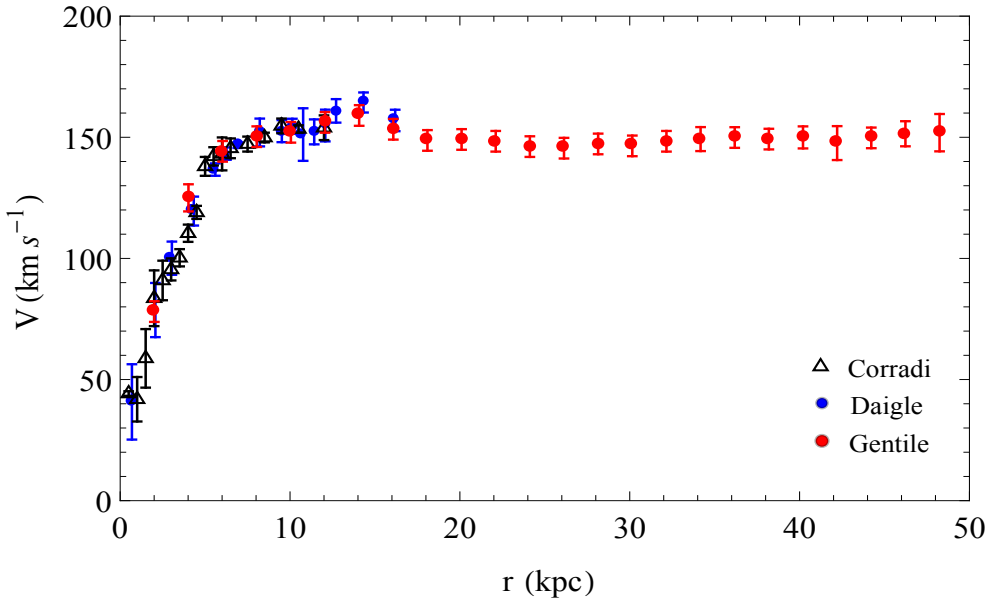


**Figure 3.1:** Comparison between H$\alpha$ and HI RCs black open triangles with error bars from Corradi et al. (1991), blue circles with error bars are from Daigle et al. (2006), and red circles with error bars are from Gentile et al. (2013).

**Table 3.1:** Stellar disk contribution $V_d$ (km s$^{-1}$) (de Blok et al., 2008) and the circular velocity $V$ (km s$^{-1}$) mainly from Gentile et al. (2013), but also from Corradi et al. (1991) and Daigle et al. (2006), of the NGC 3198 with errors d$V$ (km s$^{-1}$). The DM density profile $\rho \times 10^{-25}$ (g cm$^{-3}$) (see Sect. 5 for details).

| R (kpc) | $V_d$ (km s$^{-1}$) | $V$ (km s$^{-1}$) | d$V$ (km s$^{-1}$) | $\rho \times 10^{-25}$ (g cm$^{-3}$) |
|---|---|---|---|---|
| 2.0 | 86.2 | 79.0 | 7.0 | — |
| 3.0 | 85.4 | 97.8 | 5.0 | — |
| 4.0 | 93.6 | 118.0 | 5.6 | — |
| 5.5 | 115.7 | 139.4 | 4.3 | 2.34 |
| 6.0 | 120.8 | 144.2 | 4.3 | 2.33 |
| 7.0 | 125.4 | 143.3 | 4.5 | 2.20 |
| 8.0 | 125.5 | 150.3 | 4.3 | 2.01 |
| 9.0 | 123.5 | 149.9 | 4.3 | 1.83 |
| 10.1 | 120.1 | 152.1 | 4.3 | 1.64 |
| 11.0 | 116.6 | 151.1 | 4.5 | 1.48 |
| 12.1 | 112.6 | 156.2 | 4.3 | 1.32 |
| 14.1 | 105.2 | 161.0 | 4.3 | 1.06 |
| 16.1 | 98.6 | 155.3 | 4.3 | 0.86 |
| 18.1 | 92.7 | 148.7 | 4.3 | 0.70 |
| 20.1 | 87.5 | 149.1 | 4.3 | 0.58 |
| 22.1 | 82.8 | 148.4 | 4.3 | 0.48 |
| 24.1 | 78.7 | 146.2 | 4.3 | 0.42 |
| 26.1 | 75.1 | 145.5 | 4.3 | 0.36 |
| 28.1 | 71.9 | 147.3 | 4.3 | 0.33 |
| 30.2 | 68.9 | 146.5 | 4.3 | 0.30 |
| 32.2 | 66.3 | 148.4 | 4.3 | 0.27 |
| 34.2 | 63.9 | 149.3 | 5.0 | 0.25 |
| 36.2 | 61.8 | 149.9 | 4.3 | 0.23 |
| 38.2 | 59.8 | 149.3 | 4.3 | 0.21 |
| 40.2 | 58.0 | 150.0 | 4.6 | 0.20 |
| 42.1 | 56.4 | 147.6 | 7.0 | 0.18 |
| 44.2 | 54.9 | 149.8 | 4.3 | 0.16 |
| 46.2 | 53.5 | 151.5 | 4.3 | 0.13 |
| 48.2 | 52.2 | 151.9 | 7.7 | 0.11 |

## 3.3 Mass models

We model the spiral galaxy NGC 3198 as consisting of three "luminous" components, namely the bulge and the stellar and the gaseous disks, which are embedded in a dark halo. To study the properties of luminous and dark matter in this galaxy, we model the RC in terms of the contributions from the stellar disk, the bulge, the gaseous disk, and the dark matter halo:

$$V^2(r) = V_{\rm d}^2(r) + V_{\rm b}^2(r) + V_{\rm g}^2(r) + V_{\rm DM}^2(r). \tag{3.1}$$

### 3.3.1 Luminous matter

We define $V_{\rm d}(r)$ as the contribution of the stellar disk to the circular velocity $V(r)$. The surface brightness profile of NGC 3198 has been analysed very well by de Blok et al. (2008). We assume their one-component surface brightness profile to derive $V_{\rm d}(r)$. As a reference value we take the stellar mass-to-light ratio from de Blok et al. (2008): $\Upsilon^{3.6}_{*,\rm deBlok} = 0.8$ (referred to the Spitzer IRAC 3.6 $\mu$m band, which is a good proxy for the emission of the stellar disc). We thus set $V_{\rm d}^2(r) = (V_{\rm d}^{\rm deBlok}(r))^2 \frac{\Upsilon^{3.6}_{*,\rm fit}}{0.8}$. Then, we leave the *amplitude* of the disk contribution to the circular velocity (i.e. the disk mass) as a free parameter to be derived by fitting the RC. No results of the present paper will change by assuming any other models of the dIstribution of the stellar disk of NGC 3198 in de Blok et al. (2008) or in previous works.

The contribution from the bulge component is $V_{\rm b}(r)$. We follow de Blok et al. (2008) and we consider their 1-component model which accounts for this inner stellar component. Hence, $V_{\rm b}(r) = 0$ since the bulge is included in $V_{\rm d}^{\rm deBlok}(r)$.

The helium corrected contribution of the gaseous disk derived from the HI surface density distribution $V_{\rm g}(r)$ taken from Gentile et al. (2013). We notice that, thanks to the accuracy of the HI measurements and to the excellent knowledge of the distance of this galaxy, this component is derived here much better than in the majority of the spirals studied to resolve the core-cusp controversy.

The "luminous" component of the circular velocity of this galaxy is then well known, except for the value of the disk mass which contributes to putting NGC 3198 at the front line of DM research.

### 3.3.2 Dark matter

We define $V_{\rm DM}(r) = \int_0^r 4\pi\rho_{\rm DM}{\rm R}^2{\rm dR}$ as the contribution to $V(r)$ from the dark matter halo of the virial mass $M_{vir} = \frac{4}{3}\pi 100\rho_{crit}R_{vir}^3$ that could have a variety of density profiles. Here $\rho_{\rm DM}$ represents a DM halo density profile.

#### Burkert halo

The URC of galaxies and the kinematics of individual spirals (Salucci et al., 2007) points to dark haloes with a central constant-density core, in particular, to the Burkert halo profile (Burkert, 1995b; Salucci and Burkert, 2000a). The relative density distribution is given by

$$\rho_{\rm URC}(r) = \frac{\rho_0 r_{\rm c}^3}{(r + r_{\rm c})(r^2 + r_{\rm c}^2)} \tag{3.2}$$

where $\rho_0$ (the central density) and $r_{\rm c}$ (the core radius) are the two free parameters. The present data cannot distinguish these URC haloes from other *cored* profiles, for which $\lim_{r\to 0}\rho(r) = const.$

#### Navarro, Frenk and White (NFW) halo

In numerical simulations performed in the ($\Lambda$) CDM scenario of structure formation, Navarro et al. (1996b) found that virialized systems follow a universal DM halo profile. This is written as

$$\rho_{\rm NFW}(r) = \frac{\rho_{\rm s}}{(\frac{r}{r_s})(1 + \frac{r}{r_s})^2} \tag{3.3}$$

where $\rho_{\rm s}$ and $r_s$ are the characteristic density and the scale radius of the distribution, respectively. These two parameters can be expressed in terms of the virial mass $M_{\rm vir}$, the concentration parameter $c = \frac{R_{\rm vir}}{r_s}$, and the critical density of the Universe $\rho_{\rm crit} = 9.3 \times 10^{-30}{\rm g\,cm^{-3}}$. By using Eq. (3.3), we can write

$$\begin{aligned} \rho_s &= \frac{100}{3}\frac{c^3}{\log(1+c) - \frac{c}{1+c}}\,\rho_{\rm crit} \quad {\rm g\,cm^{-3}}, \\ r_s &= \frac{1}{c}\left(\frac{3\times M_{\rm vir}}{4\pi 100\rho_{\rm crit}}\right)^{1/3} \quad {\rm kpc}, \end{aligned} \tag{3.4}$$

where $c$ and $M_{\rm vir}$ are not independent. It is well known from simulations that a $c-M_{\rm vir}$ relationship emerges (Klypin et al., 2011; Bullock et al., 2001; Wechsler et al., 2002):

$$c \simeq 11.7 \left( \frac{M_{\rm vir}}{10^{11} M_{\odot}} \right)^{-0.075} . \tag{3.5}$$

We are testing the density profile of haloes made by collision-less cold dark matter particles. Variations in this scenario are not considered in this work, except one in Sect. 6.

## 3.4 Results from the $\chi^2$ fitting method

The mass modelling results for the Burkert and NFW profiles are shown in Figs (3.2) and (3.3), respectively. The URC Burkert halo gives an excellent fit (see Fig. 3.2) with a reduced chi-square value of $\chi^2 = 0.9$. The best-fit parameters are

$$\begin{aligned} \rho_0 &= (3.19 \pm 0.62) \times 10^{-25} \quad \mathrm{g\,cm^{-3}}; \\ r_{\rm c} &= (17.7 \pm 2.0) \quad \mathrm{kpc}; \\ \Upsilon_*^{3.6} &= (0.98 \pm 0.04). \end{aligned}$$

Then, we compute the mass of the stellar disk as

$$M_{\rm D} \simeq 1.1 \Upsilon_*^{3.6} (V_{\rm d})(R_{\rm l})^2 \frac{R_{\rm l}}{G} \tag{3.6}$$

where $V_{\rm d}(R_{\rm l})$ is the disk contribution to the circular velocity at the outermost radius $R_{\rm l} \approx 48$ kpc. This estimate is very solid and independent of the actual light profile in the inner part of the galaxy. We find $M_{\rm D} \simeq 4.4 \times 10^{10} M_{\odot}$ ($\approx 2$ times bigger than the values found by de Blok et al., 2008) with a propagated uncertainty of about ten percent. The corresponding virial mass and virial radius are $M_{\rm vir} = 5.8^{+0.4}_{-0.8} \times 10^{11} M_{\odot}$ and $R_{\rm vir} = 214^{+4}_{-11}$ kpc.The 1,2,3-$\sigma$ confidence regions for the best-fit parameters are shown in Fig. 3.4. The central points correspond to the best-fit values.

In the framework of the NFW mass models, we fitted data in terms of the free parameters: the virial mass, the concentration parameter and above defined the mass-to-light ratio ($M_{\rm vir}, c, \Upsilon_*^{3.6}$). The results of the best-fit are

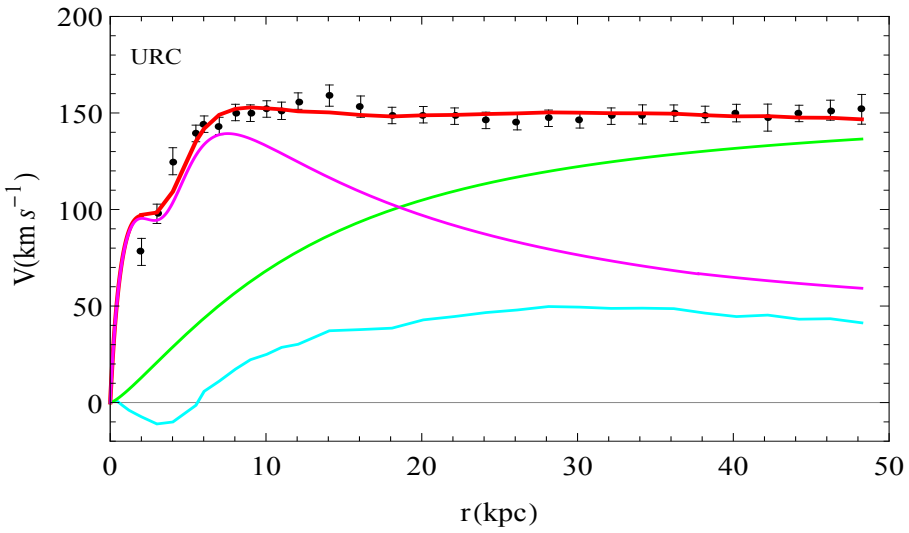


**Figure 3.2:** URC mass modelling of NGC 3198. Circular velocity data (filled circles with error bars) are modelled (thick red line) by the halo cored component (thick green line), the stellar disk (magenta line) and the HI disk (azure line).

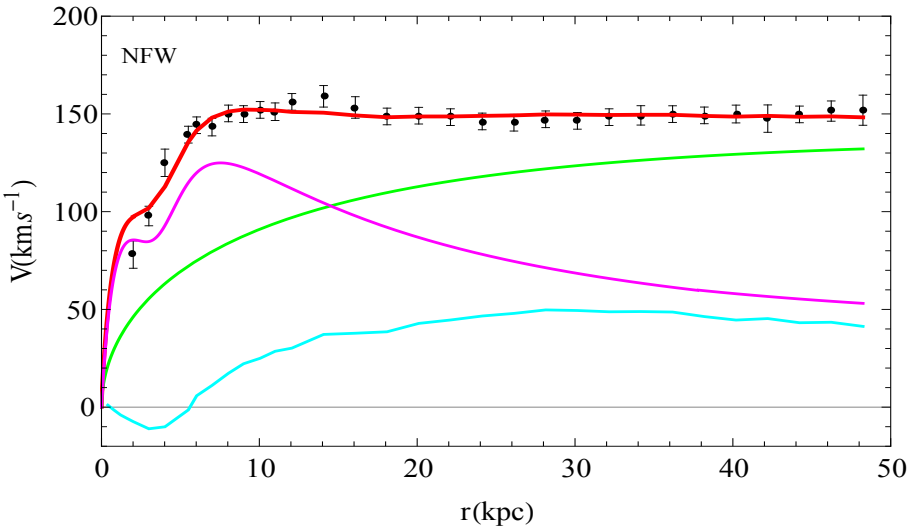


**Figure 3.3:** NFW mass modelling of NGC 3198. Circular velocity data (filled circles with error bars) are modelled (thick red line) by the stellar disk (magenta line), the NFW halo profile (green line) and the HI contribution (azure line).

$$
\begin{aligned}
M_{\rm vir} &= (8.9 \pm 2.1) \times 10^{11} \quad {\rm M}_\odot; \\
c &= (6.69 \pm 1.46); \\
\Upsilon_*^{3.6} &= (0.79 \pm 0.07).
\end{aligned}
$$

In this case the reduced chi-square is $\chi^2 = 0.8$, even slightly better value than found for the URC-halo model. The best-fit value of the concentration parameter $c = 6.69 \pm 1.46$ is found to be somewhat lower than what is expected from Eq. (3.5): $c_{\rm NFW} \approx 10 \pm 1$. It is worth recalling that in other galaxies, this discrepancy in the concentration parameter is much larger (see McGaugh et al., 2003; Salucci et al., 2010; Memola et al., 2011).

From Eq. (3.6) the disk mass, within a ten percent uncertainty, is $M_{\rm D} = 3.5 \times 10^{10} M_\odot$, a somewhat smaller value than found for the URC-halo model. The best-fit values of the scale radius and the characteristic density are $r_{\rm s} = (37.2 \pm 11.0)$ kpc and $\rho_{\rm s} = (8.0 \pm 4.1) \times 10^{-26}$ g cm$^{-3}$.

The 1,2,3-$\sigma$ best-fit parameters confidence regions are shown in Fig. 3.5. The central points correspond to the best-fit values that result somewhat higher or lower than the N-Body simulation outcome relative to a galaxy with $V_{max} \simeq 150$ km/s as NGC 3198. The discrepancy, however, is within 1.5 $\sigma$.

The standard mass modelling of the kinematical data of NGC 3198 is then not able to clearly select between a cored and a cuspy halo profile. In fact, in the case where a galaxy like NGC 3198 showing a flattish rotation curve over a wide range of radii, we have a modelling degeneracy: the same best-fit solution corresponds to very different mass models (see Appendix of Gentile et al., 2004).

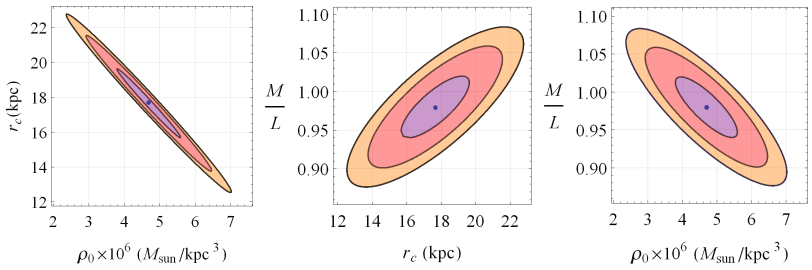


**Figure 3.4:** 1, 2, 3 $\sigma$ confidence ellipses (purple, red, orange, respectively) of the best-fit parameters in the Burkert halo case. The central points indicate the best-fitting values. $\frac{M}{L}$ is in the IRAC 3.6 $\mu$m band units.

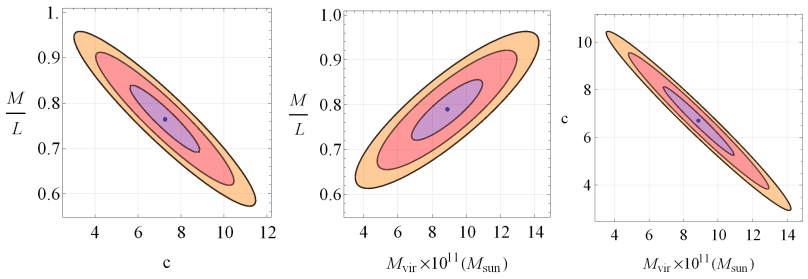


**Figure 3.5:** 1, 2, $3\sigma$ confidence ellipses (purple, red, orange, respectively) of the best-fit parameters in the NFW halo case. The central points indicate the best-fitting values. $\frac{M}{L}$ is in the IRAC 3.6 $\mu$m band units.

## 3.5 A new method of estimating the halo DM density and its results

A step forward in mass modelling spirals has come from the method of Salucci et al. (2010). This method was applied first to the Milky Way to derive the value of the DM density at the Sun's location. In this paper we are applying it, for the first time, to the outermost parts of an external galaxy. Our aim is to derive, for the spiral galaxy with the most extended kinematics, the DM density at large radii, where the influence of the stellar and HI disks is respectively negligible and known.

The idea underlying the Salucci et al. (2010) method is to resort to the equation of centrifugal equilibrium holding in spiral galaxies:

$$\frac{V^2}{r} = a_{\rm H} + a_{\rm D} + a_{\rm HI} \tag{3.7}$$

where $a_{\rm H}$, $a_{\rm D}$ and $a_{\rm HI}$ are the radial accelerations, generated, respectively, by the halo, stellar disk, and HI disk mass distributions. Within the approximation of spherical DM halo, we have

$$a_{\rm H} = 4\pi G r^{-2} \int_0^r \rho_H(r) r^2 \, dr. \tag{3.8}$$

Therefore, we compute the derivative of Eq. (3.7) by manipulating previous equations to get the DM density at any radius. We have

$$\rho_{\rm H}(r) = \frac{X_{\rm q}}{4\pi G r^2} \frac{d}{dr} \left[ r^2 \left( \frac{V^2(r)}{r} - a_{\rm D}(r) - \frac{V_{\rm HI}^2}{r} \right) \right] \tag{3.9}$$

where $X_{\rm q}$ is a factor correcting the spherical Gauss law used above in case of any oblateness of the DM halo. Since this value is very near to one, we assume $X_{\rm q} = 1$ (see details in Salucci et al., 2010).

Equation(3.9) gives a very good estimation of the density when the contribution from the luminous components is small. In short, to work well the new method requires a high-resolution, high-quality, and very extended kinematics for a spiral of known distance. Of course, we are interested in the region well outside $3R_D$.

For simplicity, we model the disk component as a Freeman stellar exponential, infinitesimally thin disk (Freeman, 1970) with the disk scale length $R_{\rm D} = 3.7$ kpc. No result in this paper will change by instead assuming the de Blok et al. (2008) disk mass profile, whose contribution to the circular velocity $V_D$ is given in Table 3.1. For $M_{\rm D}$ we use the URC mass modelling value: $M_{\rm D} \simeq 4.4 \times 10^{10} M_{\odot}$, and no result changes if assuming any other reasonable value for this quantity (see below).

The surface stellar density profile is given by

$$\Sigma(r) = \left(\frac{M_{\rm D}}{2\pi R_{\rm D}^2}\right) e^{-\frac{r}{R_{\rm D}}}. \tag{3.10}$$

We can write

$$a_{\rm D}(r) = \frac{GM_{\rm D}r}{R_{\rm D}^3}(I_0K_0 - I_1K_1) \tag{3.11}$$

where $I_{\rm n}$ and $K_{\rm n}$ are the modified Bessel functions computed at $r/(2R_{\rm D})$.

The HI disk component $V_{\rm g}(r)$ and its derivative are easily obtained from observations (Gentile et al., 2013). Finally, Eq. (3.9) becomes

$$\begin{aligned} \rho_{\rm H}(r) &= \frac{1}{4\pi G}\Big[\frac{V^2(r)}{r^2}(1+2\alpha(r)) - \frac{GM_{\rm D}}{R_{\rm D}^3}H\left(\frac{r}{R_{\rm D}}\right) \\ &- \frac{V_{\rm HI}^2(r)}{r^2}(1+2\gamma(r))\Big] \end{aligned} \tag{3.12}$$

where $2H\left(\frac{r}{R_{\rm D}}\right) = (3I_0K_0 - I_1K_1) + \frac{r}{R_{\rm D}}(I_1K_0 - I_0K_1)$ and $\alpha(r)$ and $\gamma(r)$ are the logarithmic slopes of the circular velocity and of the HI+He disk contribution to the latter, both of which known.

We stress that in galaxies with $V_d(3R_{\rm D}) \simeq V(3R_{\rm D})$, it is very difficult to use the standard mass modelling method to disentangle the circular velocity into its dark and luminous components and to obtain the DM density distribution out to $r \simeq 6R_{\rm D}$. Instead, the fundamental point of the present new method is that, for radii $r \gtrsim 3R_{\rm D}$ the second term of RHS of Eq. (3.12) always goes rapidly to zero becoming much smaller than the first and the third terms, both known. Then, by means of Eq. (3.12), we can immediately derive $\rho(r)$: the unknown term, proportional to the stellar disk mass becomes irrelevant as $r \gtrsim 3R_{\rm D}$. In Eq. (3.12), all terms have the dimensions of a density; specifically, the three terms of RHS can be considered as the *effective* density of the whole gravitating matter and the (sphericized) densities of the stellar and gaseous disks.

Thus, by means of Eq. (3.12) for $r \gtrsim 3R_{\rm D}$, we obtain a reliable dark matter density profile, the farther we get, the more precise the estimate becomes. In the range : $r \lesssim 3R_{\rm D}$, Eq. (3.12) still holds, but it cannot give information about the DM halo since this is very sub-dominant there. In this region, however, we can use the latter equation to derive the stellar disk mass. This estimate, however, may turn out to be somewhat uncertain because, in this inner region, the first term of the RHS of Eq. (3.12) has some observational errors; moreover, moderate errors in the measured value of the disk scale length can affect the third term. Incidentally, we notice that the distance of the galaxy must be known with good precision (as it is in NGC3198), because its uncertainty affects all three terms of the RHS in different ways.

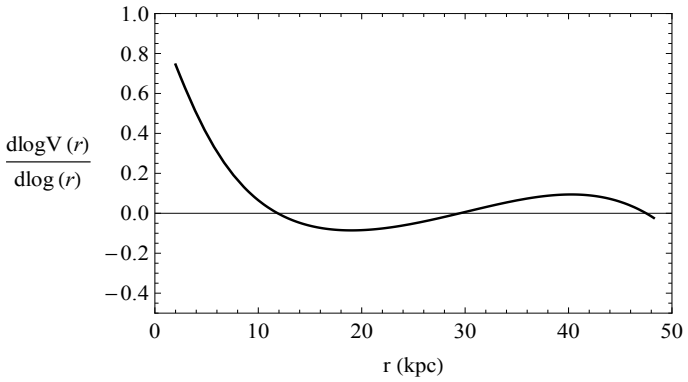


**Figure 3.6:** Logarithmic slope of the RC of NGC 3198.

In the case of NGC 3198 we take $\gamma(r) = 0$ for $r \gtrsim 3R_{\rm D}$, in order to simplify our calculations, since the gas contribution to the circular velocity, from $\sim 12$ kpc, is nearly constant (see Fig. 3.2). The logarithmic slope of the RC instead varies with radius (see Table 3.1), even at $r \sim 17$ kpc: we take $\mathrm{d}\log \mathrm{V(r)}/\mathrm{d}\log \mathrm{r}$ as in Fig. 3.6. In Fig. 3.7 we obtain the density profile of the dark halo. We list the values of the obtained DM profile

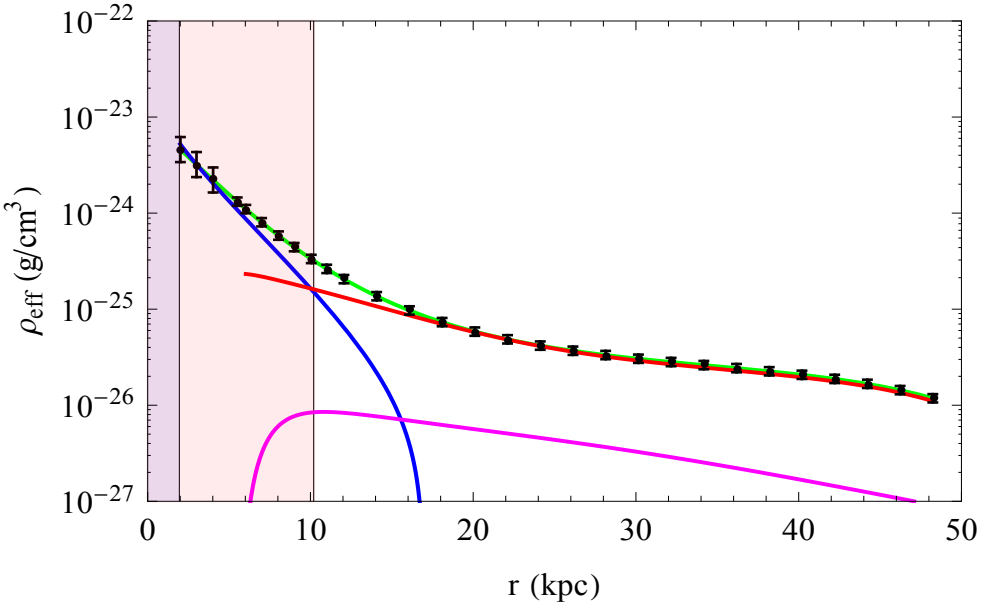


**Figure 3.7:** Density profile of the DM halo of NGC 3198 and the *effective* density of the other components. We assume $M_{\rm D} = 4.4 \times 10^{10} M_{\odot}$. The stellar disk (Blue line), the HI disk (magenta line), the dark halo (red line) and the sum of all components (green line). The different colour regions correspond to the regions a) where we do not have any kinematical information due to the lack of data (dark purple), b) where the stellar disk dominates the DM density profile (light purple) and c) where DM dominates (white).

starting from 5.5 kpc in Table 3.1. We see that the DM component starts to dominate the luminous components from $r \sim 10$ kpc; moreover, the stellar disk's contribution in the RHS of Eq. (3.12) goes further below the gravitating matter for $r \gtrsim 10$ kpc and to zero for $r \gtrsim 17$ kpc, independently of its mass. This means that, starting from $\sim 17$ kpc, the halo density profile, which obtained by means of Eq. (3.12), is virtually free from the uncertainty on the actual value of the disk mass, which usually plagues the standard mass modelling of RCs.

Next we discuss in detail the distribution of matter in the various regions of NGC 3198. In the innermost one, $r \lesssim 2$ kpc we do not have any kinematical information due to the lack of data. In the region extended from $\sim 2$ kpc to $\sim 10$ kpc, the stellar component dominates over the DM component. No direct information on the latter can be extracted here. In this region, however, we can use the fair agreement between the stellar and the dynamical density (as defined in Eq. (3.12)) to derive the value of $M_D$.

For $r \gtrsim 17$ kpc, the DM density is directly obtained by means of Eq. (3.12) see Fig. 3.7. Here, all quantities entering in Eq. (3.12) are known within a small uncertainty, and

this leads to a robust determination of $\rho(r)$.

The effect of the uncertainty in the value of the disk mass in the determination of $\rho(r)$ is shown well in Fig. 3.8. We now do not take a specific value for $M_D$, and we derive the DM density profiles through Eq. (3.12) by assuming different values for the disk mass. We see that the Salucci et al. (2010) method leads to a family of density profiles that all agree outside the stellar disk (i.e. for $r \gtrsim 3R_{\rm D}$), independently of the corresponding value of the disk mass (see the zoomed area in Fig. 3.9) .

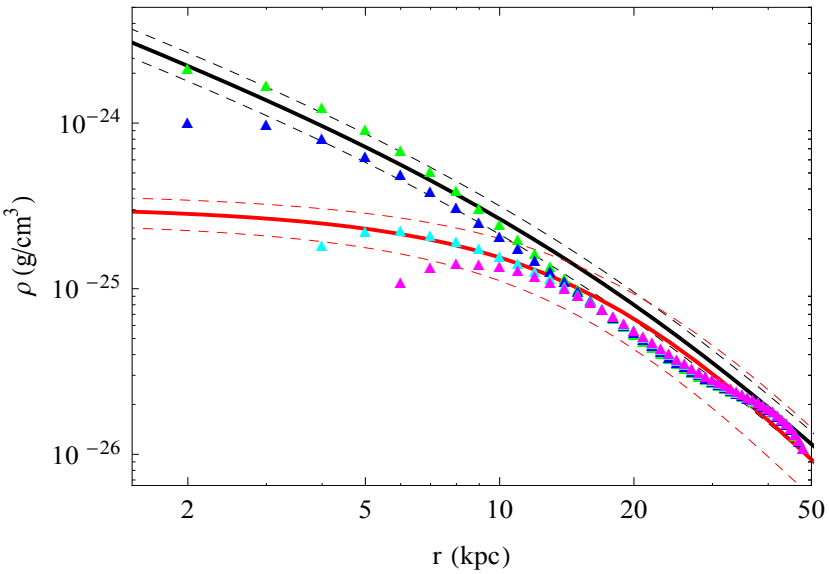


**Figure 3.8:** DM density profiles for different disk mass values $M_{\rm D} = n \times 10^{10} M_\odot$ and n=2,3,4.4,5 from the highest to the lowest curve (green, blue, azure and magenta triangles). The black solid line shows the NFW density profile with $M_{\rm vir} = 8.9 \times 10^{11} M_\odot$ corresponding to the best fit values found in the previous section. Two black dashed lines show the NFW density profiles taking $1\sigma$ uncertainties in $M_{\rm vir}$ and 10 percent of uncertainties in $c$ into account. The URC halo is shown as Red solid line. Two Red dashed lines show the URC density profiles obtained by taking $1\sigma$ uncertainties in $\rho_0, r_{\rm c}$ into account.

We compare the derived DM density with the URC and the NFW profiles, see Fig. 3.8. In the first case, the derived density bears no difference with that obtained by means of the first method, i.e. with Eqs.(3.1) and (3.2). We therefore found $M_D = (4.4 \pm 1.0) \times 10^{11} M_\odot$. This is also evident in the zoomed area of Fig. 3.8 (see Fig. 3.9). In external regions of the NGC 3198, the Salucci et al. (2010) method yields a halo that is compatible with the URC halo, as derived by chi-square fitting of the RC of NGC 3198.

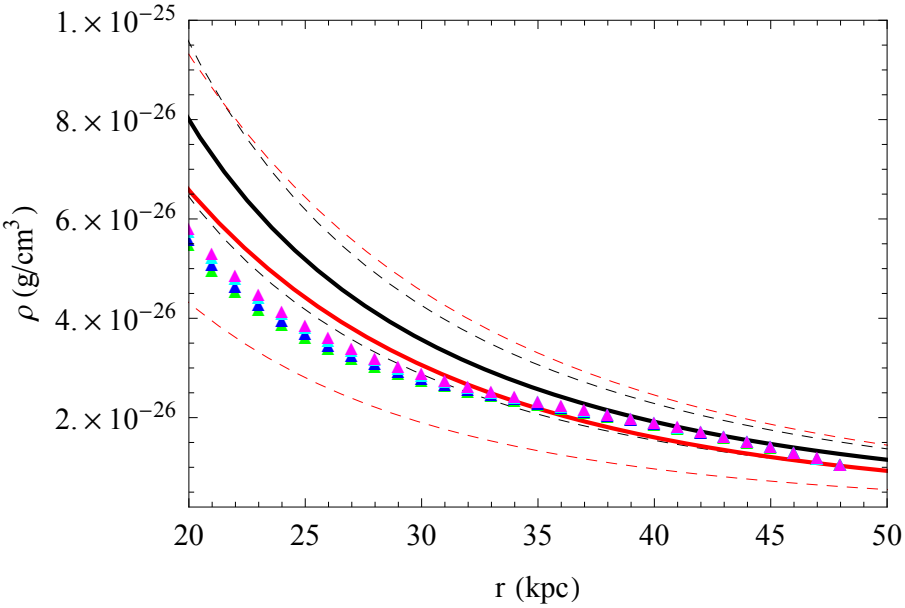


**Figure 3.9:** Zoom of Fig. 3.8 on linear scales.

For NFW haloes the situation is very different. First, in Fig. 3.9 we realize that, independently of the disk mass we assume, the best-fit NFW halo profile is in poor agreement with the derived density. We consider this fault only as a hint and not as a definitive evidence against a NFW halo. Within the new modelling method, we derive the value of $c$ and $M_{\rm vir}$ and their uncertainties by evaluating, from Eqs.(3.3), (3.4), and (3.12), the DM density (and its uncertainties) at the radius $r = 45$ kpc (where the stellar disk certainly does not contribute to the gravitating matter density profile). A more serious problem appears when we realize that the resulting values of the halo parameters $M_{\rm vir}$ and $c$ are very different from the ones derived by means of the standard method applied in the previous section. In fact, for the virial mass and the concentration parameters we get $M_{\rm vir} = (8.9 \pm 2.1) \times 10^{11} M_{\odot}$, $c = 6.69 \pm 1.46$.

In Fig. 3.10 we plot the two solutions for $(c - M_{\rm vir})$ with their uncertainties. We now compare these values of the concentration parameter and the virial mass $(c - M_{\rm vir})$ obtained by each of the mass modelling techniques also in light of the $(c - M_{\rm vir})$ relationship that emerged from numerical simulation (see Eq. (3.5)). They agree only for values of $c$ that are much lower than those emerging in numerical simulations and for values of $M_{\rm vir} > 9 \times 10^{11} M_{\odot}$ far too high for this spiral galaxy which has $V_{\rm max} \lesssim 150$ km/s.

In short, by assuming a NFW halo in NGC 3198, we have two completely *different* solutions for its structure parameters, according to whether one adopts the local or the global method of mass modelling. The best intersection of these sets of results is in total

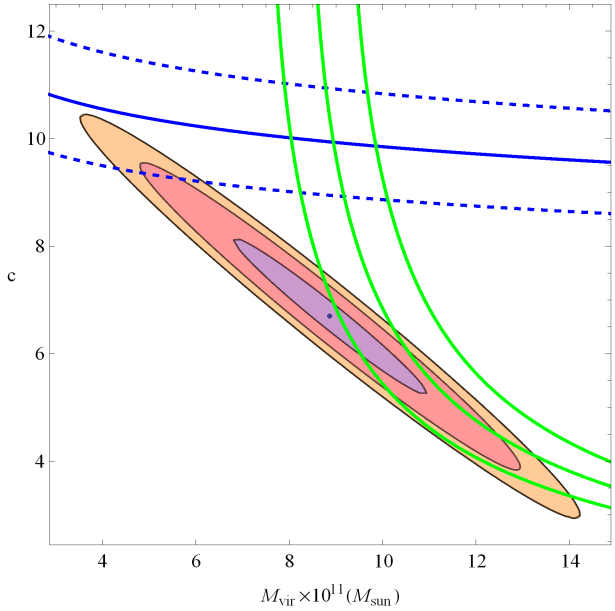


**Figure 3.10:** NFW case: the 1,2,3 - $\sigma$ (purple region, red region and orange region, respectively) confidence ellipses for the global best-fit parameters. The blue solid line shows the $c - M_{\rm vir}$ relation from numerical simulations, the dashed blue lines show its 10 percent uncertainty. The Green region shows the $c - M_{\rm vir}$ relation from the local density values obtained by the Salucci et al. (2010) method taking the 10 percent uncertainty into account.

disagreement with the properties of the simulated haloes in the N-body ΛCDM scenario. Noticeably, the problem for NFW haloes is different here and, if possible, more serious than that of the core-cusp discrepancy, usually occurring at $\sim 0.05 R_{\rm vir}$ (Donato et al., 2009b). We found, in fact, that the density of the DM halo around NGC 3198 is not very consistent with the NFW profiles well out to $0.22 R_{\rm vir}$.

Of course, NFW haloes emerge out of DM only simulations in the leading ΛCDM scenario. However, this scenario actual haloes around galaxies may have undergone a compression by the stellar disk during the formation of the latter (e.g. Gnedin et al., 2004; Katz et al., 2014) and/or suffered a baryonic feedback during the subsequent history of the galaxy (Di Cintio et al., 2014a). These processes could have modified the DM haloes original distribution. Furthermore, haloes today around galaxies, can be born within a different cosmological scenario like Warm or Self-Interacting DM, in which a NFW profile is not established (e.g. de Vega et al., 2014a).

In spite of that, in this section we focused on the failure of the NFW halo profile because: a) it is important to fully expose the discrepancy between the density distribution of the dark haloes around galaxies and the predictions of the simplest dark particle

scenario; b) NFW haloes are still used often to investigate important Cosmological issues in the belief that the discrepancy with actual galaxy haloes, though present, does not have much physical relevance; c) de facto, several cosmological investigations have been carried out considering that there is no discrepancy at all.

It goes without saying that the failure of NFW profiles is not the demise of the ΛCDM scenario (see next section).

## 3.6 Testing (Λ)CDM halo profiles modified by the physics of stellar disk formation

A line of thought holds that the cosmological core-cusp problem (CCCP) can be addressed by considering the present DM haloes around galaxies like NGC 3198 as very different with respect to those emerging out of N-body simulations. In fact, the formation and the growth in them of stellar disks and the related numerous and powerful supernova explosions could have modified the original N-body profile, by making it shallower and more in agreement with observations. We stress that such a dissolution of the CCCP is rarely studied.

One exception is the work by Di Cintio et al. (2014a) based on the analysis of hydrodynamically simulated galaxies drawn from the MaGICC project (Brook et al., 2012a; Stinson et al., 2013a). They did find, at the end of these simulations, that DM haloes had a completely new family of profiles, a generic double power-law density profile (Di Cintio et al., 2014a). This was found to vary in a systematic manner in the stellar-to-halo mass ratio of each galaxy.

The mass-dependent density profile was derived by analysing hydrodynamical cosmological simulations. This profile (hereinafter referred to as DC14) accounts for the effects of feedback on the DM haloes due to gas outflows generated in high density star-forming regions during the history of the stellar disk. The resulting radial profile is far from simple, since it starts from an $(\alpha, \beta, \gamma)$ double power-law model (see Di Cintio et al., 2014a)

$$\rho_{\rm DC14}(r) = \frac{\rho_s}{(\frac{r}{r_s})^{\gamma}\left(1+(\frac{r}{r_s})^{\alpha}\right)^{\frac{(\beta-\gamma)}{\alpha}}} \tag{3.13}$$

where $\rho_s$ is the scale density and $r_s$ the scale radius. The inner and the outer regions have logarithmic slopes $-\gamma$ and $-\beta$, respectively, and $\alpha$ indicates the sharpness of the

transition. These three parameters are fully constrained in terms of the stellar-to-halo mass ratio as shown in Di Cintio et al. (2014a):

$$\begin{aligned} \alpha &= 2.94 - \log_{10}[(10^{X+2.33})^{-1.08} + (10^{X+2.33})^{2.29}] \\ \beta &= 4.23 + 1.34X + 0.26X^2 \\ \gamma &= -0.06 + \log_{10}[(10^{X+2.56})^{-0.68} + (10^{X+2.56})] \end{aligned} \tag{3.14}$$

where $X = \log_{10}\left(\frac{M_{star}}{M_{halo}}\right)$.

The concentration parameter of the halo is $c = \frac{R_{\rm vir}}{r_s}$. An alternative definition, adopting the radius $r_{-2}$, is $c_{\rm DC14} = \frac{R_{\rm vir}}{r_{-2}}$, where $r_{-2}$ is the radius at which the logarithmic density slope of the profile is -2. This definition allows defining the same physical $r_s$ for different values of $(\alpha, \beta, \gamma)$

$$r_{-2} = \left(\frac{2-\gamma}{\beta-2}\right)^{\frac{1}{\alpha}} r_s. \tag{3.15}$$

Following Di Cintio et al. (2014a), we reach the relation between the concentration parameter in the hydrodynamical simulations and the N-body haloes as a function of the stellar-to-halo mass ratio:

$$c_{\rm DC14} = (1.0 + 0.00003e^{3.4(X+4.5)}) \times c_{\rm NFW}. \tag{3.16}$$

Using the definition of the enclosed mass, we can write down the expression for the scale density of the DC14 profile:

$$\rho_s = \frac{M_{\rm vir}}{4\pi \int_0^{R_{\rm vir}} \frac{r^2}{(\frac{r}{r_s})^\gamma [1+(\frac{r}{r_s})^\alpha]^{\frac{\beta-\gamma}{\alpha}}} {\rm dr}}. \tag{3.17}$$

To reduce the number of free parameters of the DC14 profile, it is necessary to adopt a value for the concentration parameter of the original NFW halo. For our purpose and since this quantity depends extremely weakly on the virial mass, we can adopt: $c_{\rm NFW} = 10$. By bringing together all the above equations of this section and noticing that $R_{\rm vir} = c_{\rm DC14} r_{-2}$,

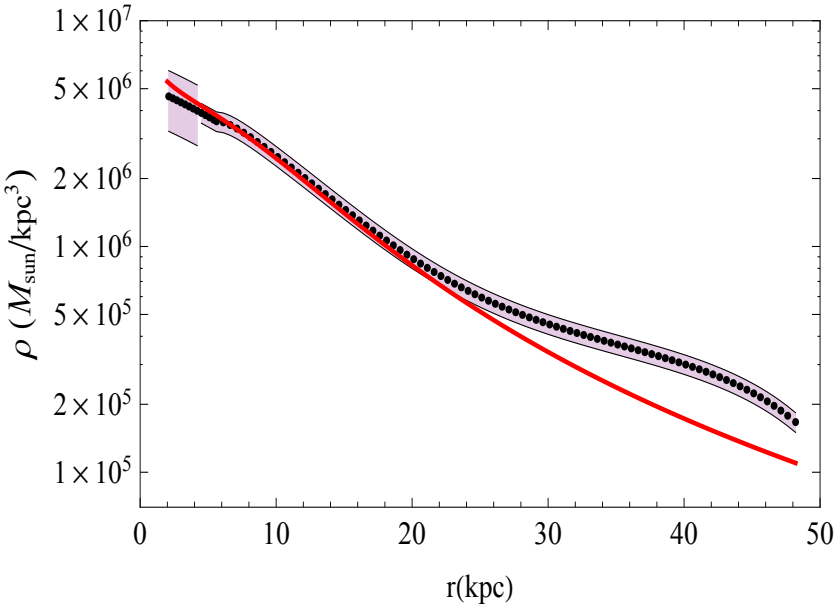


**Figure 3.11:** Observed DM halo density profile (black points) of NGC 3198 and the obtained errors by the error propagation analysis (purple area). Di Cintio et al. (2014a) mass-dependent model predictions (red line).

we can rewrite Eq. (4.12) just as a function of the scale radius and the stellar-to-halo mass ratio.

With this density profile, we can attempt a two-free parameter $(X, r_s)$ fit of the *derived* halo density profile of the NGC 3198 (Fig. 3.7). The result is in Fig. 3.11, the best-fit parameters are:

$$\begin{aligned} X &= -2.6; \\ r_s &= 12.2\text{kpc}. \end{aligned}$$

The inferred virial radius is $R_{\rm vir} \simeq 235$kpc and virial mass is $M_{\rm vir} \simeq 7.7 \times 10^{11} \mathrm{M}_{\odot}$. As result, the CCCP is only partially resolved, and the DM core we detect in NGC 3198 can be explained as an effect of the energy that, in different ways, stars have injected in the galactic ambient. However, in the outer densities of the dark halo derived for the first time in this study, there are features that may conflict with the N-body simulation predictions that should be recovered at $R > 25$ kpc from the centre of NGC 3198.

## 3.7 Conclusions

Galaxies with a flattish rotation curve between 5 kpc to 50 kpc (e.g. the spiral NGC 3198, for many years the flagship of the evidence of the DM in galaxies) amount to only a few percent of the total number of disk systems. However, they play a crucial role in the core-cusp issue of the DM density. In fact, these "flat" RCs can be well fitted by either a cored DM halo or a cuspy DM halo, just by adjusting the amount of the stellar matter content. In contrast, in spirals in which $|\mathrm{d}\log \mathrm{V(r)}/\mathrm{d}\log \mathrm{r}|$ is significantly far from zero, this quantity constraints the distribution of DM, usually towards a cored one (Gentile et al., 2005).

NGC 3198 is a special galaxy. The HI disk of this galaxy is very extended out to $\sim$ 13 disk scale lengths or out to $\sim 0.22\ R_{\rm vir}$. Furthermore, for the innermost region, many complementary optical kinematical measurements are available. This object (of known distance of 13.8 Mpc) shows a spectacular evidence of a dark force in action: baryons of this galaxy are clearly unable to account for its (very extended) kinematics. We must assume that a large part of the circular velocity of NGC 3198 is due to a DM halo. In addition, the circular velocity of this galaxy is at variance with the MOND paradigm Gentile et al. (2013), while it seems plausible within the f(R) scenario (see Salucci et al., 2014). It is then obvious that to resolve the core-cusp issue in NGC 3198 is of particular importance.

To do so, we used the old optical and new HI kinematics performed in the HALOGAS survey in combination with a new method of mass modelling a rotation curve. First, we verified that with the standard $\chi^2$ mass modelling of the RC, both URC Burkert and the NFW dark halo models fit the available data well. Then, once assured of the conditions of its applicability, we used the new refined method developed by Salucci et al. (2010) to determine the DM halo density of NGC 3198. This result is inconsistent with the NFW haloes predictions, independently of any assumption about the luminous component we can take. Moreover, the derived density profile strongly supports a cored distribution of DM, adding independent evidence to the idea of cored DM distribution in galaxies.

Today, within the $\Lambda$CDM scenario, NFW haloes are often still assumed, although it has been recognized that in this scenario the actual DM halo density is not the one emerging from cosmological N-body simulations. In fact, it has been agreed that they have been modified by the subsequent baryonic physics, leading to stellar disk formation and evolution. Di Cintio et al. (2014a) have simulated this important phase of the history of spirals and found the emerging profiles of dark matter haloes. This baryonic $\Lambda$CDM halo profile prediction fits the detected halo of NGC 3198 very well, especially in its cored region. At very large distances, 25 kpc, however, the DM halo density derived here results

in a clash; i.e., it is significantly *higher* than the outcome of the hydrodynamic N-body ΛCDM simulations. This disagreement is not an isolated one (see Gentile et al., 2007c).

# Chapter 4

# The universal rotation curve of dwarf disk galaxies

As it was introduced in our Chapter 1 the dwarf galaxies are the key objects to study the dark matter distribution. In this Chapter we use the concept of the spiral rotation curves universality (see Persic et al., 1996) to investigate the luminous and dark matter properties of the dwarf disk galaxies in the Local Volume (size $\sim$ 11 Mpc). Our sample includes 36 objects with rotation curves carefully selected from the literature. We find that, despite the large variations of our sample in luminosities ($\sim$ 2 of dex), the rotation curves in specifically normalized units, look all alike and lead to the lower-mass version of the universal rotation curve of spiral galaxies found in Persic et al. (1996).

We mass model $V(R/R_{opt})/V_{opt}$, the double normalized universal rotation curve of dwarf disk galaxies: the results show that these systems are totally dominated by dark matter whose density shows a core size between 2 and 3 stellar disk scale lengths. Similar to galaxies of different Hubble Types and luminosities, the core radius $r_0$ and the central density $\rho_0$ of the dark matter halo of these objects are related by $\rho_0 r_0 \sim 100 M_{\odot} pc^{-2}$.

The structural properties of the dark and luminous matter emerge very well correlated. In addition, to describe these relations, we need to introduce a new parameter, measuring the compactness of light distribution of a (dwarf) disk galaxy. These structural properties also indicate that there is no evidence of abrupt decline in the baryonic to halo mass relation at the faint end of spiral disks.

## 4.1 Introduction to the problem

Let us recall that although the well known (Λ)CDM scenario is successful in describing the large structure of the Universe, at the galactic scales, this scenario has significant challenges. We will shortly describe these challenges below (for more details see Chapter 1).

Firstly, the apparent mismatch between the number of the detected satellites around the Milky Way and the predictions of the corresponding simulations, known as the "missing satellite problem" (Klypin et al., 1999; Moore et al., 1999), which also occurs in the field galaxies (Zavala et al., 2009; Papastergis et al., 2011; Klypin et al., 2015). This discrepancy widens up when the masses of the detected satellites are compared to those of the predicted subhalos (i.e. "too big to fail problem") (see Boylan-Kolchin et al., 2012; Ferrero et al., 2012; Garrison-Kimmel et al., 2014a; Papastergis et al., 2015).

Furthermore, there is the "core-cusp" controversy: the inner DM density profiles of galaxies generally appear to be cored, and not cuspy as predicted in the simplest (Λ)CDM scenario (e.g., Salucci, 2001; de Blok and Bosma, 2002a; Gentile et al., 2005; Weinberg et al., 2013; Bosma, 2004; Simon et al., 2005; Gentile et al., 2004, 2007c; Donato et al., 2009a; Oh et al., 2011, to name few).

These apparent discrepancies between the observations and the predictions of the DM-only simulations suggest to either abandon the (Λ)CDM scenario in favour of the others: (e.g., selfinteracting DM Vogelsberger et al., 2014; Elbert et al., 2015 or warm DM de Vega and Sanchez, 2013; de Vega et al., 2013; Lovell et al., 2014; de Vega et al., 2014b) or upgrade the role of baryonic physics in the galaxy formation process by including strong gas outflows, triggered by stellar and/or AGN feedback that are thought to strongly modify the original (Λ)CDM halo profiles out to a distance as large as the size of the stellar disk (e.g., Navarro et al., 1996a; Read and Gilmore, 2005; Mashchenko et al., 2006; Pontzen and Governato, 2012, 2014; Di Cintio et al., 2014b).

Although these issues are present in galaxies of any luminosity, however in low luminosity systems they emerge more clearly and appear much more difficult to be resolved within the ΛCDM scenario. Galaxies with I-band absolute magnitude $M_I \gtrsim -17$ play a pivotal role since observationally, these objects are dark matter dominated at all radii while, theoretically, they may be related to the building blocks of more massive galaxies. It is well known the importance of dwarf spheroids in various DM issues (see, e.g., Gilmore et al., 2007). However, down to $M_I \sim -11$ there is no shortage of disk systems, although a systematic investigation is lacking. These rotationally supported systems have a rather simple kinematics suitable for investigating the properties their dark matter content.

In normal spirals, one efficient way to represent and model their rotation curves (RCs) comes from the concept of a universal rotation curve (URC), i.e. a single function of the total galaxy luminosity and of a characteristic radius of the luminous matter[1] distribution which represents the RCs of all spirals.

This concept, implicit in Rubin et al. (1985), pioneered by Persic and Salucci (1991), set by Persic et al. (1996) (PSS, Paper I) and extended to large galactocentric radii by Salucci et al. (2007) has provided us the mass distribution of (normal) disk galaxies in the magnitude range $-23.5 \lesssim M_I \lesssim -17$[2]. This curve, therefore, encodes all the main structural properties of the dark and luminous matter of every spiral (PSS, Yegorova and Salucci, 2007). In this Chapter, we work out to extend RCs universality to any disk systems and then, to use it to investigate the DM distribution in dwarf disk galaxies.

Noticeably, for this population of galaxies the approach of stacking the available kinematics is very useful. In fact, presently, for disk systems with the optical velocity $V_{opt} \lesssim 61 km/s$, some kinematical data have become available. However, still there are not enough individual *high quality high resolution extended* RCs to provide us with a solid knowledge of their internal distribution of mass. Instead, we will prove that the 36 selected in literature *good quality good resolution reasonably extended* RCs (see below for these definitions), once coadded, provide us with a reliable kinematics yielding to their mass distribution.

In this work, we construct a sample of dwarf disks from the Local Volume catalog (LVC) (Karachentsev et al., 2013, hearafter K13), which is $\sim$ 70% complete down to $M_B \approx -14$ and out to 11 Mpc, with the distances of galaxies obtained by means of primary distance indicators.

Using LVC, we go more than 3 magnitudes fainter with respect to the sample of spirals of PSS. Moreover the characteristics of the LVC guarantee us against several luminosity biases that may affect such faint objects. The total number of objects in this catalog is $\sim$900 of which $\sim$ 180 are dwarf spheroidal galaxies, $\sim$ 500 are dwarf disk galaxies and the rest are ellipticals and spirals. We stress that, according to the current cosmological paradigm, studying the nearest galaxies provides an observational window on high redshift galaxy evolution that even the next generation of high redshift galaxy surveys will not be able to provide. For example, Boylan-Kolchin et al. (2016) explored how the Local Group ($\sim$ 2 Mpc diameter) might be representative of its ancestors in the proto-Local-Group at high redshift ($z \sim 7$). The authors concluded that the Local Group dwarfs are expected to provide a direct window to low-mass systems in the high-redshift University.

[1] i.e. optical radius $R_{opt}$ defined as the radius encompassing 83 % of the total luminosity.

[2] Extensions of the URC to other Hubble types are investigated in Salucci and Persic (1997); Noordermeer et al. (2007).

All our galaxies are low mass bulgeless disk systems in which the rotation corrected for the pressure support totally balances the gravitational force. Morphologically, they can be divided into two main types: gas-rich dwarfs that are forming stars at a relatively-low rate, named irregulars (Irrs) and starbursting dwarfs that are forming stars at an unusually high rate, named blue compact dwarfs (BCD). The dwarf Irr galaxies are named "irregulars" due to the fact that they usually do not have a defined shape and the star formation is not organized in spiral arms. However, some gas-rich dwarfs can have diffuse, broken spiral arms and be classified as late-type spirals (Sd) or as a Magellanic spiral (Sm). The starbursting dwarfs are classified as BCD due to their blue colours, high surface brightness and low luminosities. Notice that it is not always easy to distinguish among these types since the galaxies we are considering often share the same parameters space for many structural properties (e.g., Kormendy, 1985; Binggeli, 1994; Tolstoy et al., 2009).

In this work, we neglect the morphology of the baryonic components as far they are in rotating disks; the identifiers of a galaxy are $V_{opt}$, its disk length scale $R_D$ and its $K$-band magnitude $M_K$ that can be substituted by its disk mass. We refer to disk systems of any morphologies and $M_K \gtrsim -18$ as dwarf disks (DD).

In order to compare galaxy luminosities in different bands, we write down the DD relation between the magnitudes in different bands $< B-K > \simeq 2.35$ (Jarrett et al., 2003) and $< B-I > \simeq 1.35$ (Fukugita et al., 1995).

The plan of this Chapter is in following: in Section 4.2 we describe the sample that we are going to use; in Section 4.3 we introduce the analysis used to build the synthetic RC; in Section 4.4 we do the mass modelling of the synthetic RC; in Section 4.5 we introduce the results of the mass modelling and we denormalize it in order to describe individually our sample of galaxies; in Section 4.6 we introduce a new quantity, which we call "compactness"; in Section 4.7 we discuss our main results.

## 4.2 The sample

We construct our (DD) sample out of the LVC (Karachentsev et al., 2013) by adopting the following 4 selection criteria:

1. We include disk galaxies with the optical velocity less than $\sim 61\ km/s$ (disk systems with larger velocity amplitude are studied in PSS);

2. The rotation curves extend to at least 3.2 disk scale lengths [1]. However, we allowed ourselves to extrapolate modestly the RCs of UGC1501, UGC8837, UGC5272 and IC10 due to their smoothness;

[1] $R_{opt} \simeq 3.2 R_D$

3. The RCs are symmetric, smooth and with an average internal uncertainty lesser than 20 %;

4. The galaxy disk length scale $R_D$ and the inclination function $1/\sin i$ are known within 20 % uncertainty.

It is worth noticing that for a RC to fulfil criteria (2), (3) and (4) it is sufficient to qualify it for the *coaddition* procedure but not necessarily it is so for the *individual* modelling.

The kinematical data used in our analysis are HI and $H_\alpha$ rotation curves available in the literature (see Table 4.1), which are corrected for inclination and instrumental effects. Furthermore, circular velocities of low mass galaxies, with $V_{max} \lesssim 50\,km/s$, require to be checked for the pressure support correction, the latter can be done using the so-called "asymmetric drift correction" (Dalcanton and Stilp, 2010). Therefore, most of the RCs in our sample either have the asymmetric drift correction applied (the ones chosen Oh et al., 2011, 2015; Lelli et al., 2014; Gentile et al., 2010, 2012) or pressure support has been determined and is too small to affect the RC (those coming from Swaters et al., 2009; Weldrake et al., 2003; Karachentsev et al., 2016). Although, we leave three galaxies (UGC1501, UGC5427 and UGC7861) for which circular velocities were not corrected. However, their $V_{max}$ are larger than 50 $km/s$, therefore the effect should be minor. In the innermost regions of galaxies, when available, we use also $H_\alpha$ data not corrected for the asymmetric drift since such term is negligible as it was pointed out by e.g. Swaters et al. (2009); Lelli et al. (2012).

**Table 4.1:** sample of dwarf disk galaxies. Columns: **(1)** galaxy name; **(2)** galaxy distance; **(3)** rotation curve source; **(4)** exponential scalelength of a galaxy stellar disk; **(5)** disk scalelenght source; **(6)** rotation velocity at the optical radius; **(7)** absolute magnitude in K-band.

| Name | D | RCs refs | $R_D$ | $R_D$ refs | $V_{opt}$ | $M_K$ |
|---|---|---|---|---|---|---|
| — | Mpc | — | kpc | — | km/s | mag |
| (1) | (2) | (3) | (4) | (5) | (6) | (7) |
| | | $H_\alpha$; HI | | | | |
| UGC1281 | 4.94 | 1; 2 | 0.99 | a | 53.8 | -17.97 |
| UGC1501 | 4.97 | 1; - | 1.32 | a | 50.2 | -18.19 |
| UGC5427 | 7.11 | 1; - | 0.38 | e | 54.0 | -17.06 |
| UGC7559 | 4.88 | -;2, 3 | 0.88 | b | 37.4 | -16.91 |
| UGC8837 | 7.21 | -; 2 | 1.55 | b | 47.6 | -18.25 |
| UGC7047 | 4.31 | -; 2,4 | 0.57 | c | 37.0 | -17.41 |
| UGC5272 | 7.11 | -; 2 | 1.28 | b | 55.0 | -16.81 |

| | | | | | | |
|---|---|---|---|---|---|---|
| DDO52 | 10.28 | -; 3 | 1.30 | b | 60.0 | -17.69 |
| DDO101 | 16.1 | -; 3 | 0.94 | b | 58.8 | -19.01 |
| DDO154 | 4.04 | -; 3 | 0.75 | b | 38.0 | -15.70 |
| DDO168 | 4.33 | -; 3 | 0.83 | b | 60.0 | -17.07 |
| Haro29 | 5.68 | -; 3,4 | 0.28 | b | 32.6 | -16.26 |
| Haro36 | 8.9 | -; 3 | 0.97 | h | 56.5 | -17.63 |
| IC10 | 0.66 | -; 3 | 0.38 | b | 41.0 | -17.59 |
| NGC2366 | 3.19 | -; 3,4 | 1.28 | b | 55.0 | -18.38 |
| WLM | 0.97 | -; 3 | 0.55 | b | 33.0 | -15.93 |
| UGC7603 | 8.4 | -; 2 | 1.11 | 2 | 60.3 | -19.07 |
| UGC7861 | 7.9 | -; 5 | 0.62 | i | 61.0 | -19.74 |
| NGC1560 | 3.45 | -; 6 | 1.10 | 6 | 56.1 | -18.43 |
| DDO125 | 2.74 | 1; 2 | 0.49 | c | 17.0 | -16.96 |
| UGC5423 | 8.71 | 1; 3 | 0.52 | d | 27.5 | -17.71 |
| UGC7866 | 4.57 | -; 2 | 0.54 | 2 | 28.7 | -17.18 |
| DDO43 | 5.73 | -; 2 | 0.57 | b | 35.3 | -15.72 |
| IC1613 | 0.73 | -; 3 | 0.60 | b | 19.0 | -16.89 |
| UGC4483 | 3.21 | -; 4 | 0.16 | f | 20.8 | -14.20 |
| KK246 | 7.83 | -; 9 | 0.58 | 9 | 34.6 | -16.17 |
| NGC6822 | 0.5 | -; 10 | 0.56 | b | 35.0 | -17.50 |
| UGC7916 | 9.1 | -; 2 | 1.63 | h | 37.0 | -16.22 |
| UGC5918 | 7.45 | -; 2 | 1.23 | 2 | 45.0 | -17.50 |
| AndIV | 7.17 | -;11 | 0.48 | 11 | 32.2 | -14.78 |
| UGC7232 | 2.82 | -; 2 | 0.21 | f | 37.0 | -16.46 |
| DDO133 | 4.85 | -; 3 | 0.9 | g | 42.4 | -17.31 |
| UGC8508 | 2.69 | 1; 3 | 0.28 | j | 25.5 | -15.58 |
| UGC2455 | 7.8 | -; 2 | 1.06 | h | 47.0 | -19.91 |
| NGC3741 | 3.03 | -; 7 | 0.18 | c | 22.0 | -15.15 |
| UGC11583 | 5.89 | -; 8 | 0.17 | 8 | 52.2 | -16.55 |

**Notes.** RC & $R_D$ references: Moiseev (2014)-1, Swaters et al. (2009)-2, Oh et al. (2015)-3, Lelli et al. (2014)-4, Epinat et al. (2008)-5, Gentile et al. (2010)-6, Gentile et al. (2007c)-7, Begum and Chengalur (2004)-8; Gentile et al. (2012)-9, Weldrake et al. (2003)-10, Karachentsev et al. (2016)-11, van Zee (2001)-a, Hunter and Elmegreen (2004)-b, Sharina et al. (2008)-c, Parodi et al. (2002)-d, Simard et al. (2011)-e, Martin (1998)-f, Hunter et al. (2011)-g, Herrmann et al. (2013)-h, Yoshino and Yamauchi (2015)-i, Hunter et al. (2012)-j. Distance $D$ and absolute magnitude in K-band $M_K$ are from Karachentsev et al. (2013).

We stress that the above selection process has left out few objects whose RCs are sometimes considered in literature, e.g. the RC of DDO 70 described by Oh et al. (2015) has failed our criteria (3) because of its abnormal shape. Our approach stands firmly that, in order to provide us with proper and correct information about a galaxy dark and luminous mass distribution, the relative kinematical and the photometric data must reach a well defined level of quality, otherwise they will be confusing rather that enlightening the issue.

Therefore, we ended with the final sample of 36 galaxies spaning the magnitude and disk radii intervals, $-19 \lesssim M_I \lesssim -13$, $0.18\,kpc \lesssim R_D \lesssim 1.63\,kpc$ and the optical velocities $17\,km/s \lesssim V_{opt} \lesssim 61\,km/s$ (see Table 3.1, the references for HI and H$\alpha$ RCs of our sample are also given in the table and the individual RCs are plotted in Fig.4.A.1 of Appendix A ).

The log average optical radius $\langle R_{opt} \rangle$ and the log average optical velocity $\langle V_{opt} \rangle$ are $2.5\,kpc$, $39.6\,km/s$, respectively, (these values will be specifically needed in Section 5). For a comparison, the galaxy sample of PSS spans the magnitude interval $-23.5 \lesssim M_I \lesssim -17$, the disk scale radii $2\,kpc \lesssim R_D \lesssim 30\,kpc$, and the optical velocities between $70\,km/s$ and $300\,km/s$. Therefore, our sample will extend the URC of PSS by more than 2 orders of magnitudes down in galaxy luminosity.

## 4.3 The URC of Dwarf Disks

First, we plot the RCs of galaxies in our sample expressed in physical units in log-log scales (see the left panel of Fig. 4.1). We realize, even at a first glance, that, contrary to the RCs of normal spirals (e.g., Yegorova and Salucci, 2007, PSS), each DD galaxy has a RC with a very different profile, as it has also been noticed by Oman et al. (2015). All curves are rising with radius but at a very different place.

Surprisingly, the origin of such diversity is closely linked with the very large scatter that the DDs show in the relationship between the optical radius $R_{opt}$ and the luminosity $L_K$ shown in Fig. 4.2. In our sample the relation still holds but the scatter remarkably increased, while in normal Spirals luminosities and disk sizes are very well correlated.

Thus, also in DD galaxies, by following the analogous PSS procedure, we derive a universal profile of their RCs. As an initial step of the co-addition procedure (see PSS for details) each of the 36 $V(R)$ has been normalized to its own optical radius $R_{opt}$ and to its optical velocity $V_{opt}$ obtained by RC data interpolation. We then derive the quantity $V(R/R_{opt})/V(R_{opt})$. This double normalization (DN) eliminates most of the individualities of the RCs. It can be seen in the right panel of Fig. 4.1 that as a consequence of the

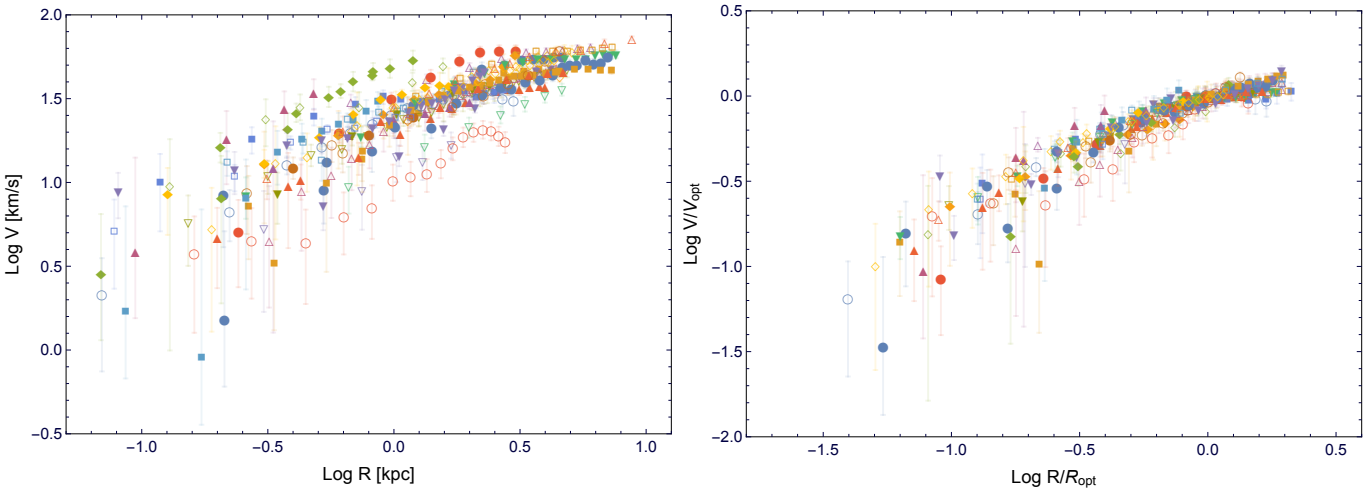


**Figure 4.1:** Individual RCs. *Left panel:* in physical units. *Right panel:* after double normalization on $R_{opt}$ and $V_{opt}$.

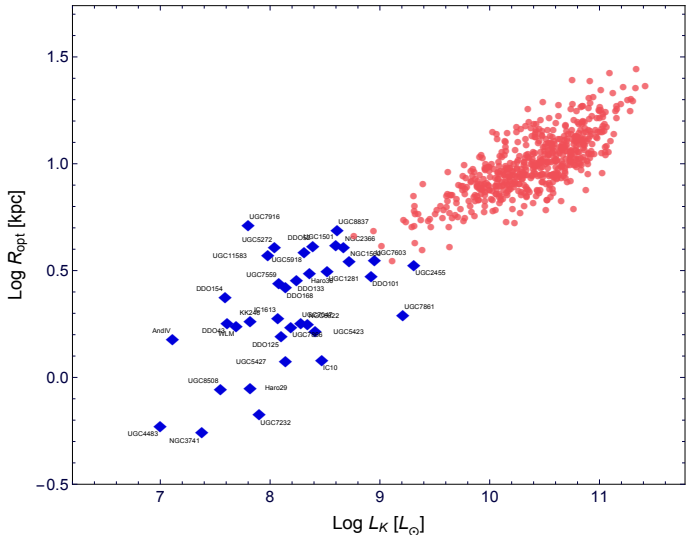


**Figure 4.2:** The optical radius versus the total luminosity. Red circles indicate the normal spiral galaxies from the sample of PSS and blue squares are the dwarf galaxies of the present work.

DN, all RCs have become similar to each other, leading to a profile very similar to that coadded of the least luminous normal spirals (green diamonds of Fig. 4.B.1).

This effect is not new: in Verheijen and de Blok (1999); Salucci and Persic (1997) (see also McGaugh, 2014) the variety of RCs shapes in physical units between high surface

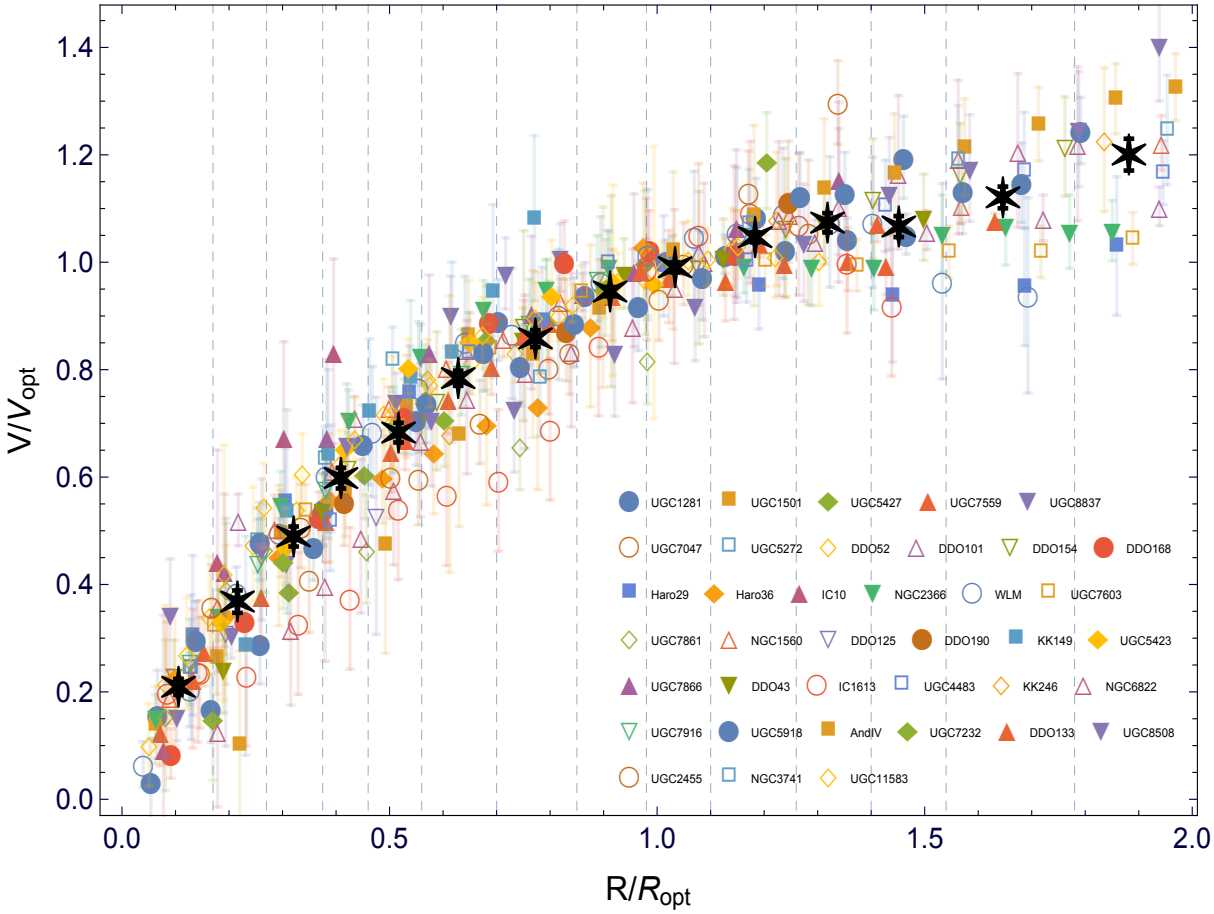


**Figure 4.3:** Individual RCs normalized to $R_{opt}, V_{opt}$. Black stars indicate the synthetic RC. Bins are shown as vertical dashed grey lines.

brightness galaxies and LSB objects of similar maximum velocities was eliminated by normalizing $V(R)$ on the corresponding disk scale lengths.

In investigating our sample of RC *profiles* we will construct just one luminosity bin, because of the data limitation. At its support, lets us note that the URC at low luminosities converges to a profile independently of luminosity. The DN velocity data are co-added as it follows: we set 14 radial bins in the position $r_i$[1] given by the vertical dashed grey lines in Fig. 4.3 and reported in Table 4.2. Each bin is equally divided in two, we adopt that every RC can contribute to each of the 28 semi bins at most with one data point. When, for a RC more data points concurring to the same semi bin, these are averaged accordingly. The last bin is set at $r_i = 1.9$ due to the lack of outer data.

[1]Calculated as a mean value in a bin.

**Table 4.2:** Data in the radial bins. Columns: **(1)** bin number; **(2)** number of data points; **(3)** the central value of a bin; **(4)** the average coadded weighted normalized rotation velocity; **(5)** r.m.s. on the average coadded rotation velocity **(6)** denormalized on $\langle R_{opt} \rangle$ values of radii, *kpc* **(7)** denormalized on $\langle V_{opt} \rangle$ values of velocities, $km/s$ **(8)** r.m.s. on the denormalized rotation velocity

| i | N | $r_i$ | $v_i$ | $dv_i$ | $R_i$ | $V_i$ | $dV_i$ |
|---|---|---|---|---|---|---|---|
| (1) | (2) | (3) | (4) | (5) | (6) | (7) | (8) |
| 1 | 31 | 0.11 | 0.21 | 0.015 | 0.27 | 8.28 | 0.59 |
| 2 | 30 | 0.22 | 0.37 | 0.021 | 0.54 | 14.57 | 0.82 |
| 3 | 21 | 0.32 | 0.49 | 0.019 | 0.81 | 19.37 | 074 |
| 4 | 26 | 0.41 | 0.60 | 0.019 | 1.03 | 23. 68 | 0.78 |
| 5 | 25 | 0.52 | 0.68 | 0.018 | 1.30 | 27.03 | 0.72 |
| 6 | 33 | 0.63 | 0.78 | 0.014 | 1.58 | 31.04 | 0.56 |
| 7 | 34 | 0.77 | 0.86 | 0.016 | 1.94 | 34.0 | 0.63 |
| 8 | 28 | 0.91 | 0.95 | 0.009 | 2.29 | 37.42 | 0.35 |
| 9 | 25 | 1.03 | 0.99 | 0.009 | 2.60 | 39.21 | 0.37 |
| 10 | 28 | 1.18 | 1.05 | 0.010 | 2.97 | 41.43 | 0.38 |
| 11 | 18 | 1.32 | 1.07 | 0.018 | 3.31 | 42.50 | 0.71 |
| 12 | 17 | 1.45 | 1.07 | 0.020 | 3.65 | 42.22 | 0.78 |
| 13 | 20 | 1.65 | 1.12 | 0.020 | 4.13 | 44.37 | 0.80 |
| 14 | 14 | 1.88 | 1.20 | 0.030 | 4.73 | 47.53 | 1.17 |

Since a galaxy cannot contribute more than twice to every bin $i$, each of them, centred at $r_i$ (see Table 4.2) and with boundaries shown in Fig. 4.3, has a number $N_i$ data (see Table 4.2) which runs from a maximum of 68 and a minimum that we have set to be 14. Then, from $N_i$ data in each radial bin $i$ we compute the average weighted rotation velocity, where the weights are taken from the uncertainties in the rotation velocities (given online).

In Table 4.2 we report, the 14 $r_i$ positions, the values of the coadded DN curve $v = V(R/R_{opt})/V(R_{opt})$ and of their uncertainties $dv$, calculated as the standard deviation with respect to the mean [1]. The universality of this curve can be infered from its very small r.m.s. values (see Fig. 4.3). Further, we investigate the universality in deep by calculating the residuals of each individual RC with respect to the emerging coadded curve (Table 4.2 column 5):

$$\chi^2 = \frac{\sum_{ij} \frac{(v_{ij}-v_i)^2}{\delta_{ij}^2}}{N}, \tag{4.1}$$

where $v_{ij}$ are the individual RC data referring to the bin $i$ of the DN RC of the $j$ dwarf disk ($j$ from 1 to 36), $v_i$ is the double normalized coadded $i$ value ($i$ from 1 to 14) (see Fig. 4.3), $\delta_{ij}$ are the observational errors of the normalized circular velocities and $N$ is the total number of the data points ($N = 350$) [2].

We consider the 14 $v_i$ as an exact numerical function which we attempt to fit with DN velocity data $v_{ij}$: we found that the fit is excellent, the reduced chi-square is $\sim 1.0$ and the reduced residuals $dv_{ij} = v_{ij} - v_i$ are very small, see Fig. 4.4. In fact $\sim 72\%$ of the residuals is smaller than $1\delta_{ij}$, $\sim 26\%$ falls inside 3 $\delta_{ij}$ and only the remaining $\sim 2\%$ is anomalously large.

Finally, in order to check the existence of biases, we investigate, in all 14 bins, whether the $dv_{ij}$ residuals have any correlation with the optical velocity $logV_{opt}^{ij}$ of the corresponding galaxy (see Fig. 4.5). However, we did not find any correlation see Fig. 4.5; DD galaxies of any luminosity (and $V_{opt}$) show the same DN RC profile. In fact, our accurate analysis shows no evidence of DD with a DN rotation curve relevantly different from the coadded $v_i(r_i)$ derived in this section and given in Table 4.2.

It is worth to compare the present results with those of PSS, in Fig 4.B.1 our coadded RC is plotted alongside with the similar curve of the PSS's first luminosity bin containing 30 normal spirals with the average I-band magnitude of $\langle M_I \rangle = -18.29$. Noticeably, both coadded DN RCs are in a very good agreement, which indicates that, starting

[1] Lowercase letters refer to normalized values, while capital letters to the values in physical units.
[2] $i$ is the index number of a radial bin and $ij$ are the index numbers of a data $j$ in a bin $i$.

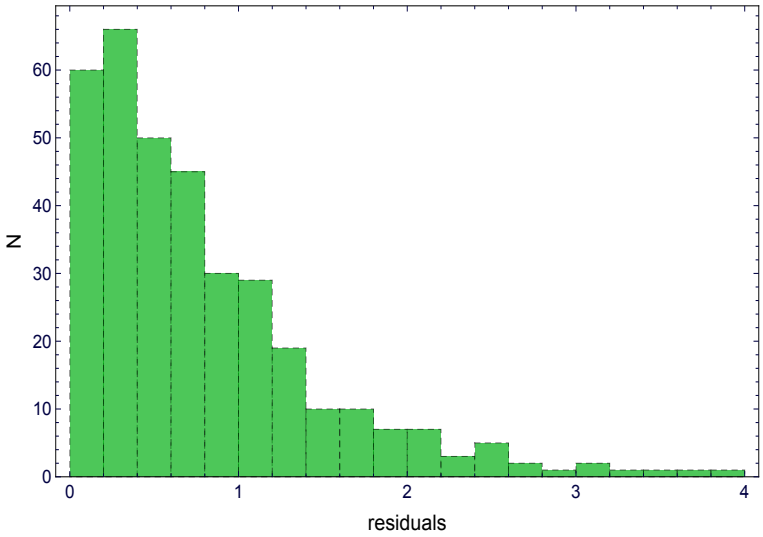


**Figure 4.4:** The distribution of residuals in terms of rms, which are listed in column 5 of Table 4.2.

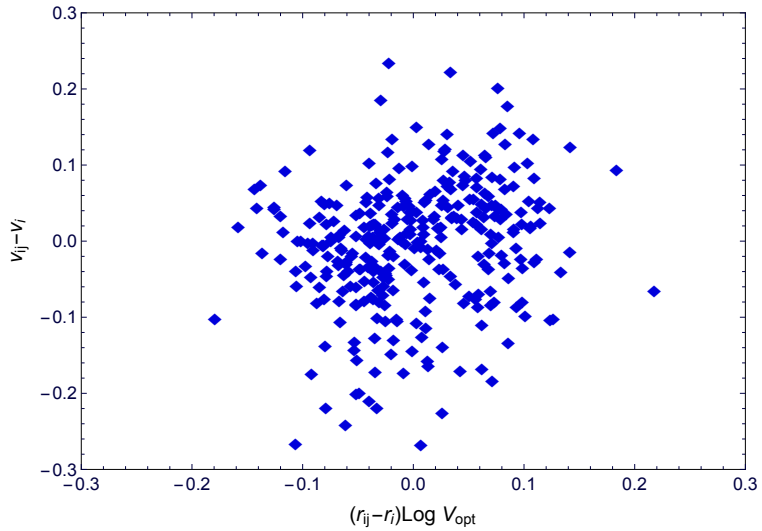


**Figure 4.5:** The $v_{ij}$ residuals in the 14 bins versus the optical velocity $logV_{opt}$. Coefficient of correlation $R^2$ is $\sim 0.06$.

from $M_I \sim -18$ and down to the smallest disk systems, the mass structure of disk galaxies is simply a dominated dark halo with a density core radius as big as the stellar disk. Additionally, in the same plot we show 5 galaxies used in PSS sample (the data are published in Persic and Salucci, 1995), which have $V_{opt} \lesssim 61\ km/s$, for details see Appendix B.

Therefore, we conclude the existence of the coadded RC for the DD population. This is the first step to obtain that the kinematics of DD galaxies can be described by a smooth universal function, exactly as it happens in normal spirals (PSS, Salucci et al., 2007).

## 4.4 Modelling the DN Coadded RC of DD galaxies

As in normal spirals (see PSS) we mass model the coadded RC data that represent the whole kinematics of DDs. More precisely,

1. the coadded (double normalized) RC (see Table 4.2), once proven to be universal, is the basic data with which we build the mass model of DD galaxies;

2. for simplicity, we rescale the 14 normalized velocities $v_i$ to the log average values of the sample $\langle V_{opt}\rangle$ and $\langle R_{opt}\rangle$, 39.6 km/s and 2.1 kpc, respectively. In details, we write:

$$\begin{aligned} \langle V_i\rangle &= v_i\langle V_{opt}\rangle; \\ \langle R_i\rangle &= r_i\langle R_{opt}\rangle, \end{aligned} \tag{4.2}$$

the 14 values of $\langle V_i\rangle$ and $\langle R_i\rangle$ are also reported in Table 4.2 (columns 6-7), where angle brackets indicate normalization to the log average values of optical radius and optical velocity. This RC is the fiducial curve for DD systems. In fact, we take the coadded DN curve Table 4.2 (columns 3-5) and we apply it to a galaxy with the values of $R_{opt}$ and $V_{opt}$ equal to the average values in our sample. Since all DD RCs have the same DN profile, the parameters of the resulting mass model can be easily rescaled back to cope with galaxies of different $V_{opt}$ and $R_{opt}$.

The fiducial rotation curve (Table 4.2 columns 6-8) of DD consists of 14 velocity data points extended out to 1.9 $\langle R_{opt}\rangle$. The uncertainties on the velocities are at the level of $\sim 3\%$ (see Fig 4.3).

The circular velocity model $V_{tot}(R)$ consists into the sum, in quadrature, of three terms $V_D, V_{HI}, V_{DM}$ that describe the contribution from the stellar disk ,the HI disk and dark halo and that must equate to the observed circular velocity:

$$V^2_{tot}(R) = V_m(R) \equiv V^2_D(R) + V^2_{HI}(R) + V^2_{DM}(R). \tag{4.3}$$

Notice in the RHS of eq. 4.3, we have neglected the stellar bulge contribution that is, in fact, absent in DDs.

### 4.4.1 Stellar component

With a constant stellar mass to light ratio as function of radius (see e.g Bell and de Jong, 2001) all 36 DDs have the same surface density stellar profile $\Sigma_D$ well represented by the Freeman disk (Freeman, 1970):

$$\Sigma_D(R) = \frac{M_D}{2\pi R_D^2} e^{-\frac{R}{R_D}} \tag{4.4}$$

then, the contribution of the stellar disk $V_D(R)$ is

$$V_D^2(R) = \frac{1}{2}\frac{GM_D}{R_D}(3.2x)^2(I_0K_0 - I_1K_1), \tag{4.5}$$

where $x = R/R_{opt}$ and $I_n$ and $K_n$ are the modified Bessel functions computed at 1.6 x.

Noticeably, the absence of a significant bulge in these objects simplifies the study.

### 4.4.2 Gas disk

For each galaxy the gaseous mass $M_{HI}$ was taken from K13, log averaged and then multiplied by a factor 1.33 to account for the He abundance, then we obtain $\langle M_{HI} \rangle = 1.7 \times 10^8 M_\odot$. The HI surface density profile is not available for all DD galaxies of our sample, therefore we model it, by following Tonini et al. (2006), as a Freeman distribution with a scale length three times larger that of the stellar disk $\Sigma_{HI}(R) = \frac{M_{HI}}{2\pi(3R_D)^2} e^{-\frac{R}{3R_D}}$, then, the contribution of the gaseous disk $V_{HI}(R)$ is

$$V_{HI}^2(R) = \frac{1}{2}\frac{GM_{HI}}{3R_D}(1.1x)^2(I_0K_0 - I_1K_1), \tag{4.6}$$

where $x = R/R_{opt}$ and $I_n$ and $K_n$ are the modified Bessel functions computed at 0.53 x.

This scheme is fairly well supported in DDs for which the HI surface density data are available (e.g., data from Oh et al., 2015; Gentile et al., 2010, 2012). In order to clarify the latter, we plot in Fig. 4.6, alongside the observed RC of HI component and our approximation of the HI distribution for 5 galaxies of our sample.

In addition, let us stress that the gas contribution is always a minor component to the DD circular velocities, so that, possible errors in its estimate do not alter the mass modelling neither affect any result of this paper.

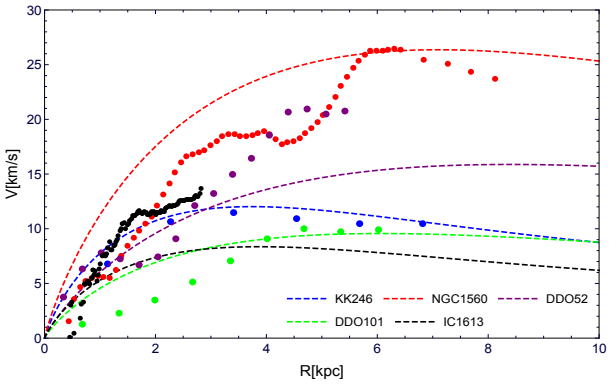


**Figure 4.6:** The observed circular velocities of HI taking from Gentile et al. (2010, 2012); Oh et al. (2015) (points) and the approximation for the distribution of HI component as described in Tonini et al. (2006) (dashed lines).

### 4.4.3 Dark halo

Many different halo radial mass profiles have been proposed over the years, in this work we are going to test the following profiles.

#### Burkert profile

The URC of normal spirals and the kinematics of individual objects (Salucci and Burkert, 2000b) point to dark halos density profiles with a constant core, and, in particular, to the Burkert halo profile (Burkert, 1995a), for which:

$$\rho_{B,URC}(r) = \frac{\rho_0 r_c^3}{(r + r_c)(r^2 + r_c^2)}, \tag{4.7}$$

where $\rho_0$ (the central density) and $r_c$ (the core radius) are the two free parameters and $\rho_{B,URC}$ means that we have adopted the Burkert profile for the URC DM halo component. Hereafter, we will freely exchange the two denominations according to the issue considered.

Adopting spherical symmetry, the mass distribution of the Burkert halos is given by:

$$M_{URC}(r) = 2\pi\rho_0 r_c^3 \left[ln\left(1 + \frac{r}{r_c}\right) - tg^{-1}\left(\frac{r}{r_c}\right) + 0.5ln\left(1 + \left(\frac{r}{r_c}\right)^2\right)\right] \tag{4.8}$$

#### NFW profile

We will investigate also NFW profile. Navarro et al. (1996b) found, in numerical simulations performed in the ($\Lambda$) CDM scenario of structure formation, that virialized systems

follow a universal dark matter halo profile. This is written as:

$$\rho_{NFW}(r) = \frac{\rho_0}{(\frac{r}{r_s})(1+\frac{r}{r_s})^2}, \tag{4.9}$$

where $\rho_0$ and $r_s$ are, respectively, the characteristic density and the scale radius of the distribution. These two parameters can be expressed in terms of the virial mass $M_{vir} = 4/3\pi 100 \rho_{crit} R_{vir}^3$, the concentration parameter $c = \frac{R_{vir}}{r_s}$ and the critical density of the Universe $\rho_{crit} = 9.3 \times 10^{-30} g\ cm^{-3}$. By using eq.(4.9), we can write:

$$\begin{aligned} \rho_0 &= \frac{100}{3} \frac{c^3}{\log(1+c) - \frac{c}{1+c}} \rho_{crit} \quad g\, cm^{-3}; \\ r_s &= \frac{1}{c} \left( \frac{3 \times M_{vir}}{4\pi 100 \rho_{crit}} \right)^{1/3} \quad kpc. \end{aligned} \tag{4.10}$$

Then, the RC curve for the NFW DM profile is

$$V_{NFW}^2(r) = V_{vir}^2 \frac{log(1+cx) - cx/(1+cx)}{x[log(1+c) - c/(1+c)]}, \tag{4.11}$$

where $x = r/R_{vir}$ and $V_{vir}$ represents the circular velocity ar $R_{vir}$.

Let us point out that, within the ($\Lambda$)CDM scenario, this profile maybe not the one the present day dark halos around spirals. Baryons, during the formation of the stellar disks, may have been able to modified the original DM density distributions (see, e.g., Pontzen and Governato, 2012, 2014; Di Cintio et al., 2014b). We then consider eq. (4.11) as the fiducial profile of ($\Lambda$)CDM scenario, a working assumption useful to frame changes of the latter.

### DC14 profile

A solution for the existence of cored profiles in ($\Lambda$)CDM scenario may have emerged by considering the recently developed DM density profile (see Di Cintio et al., 2014b). This profile (hereinafter referred to as DC14) accounts for the effects of feedback on the DM halos due to gas outflows generated in high density starforming regions during the history of the stellar disk. The resulting radial profile is far from simple, since it starts from an $(\alpha, \beta, \gamma)$ double power-law model (see Di Cintio et al., 2014b)

$$\rho_{DC14}(r) = \frac{\rho_s}{(\frac{r}{r_s})^\gamma \left(1 + (\frac{r}{r_s})^\alpha\right)^{\frac{(\beta-\gamma)}{\alpha}}} \tag{4.12}$$

where $\rho_s$ is the scale density and $r_s$ is the scale radius. The inner and the outer regions have logarithmic slopes $-\gamma$ and $-\beta$, respectively, and $\alpha$ indicates the sharpness of the transition. These three parameters are fully constrained in terms of the stellar-to-halo mass ratio as shown in Di Cintio et al. (2014b):

$$\begin{aligned} \alpha &= 2.94 - log_{10}[(10^{X+2.33})^{-1.08} + (10^{X+2.33})^{2.29}] \\ \beta &= 4.23 + 1.34X + 0.26X^2 \\ \gamma &= -0.06 + log_{10}[(10^{X+2.56})^{-0.68} + (10^{X+2.56})] \end{aligned} \tag{4.13}$$

where $X = log_{10}\left(\frac{M_D}{M_{halo}}\right)$.

Then, using the definition of the enclosed mass, we can write down the expression for the scale density of the DC14 profile:

$$\rho_s = \frac{M_{vir}}{4\pi \int_0^{R_{vir}} \frac{r^2}{(\frac{r}{r_s})^{\gamma}[1+(\frac{r}{r_s})^{\alpha}]^{\frac{\beta-\gamma}{\alpha}}} dr}. \tag{4.14}$$

Finally, by combining the above eqs. (4.12-4.14) we obtain a density profile as a function of three parameters $r_s$, $M_{halo}$ and $M_D$, which we use in order to define the RC curve for the DC14 DM profile.

Despite the complexity of the proposed scheme, it is worth to test such DM density profile based on the analysis of hydro-dynamically simulated galaxies (see Di Cintio et al., 2014b) drawn from the MaGICC project (Brook et al., 2012b; Stinson et al., 2013b).

### 4.4.4 Results

In Fig. 4.7 we show that the modelling of the fiducial RC by means of the Dwarf Disk Universal Rotation Curve (DDURC) mass model: an exponential Freeman disk, a gaseous disk plus a Burkert halo profile. This result is very successful (see Fig. 4.4) with $\chi^2_{red} < 1$. The best-fit parameters of the fiducial RC are:

$$\begin{aligned} log\langle\rho_0\rangle &= 7.53 \pm 0.04 \quad M_\odot\, kpc^{-3}; \\ \langle r_c\rangle &= 2.34 \pm 0.14 \quad kpc; \\ log\langle M_D\rangle &= 7.72 \pm 0.15 \quad M_\odot. \end{aligned} \tag{4.15}$$

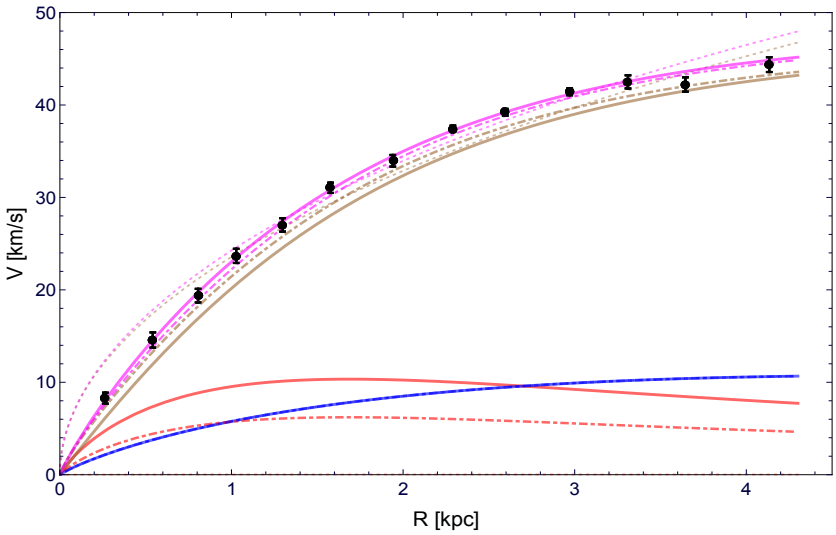


**Figure 4.7:** The synthetic RC (filled circles with uncertainties) and URC with its separate dark/luminous contributions (red line: disk; blue line: gas; brown line: halo) in case of two DM profiles: the Burkert DM profile (solid lines), NFW profile (dashed lines) and DC14 profile (dot-dashed line).

The resulting virial mass is $\langle M_{vir} \rangle = (1.38 \pm 0.05) \times 10^{10} M_{\odot}$. Note that quite large fitting uncertainties in the estimate of the stellar disk masses come from the fact that the stellar disks are subdominant components in these galaxies.

It is worth to remind that the coadded DN RC of DD (Table 4.2 columns 3-5) would be identically well fitted and the relative structure parameters can easily be obtained via the transformation laws in eq. (4.2).

NFW profile fails to reproduce the synthetic RC (see Fig. 4.7), the reduced chi-square is $\approx 12$ and the best-fit parameters

$$\begin{aligned} log\langle M_{vir} \rangle &= 11.74 \pm 0.94 \quad M_{\odot}; \\ \langle c \rangle &= 4.46 \pm 3.19; \\ log\langle M_{D} \rangle &= 2.60^{+?}_{-2.60} \quad M_{\odot}. \end{aligned}$$

lead to totally unrealistic estimates of the stellar disk and halo masses.

The DC14 profile shows the same good quality fit (see Fig. 4.7) as the URC profile with $\chi^2_{red} < 1$ and similar values of the structural parameters

$$log\langle M_{vir} \rangle = 10.29 \pm 0.02 \quad M_{\odot};$$

$$\begin{aligned} \langle r_s \rangle &= 2.09 \pm 0.14; \\ log\langle M_D \rangle &= 7.27 \pm 0.14 \quad M_\odot. \end{aligned}$$

Then, in spite of the fact that the galaxies in our sample vary by $\sim 6$ magnitudes in the $I$ band, we obtain a Universal Function of the normalized galactocentric radius, similar to that set up in PSS, that is able to fit well the DN coadded RCs of DN galaxies, when extrapolated to our much lower masses.

To summarise, we have worked out the DDURC, i.e. an analytical model for the DD coadded curve, that represents the RC of DD galaxies. This function is given by eqs. 4.3,4.5,4.8 and by eq. 4.15.

## 4.5 Denormalisation of the DDURC mass model

In this section we will construct a URC for the DD in the physical units that will cope with the diversity of RCs evident in Fig. (4.2). In spirals (see PSS) we can easily go back from a double normalized URC $V(R/R_{opt})/V_{opt}$ to a RC expressed in physical units $V(R/kpc, M_I)km/s$, where $R_{opt}$, $V_{opt}$ and $M_I$ are altogheter well correlated. This is not the case for DDs where another quantity, the concentration, enters in the above 3-quantity link.

Let us first remind that in every radial bin the residuals do not correlate with the optical velocity of the corresponding galaxy (see Section 3). This implies that the DDs structural parameters of the dark and luminous matter have a negligible direct dependence on luminosity/optical velocity different from that inherent to the two normalizations we apply to the individual RCs.

Moreover, given the very small intrinsic scatter of the fiducial DN coadded RC and the extremely good fit of the DDURC to it, we can write

$$\frac{M_{D,HI}}{V_{opt}^2 R_{opt}} = \frac{\langle M_{D,HI} \rangle}{\langle V_{opt}^2 \rangle \langle R_{opt} \rangle} \equiv const, \tag{4.16}$$

and derive, in all objects, a direct proportionality between the halo core radius $r_c$ and the disk scale-length $R_D$ in agreement with the extrapolation of the corresponding relationship to that found in Spirals of much higher mass (see Fig. 4.8) (Salucci et al., 2007): $log(r_c) = 0.47 + 1.38log(R_D)$.

We also assume that $\frac{V_D^2(R_{opt})}{V_{HI}^2(R_{opt})}$ is constant among galaxies and it equals to the value of the average case $\frac{\langle V_D^2(R_{opt}) \rangle}{\langle V_{HI}^2(R_{opt}) \rangle} \simeq 1.1$.

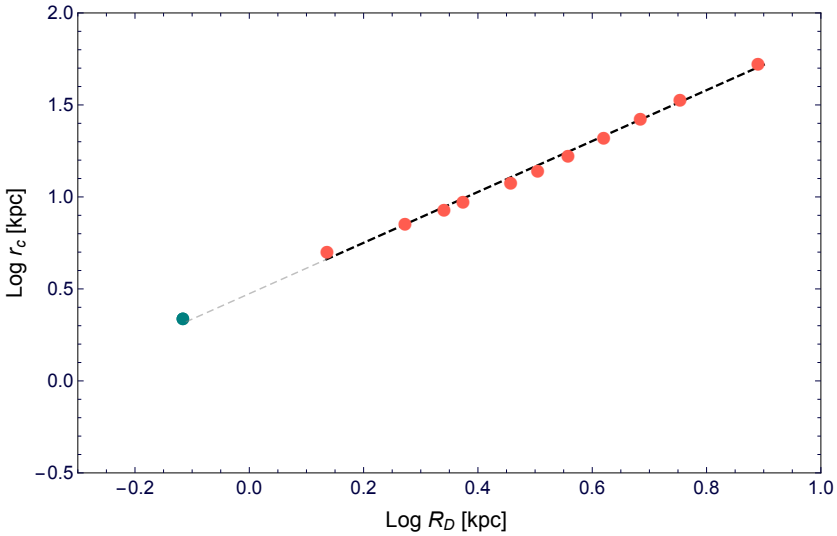


**Figure 4.8:** The core radius versus disk scalelength. Red circles represent the values of the URC of normal spirals and green circle represents the best fit values found in the previous section. Black dashed line is a linear fit to the data of the URC of normal spirals and the grey dashed line is the extrapolation of the linear fit to the DD regime.

Consequently with the above assumptions, for each galaxy of the sample, we have

$$M_{DM}(R_{opt}) = (1-\alpha)V_{opt}^2 R_{opt} G^{-1}, \tag{4.17}$$

where $M_{DM}$ is the Burkert DM mass inside the optical radius $R_{opt}$ and $\alpha$ is the fraction which baryonic matter contributes to the total circular velocity:

$$\begin{aligned} \alpha &= \frac{\langle V_{HI}^2(R_{opt})\rangle + \langle V_D^2(R_{opt})\rangle}{\langle V_{tot}^2(R_{opt})\rangle} = \\ &= 0.12 \equiv const. \end{aligned} \tag{4.18}$$

Notice that in some galaxies the fractional contribution to $V$ from the HI disk can be different from the assumed value of $\sim 0.06$. However, this has no effect on our investigation. In fact, at the radii where the HI disk is more relevant that the stellar disk, the contribution of the DM halo becomes overwhelming (Evoli et al., 2011).

By simple manipulations of eqs. (4.16-4.18) with the individual values of $R_{opt}, V_{opt}$, we get, for each galaxy, the structural parameters of the dark and the luminous matter. In Table 4.3 we list them along side with their uncertainties obtained from those of the URC mass model given in eq. (4.15).

**Table 4.3:** sample of DD galaxies. Columns: **(1)** galaxy name; **(2)** the stellar disk mass; **(3)** the stellar disk mass using K-band luminosities; **(4)** the gas mass; **(5)**the gas mass listed in Karachentsev et al. (2013); **(6)** the core radius; **(7)** the central density; **(8)** the halo mass.

| Name | $M_D$ | $M_D(K_S)$ | $M_{HI}$ | $M_{HI}(K13)$ | $r_c$ | $log(\rho_0)$ | $M_h$ | c |
|---|---|---|---|---|---|---|---|---|
| — | $\times 10^7$ | $\times 10^7$ | $\times 10^7$ | $\times 10^7$ | — | — | $\times 10^9$ | — |
| — | $M_\odot$ | $M_\odot$ | $M_\odot$ | $M_\odot$ | kpc | $g/cm^3$ | $M_\odot$ | — |
| (1) | (2) | (3) | (4) | (5) | (6) | (7) | (8) | (9) |
| UGC1281 | 12.2 | 19.9 | 39.5 | 22.1 | 2.93 | -23.6 | 32.2 | 1.05 |
| UGC1501 | 15.1 | 23.9 | 48.8 | 38.4 | 4.32 | -23.9 | 43.8 | 0.87 |
| UGC5427 | 4.63 | 8.28 | 15.02 | 3.93 | 0.76 | -22.5 | 8.85 | 1.80 |
| UGC7559 | 5.2 | 7.21 | 16.8 | 13.9 | 2.46 | -23.8 | 11.8 | 0.81 |
| UGC8837 | 14.9 | 24.4 | 48.2 | 29.8 | 5.40 | -24.2 | 44.4 | 0.74 |
| UGC7047 | 3.28 | 11.4 | 10.6 | 15.3 | 1.34 | -23.3 | 6.50 | 1.02 |
| UGC5272 | 16.4 | 6.58 | 53.1 | 23.1 | 4.14 | -23.8 | 47.8 | 0.93 |
| DDO52 | 19.8 | 14.7 | 64.3 | 27.8 | 4.24 | -23.8 | 59.8 | 1.0 |
| DDO101 | 13.8 | 49.9 | 44.7 | 16.0 | 2.71 | -23.4 | 36.6 | 1.17 |
| DDO154 | 4.58 | 2.33 | 14.9 | 25.3 | 1.98 | -23.6 | 9.99 | 0.90 |
| DDO168 | 12.7 | 8.28 | 41.1 | 29.8 | 2.28 | -23.3 | 32.4 | 1.28 |
| Haro29 | 1.26 | 3.96 | 4.11 | 7.65 | 0.51 | -22.6 | 2.01 | 1.34 |
| Haro36 | 3.92 | 13.8 | 15.8 | 14.9 | 2.84 | -23.5 | 35.0 | 1.11 |
| IC10 | 2.31 | 17.7 | 8.80 | 13.3 | 0.78 | -22.8 | 4.91 | 1.39 |
| NGC2366 | 16.4 | 28.1 | 53.2 | 54.2 | 4.16 | -23.8 | 47.97 | 0.93 |
| WLM | 1.79 | 2.94 | 8.23 | 9.0 | 1.29 | -23.4 | 4.84 | 0.94 |
| UGC7603 | 17.1 | 53.5 | 55.6 | 55.4 | 3.42 | -23.6 | 48.8 | 1.09 |
| UGC7861 | 9.74 | 97.3 | 31.6 | 41.1 | 1.51 | -23.0 | 22.5 | 1.53 |
| NGC1560 | 14.7 | 31.5 | 47.6 | 142.5 | 3.37 | -23.7 | 40.7 | 1.03 |
| DDO125 | 0.60 | 7.55 | 1.95 | 4.02 | 1.1 | -23.8 | 0.92 | 0.55 |
| UGC5423 | 1.66 | 15.4 | 5.39 | 9.2 | 1.19 | -23.5 | 2.97 | 0.82 |
| UGC7866 | 1.90 | 9.29 | 6.15 | 10.6 | 1.27 | -23.5 | 3.47 | 0.83 |
| DDO43 | 3.0 | 2.44 | 9.72 | 9.42 | 1.35 | -23.3 | 5.88 | 0.98 |
| IC1613 | 0.92 | 7.05 | 3.0 | 7.8 | 1.46 | -23.9 | 1.52 | 0.54 |
| UGC4483 | 0.34 | 0.6 | 1.11 | 4.4 | 0.29 | -22.6 | 4.51 | 1.12 |
| KK246 | 2.51 | 3.96 | 9.56 | 15.6 | 1.40 | -23.4 | 5.79 | 0.95 |
| NGC6822 | 2.94 | 13.1 | 9.41 | 18.8 | 1.32 | -23.3 | 5.65 | 0.98 |
| UGC7916 | 9.45 | 3.79 | 30.7 | 35.8 | 5.80 | -24.4 | 26.2 | 0.57 |
| UGC5918 | 10.4 | 12.3 | 33.9 | 23.1 | 3.88 | -23.0 | 28.2 | 0.80 |
| AndIV | 2.08 | 0.77 | 6.76 | 27.8 | 1.06 | -23.2 | 3.79 | 0.99 |
| UGC7232 | 1.23 | 4.77 | 4.0 | 3.84 | 0.34 | -22.2 | 1.87 | 1.75 |
| DDO133 | 6.85 | 10.4 | 22.2 | 21.1 | 2.55 | -23.7 | 16.4 | 0.90 |

| | | | | | | | | |
|---|---|---|---|---|---|---|---|---|
| UGC8508 | 0.77 | 2.13 | 2.48 | 2.65 | 0.50 | -22.8 | 1.15 | 1.08 |
| UGC2455 | 9.93 | 122.5 | 32.2 | 87.9 | 3.21 | -23.8 | 25.9 | 0.90 |
| NGC3741 | 0.36 | 1.44 | 1.16 | 10.1 | 0.27 | -22.4 | 0.47 | 1.22 |
| UGC11583 | 13.5 | 5.73 | 43.9 | 24.8 | 3.67 | -23.8 | 37.6 | 0.93 |

### 4.5.1 HI gas mass and stellar mass

We now check the validity of the assumptions in the previous subsection. We compare our estimation values of the galaxy HI masses, eq. (4.16), with those given by K13 (calculated using total $H_I$ flux, for more details see K13). We find:

$$\begin{aligned} logM_{HIkin} &= (-0.18 \pm 1.20) + \\ &+ (1.01 \pm 0.16) logM_{HIK13} \end{aligned} \tag{4.19}$$

with a r.m.s of 0.3 dex. The value of the slope and the small r.m.s., despite the presence of some outliers most probably originating from the large range in luminosities and morphologies of our sample, suggest that $M_{HIkin}$ are good proxies of $M_{HIK13}$ and to adopt them does not influence any result of this paper.

We also compare the kinematical derivation of the stellar disk masses for the objects in our sample with those obtained for the same objects from $K_S$ band photometry (provided by K13). Following Bell et al. (2003); McGaugh and Schombert (2015) we adopt a constant mass-to-light ratio of $M/L_K = 0.6 \times M_\odot/L_\odot$ and we report them in Table 4.3 as $M_D(K_S)$. We find a good correlation between the two estimates:

$$\begin{aligned} logM_{Dkin} &= (2.58 \pm 1.01) \\ &+ (0.64 \pm 0.13) logM_{DK_S} \end{aligned} \tag{4.20}$$

with a r.m.s of 0.4 dex. The two estimates are therefore mutually consistent especially by considering that the kinematical estimate has an uncertainty of 0.3 dex (see Salucci et al., 2008). Let us also notice that in DD the conversion between luminosity and stellar masses is subject to a similarly large systematical uncertainty, especially in actively star-forming galaxies like those present in our sample.

These results, therefore, support well the scheme used in this paper to deal with the luminous components of DDs.

Furthermore, we compare our results with Lelli et al. (2016), where the authors analyse a sample of 176 disk galaxies and quantify for them the ratio of baryonic-to-observed

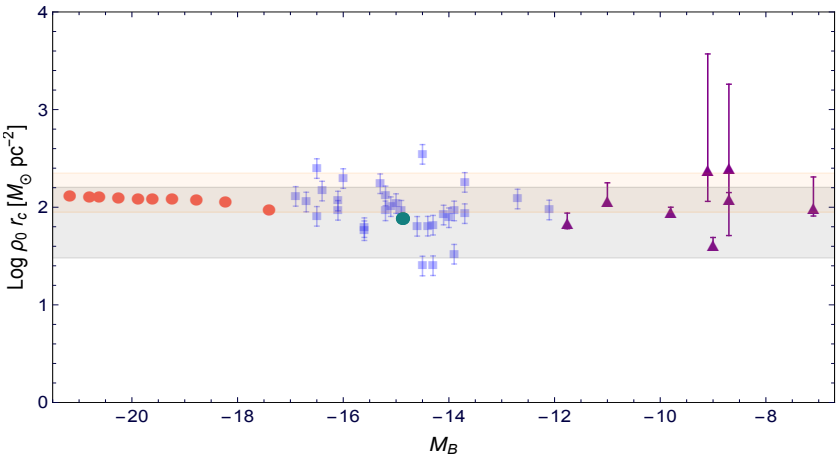


**Figure 4.9:** $\rho_0 r_c$ in units of $M_\odot pc^{-2}$ as a function of galaxy magnitude for different galaxies and Hubble types. The data are: the Salucci et al. (2012) the URC of normal spiral galaxies (red circles); scaling relation from Donato et al. (2009a) (orange shadowed area); Milky Way dSphs (black triangles) Salucci et al. (2012); DD galaxies (blue squares-this work), B magnitudes are taking from KK13; empirically inferred scaling relation: $\rho_0 r_c = 75^{+85}_{-45} M_\odot pc^{-2}$ from Burkert (2015)(grey shadowed area).

velocity. We have, that this ratio at 2.2 disk scale lengths (following Lelli et al., 2016) is $\sim 0.4$, which is consistent with their values found for a sample of dwarf disk galaxies. Moreover, we found that the value of gas fraction ($f_{gas} \equiv \frac{M_{HI}}{M_{bar}} \sim 0.8$) in our sample is consistent with the value found by Lelli et al. (2016), where the authors say that low-luminosity end disk galaxies are extremely gas dominated with $f_{gas} \simeq 0.8 - 1.0$.

### 4.5.2 The scaling relations

Let us plot, the central surface density of the DM haloes of our sample, i.e. the product of $\rho_0 r_c$, as a function of B magnitude (see Fig. 4.9). A constancy of this product has been found over 18 blue magnitudes and in objects ranging from dwarf galaxies to giant galaxies (e.g Kormendy and Freeman, 2004; Gentile et al., 2009; Donato et al., 2009a; Plana et al., 2010; Salucci et al., 2012). For the case of DDs, in Fig. 4.9, one can see that most of the objects of our sample fall inside the extrapolation of Donato et al. (2009a) relation (see the orange shadowed are of Fig. 4.9) with a scatter of about 0.3 dex of an uncertain origin.

We now work out the relationships among the various structural properties of the dark and luminous matter of each galaxy in our sample. These will provide us with crucial

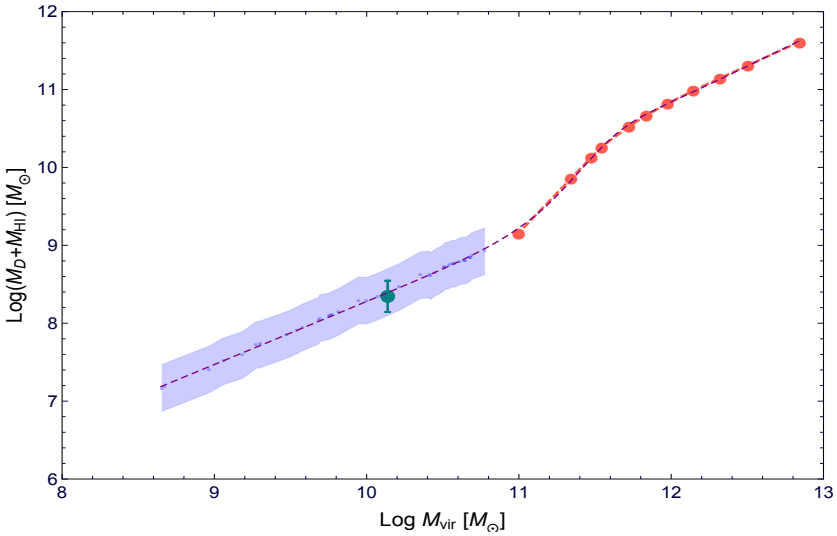


**Figure 4.10:** The baryonic mass versus the virial mass for normal spirals (joined red circles) and for the dwarf dIs (blue shadowed area assuming 0.3 dex scatter, the green circle with error bars represents the average point of the region). Purple dashed line corresponds to the parameterised eq. (4.21) of the galaxy baryonic mass as a function of halo mass.

information on the relation between dark and baryonic matter as well as on the DM itself. Obviously they are necessary to establish a URC for the present sample.

We first derive the galaxy baryonic mass versus halo virial mass relation and compare it with that of normal spiral galaxies (Salucci et al., 2007), see Fig. 4.10. We take 0.3 dex as 1-$\sigma$ error in the baryonic mass (blue shadowed area). Fig. 4.10 highlights that galaxies of our sample, i.e. DD objects live in haloes with masses below $5 \times 10^{10} M_{\odot}$ and above $4 \times 10^{8} M_{\odot}$. A similar result was found by Ferrero et al. (2012), who analysed a sample of dwarf disk galaxies either by using the individual mass modelling or the outermost values of their RCs in order to define the galactic virial mass.

The relation has a small scatter of 0.02 dex, so that, by following Ferrero et al. (2012), we can derive $M_{bar}$ as a function of $M_{vir}$ by fitting it with the function of 7 free parameters:

$$\begin{aligned} M_{bar} &= M_{vir} \times A \left(1 + \left(\frac{M_{vir}}{10^{M_1}}\right)^{-2}\right)^{\kappa} \\ &\times \left(\left(\frac{M_{vir}}{10^{M_0}}\right)^{-\alpha} + \left(\frac{M_{vir}}{10^{M_0}}\right)^{\beta}\right)^{-\gamma}, \end{aligned} \tag{4.21}$$

we found $A = 0.070$, $\kappa = 1.80$, $M_1 = 11.36$, $M_0 = 11.59$, $\alpha = 3.43$, $\beta = 0.042$, $\gamma = 1.8$(see

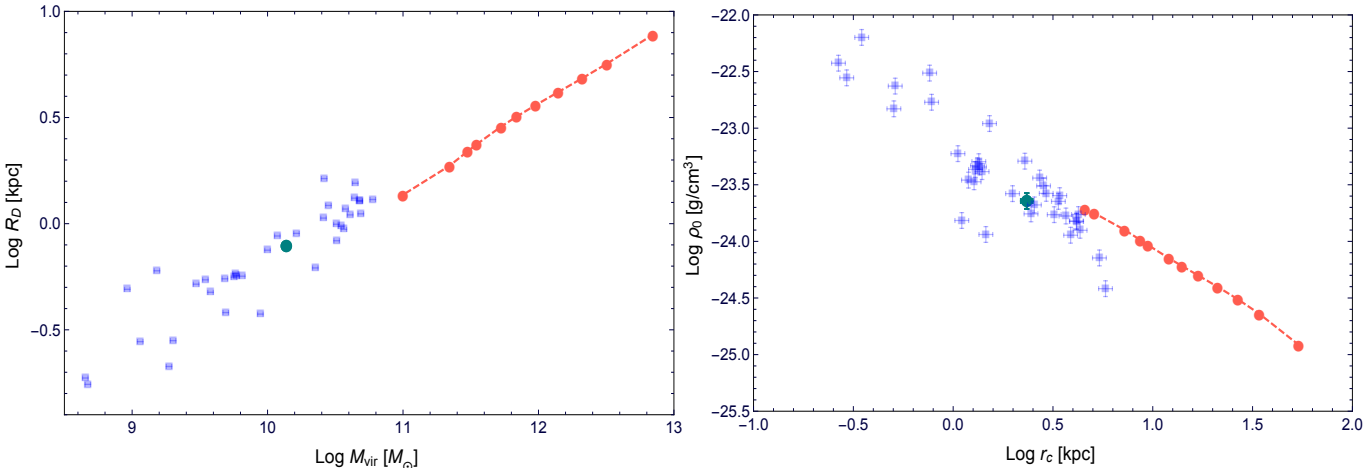


**Figure 4.11:** *Left panel:* the disk scalelenght versus virial mass. *Right panel:* the central density versus core radius. Red circles represent normal spirals, blue squares with error bars correspond to dwarf disks of this work and the green circle with error bars represents the average point.

Fig. 4.10).

The other two relationships which are necessary to establish a URC of DD also in physical units i.e. $R_D$ - $M_{vir}$ or $\rho_0$ -$r_c$, show a very large scatter (see Fig. 4.11) as a consequence of the presence of DD galaxies in the sample (and in the Universe) with almost the same stellar mass (luminosity) but with a different size of their stellar disks. At the face value, relationships in Fig. 4.11 may lead us to exclude the existence of URC in physical units for dwarf disk galaxies.

Instead, we can proceed and show that the universality is restored by introducing a new parameter, which we call "compactness" $C$. We define, for galaxies in the (DD) sample, the quantity $C$ as the ratio between the value of $R_D$ measured from photometry and that *predicted* from the measured galaxy disk mass $M_D$ according to the simple linear regression $M_D$ vs $R_D$ tof the whole sample. As regard, we find:

$$logR_D = -3.62 + 0.45\, logM_D. \tag{4.22}$$

Then, we obtain the following expression of $C$,

$$C = \frac{10^{(-3.62+0.45\, logM_D)}}{R_D} \tag{4.23}$$

that obviously describes the differences of the sizes of the stellar disks reduced at a same stellar mass. $C$ varies from -0.27 to 0.26 and its distribution in our sample is listed in

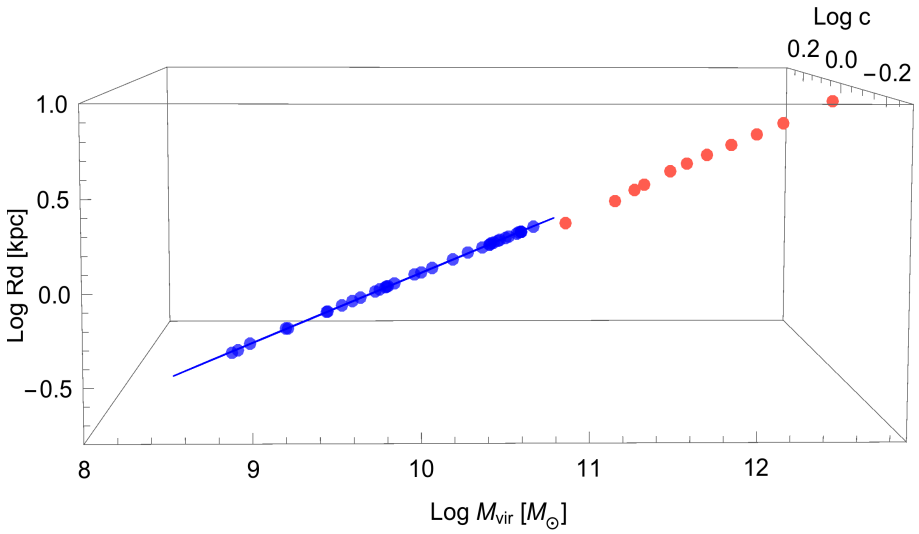


**Figure 4.12:** The disk scalelenght versus virial mass and the compactness parameter C. Red circles represent normal spirals, blue squares with error bars correspond to dwarf disks of this work and blue line is the result of the fit (for details see text).

Table 4.3.

By fitting $logR_D$ to $logM_{vir}$ with an additional variable $logC$, we obtain a excellent fit shown in Fig. 4.12. The model function being,

$$logR_D = -3.90 + 0.37\, logM_{vir} - 0.94\, logC. \tag{4.24}$$

this relation just acknowledges the existence of another player in the stellar disk mass-size interplay.

Then we fit $log\rho_0$ to $logM_{vir}$ and $logC$:

$$log\rho_0 = -18.60 - 0.48\, logM_{vir} + 3.44\, logC. \tag{4.25}$$

Finally, we fit $log\rho_0$ -$logr_c$ by adding $logC$ as a free parameter. The result of the fit is shown on Fig. 4.13 and the model function is,

$$log\rho_0 = -23.19 - 0.93\, logr_c + 2.23\, logC. \tag{4.26}$$

It is remarkable that a basic property of the stellar disks enters to set the relationship between two DM structural quantities. Therefore, the scatter, which appears in DD when we try to relate the local properties of either baryonic or DM can be eliminated by using an additional parameter $C$.

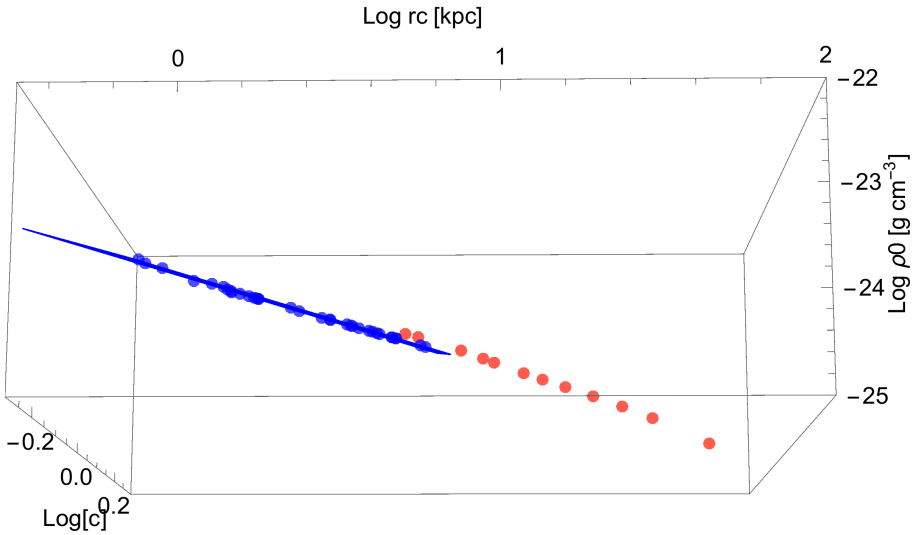


**Figure 4.13:** The central density versus core radius and the compactness parameter C. The lines and symbols are as in Fig. 4.12.

Finally, by using eqs. (4.5,4.6,4.8,4.21,4.23-4.26) we derive $V_{DDURC}(R, M_D, C)$ the Universal Function that describes the DD RCs in physical units. Differently, from normal Spirals it has 2 parameters, disk mass $M_D$ and concentration $C$, to account to the diversity of the mass distribution of these galaxies.

## 4.6 Summary and Conclusions

We have compiled literature data for a sample of DD galaxies in the Local Volume ($\lesssim 11\ Mpc$) with HI and $H_\alpha$ RCs in order to establish their URC in normalized and physical units and to investigate the related dark and luminous matter properties, not yet studied statistically in these galaxies. Our sample spans $\sim 2$ decades ($\sim 10^6 - 3 \times 10^8 L_\odot$) in luminosity, coincides with the faint end of the luminosity function of disk galaxies. In magnitude extension is as large as the whole range of normal Spirals usually investigated. The galaxies in the sample are up to $\sim 4$ magnitudes fainter than the lowest limit in the PSS sample.

We find that, the large variations of our sample in luminosity and morphologies require double normalization, after that we have that all RCs in double normalized units are alike. This implies that the structural parameters of the dark and luminous matter for the galaxies in our sample do not have any explicit dependence from luminosity except those coming from the normalizing process. Additionally, the good agreement of our coadded RC with that of the first PSS's luminosity bin indicates that in such small galaxies the

mass structure is already dominated by a dark halo with a density core as big as a stellar disk.

Then by applying to the DN rotation curve the standard $\chi^2$ mass modelling of RCs, we tested three DM density profiles. The NFW profile fails to reproduce the coadded curve, while the Burkert and DC14 profiles show excellent quality fits with $\chi^2_{red} < 1$. This result points out to the manifestation of the cored DM distribution in DD galaxies. The same conclusion was drawn in the papers on Things and Little Things dwarfs galaxies (see, e.g., Oh et al., 2011, 2015), where the authors found for their dwarfs much shallower inner logarithmic DM density slopes than those predicted by DM-only ΛCDM simulations. The present analysis has the advantages of bigger statistics, but above all, is immune from systematics that can affect the mass modelling of individual galaxies.

We also found, galaxy by galaxy, the values of the dark and luminous matter structural parameters. Surprisingly, a new actor enters the scene of the distribution of matter in galaxies, the compactness of the stellar component, which allows us to establish the DDURC.

As a consequence of the derived mass distributions, there is no evidence for the sharp decline in the baryonic to halo mass relation. Similar result, for dwarf galaxies in the field, was found by Ferrero et al. (2012) (see also Pace, 2016). The latter contradicts to the general predictions of the abundance matching or semianalytical models of galaxy formation, which predict that there are no DD galaxies in halos with virial mass below $10^{10} M_{\odot}$. Consequently, since in the present study it cannot be just misinterpretation of the observed RCs (for references see Oman et al., 2016; Pineda et al., 2016), then this result is an important challenge for the ΛCDM model of galaxy formation and specifically to the abundance matching technique since there are no obvious explanations for such behaviour.

Moreover, the S-shape of $M_{vir} - M_{bar}$ relation, may be interpreted as different physical mechanism occurring along the mass sequence of disk galaxies. Theoretically, it has been shown that the energetics of star formation differs among different galaxies with a characteristic dependence on the halo-to-stellar mass ratio (Di Cintio et al., 2014b; Chan et al., 2015) and possibly also on star formation history (Oñorbe et al., 2015).

Finally we recall that the study of the DDURC has lead to the main properties of dark matter in DDs, it will be integrated by future analyses of suitable individual RCs, once they will be available in a sufficient number.

## 4.A Sample of rotation curves

In Fig 4.A.1 we show the rotation curves of all observed galaxies used in our analyses, i.e. the same galaxies as appear in Table 3.1. We note that rotation curves of UGC1501, UGC5427, UGC8837, UGC5272, IC10, KK149 and UGC3476a are not extended to 3.2 $R_D$ (the verdical dashed gray line of Fig. 4.A.1 indicates the position of 3.2 $R_D$ for each galaxy), therefore, in order to know, the value of the circular velocity at these radii we made extrapolations.

## 4.B Comparison of the current URC and the URC of PSS

In Fig. 4.B.1, as already discussed in Section 3, we plot our URC alongside with the URC of the PSS's first luminosity bin containing 30 normal spirals. Then, among these 30 normal spirals, the individual RCs of which are published in Persic and Salucci (1995), we selected 5 galaxies that fit our selection criteria, however not the first one since these are not Local Volume galaxies. As one can see from the Fig. 4.B.1 all 5 RCs have more or less the same profile similar to our synthetic RC.

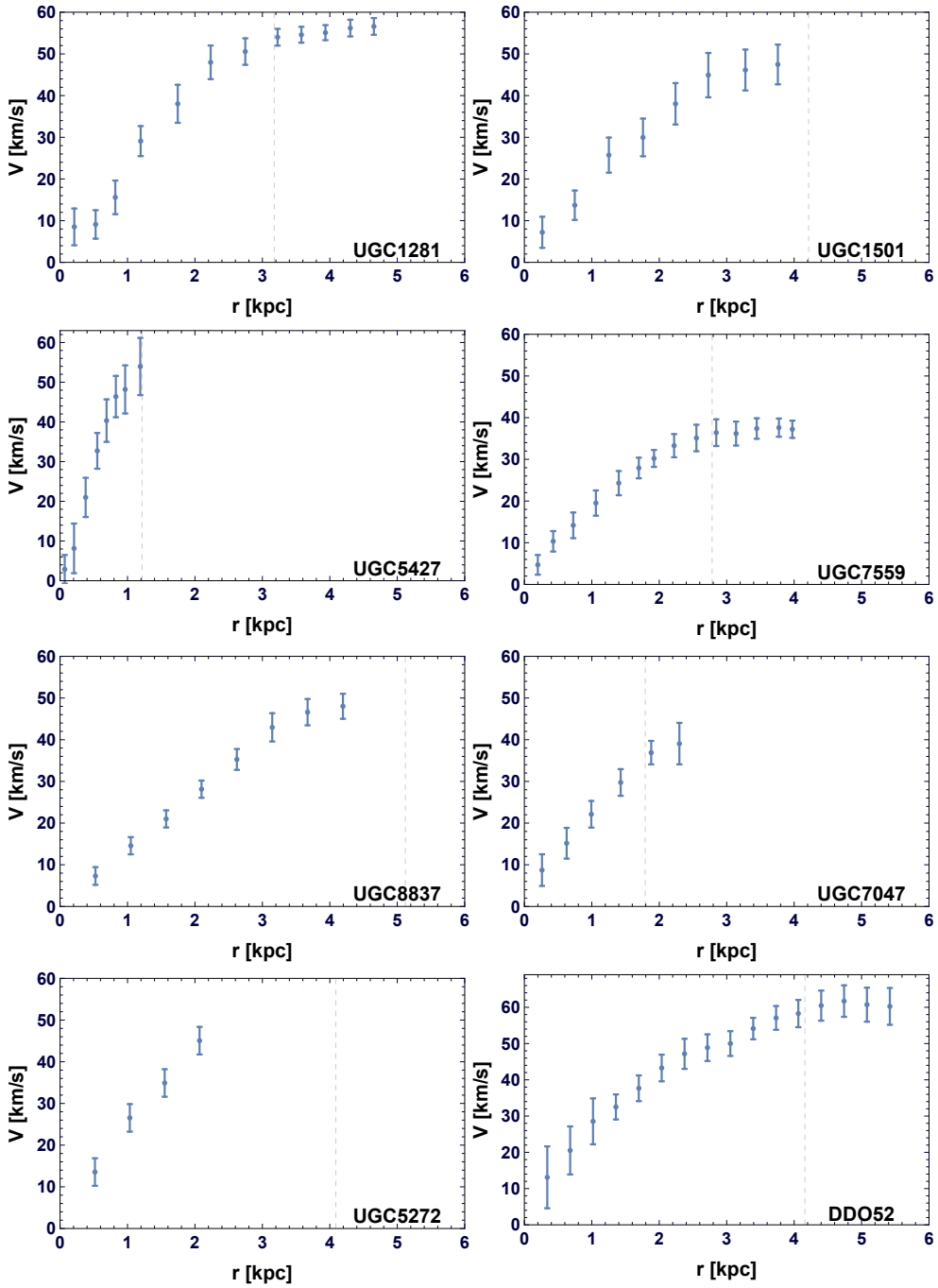


**Figure 4.A.1:** Individual RCs. Here the $R_{opt}$ are indicated by dashed vertical lines.

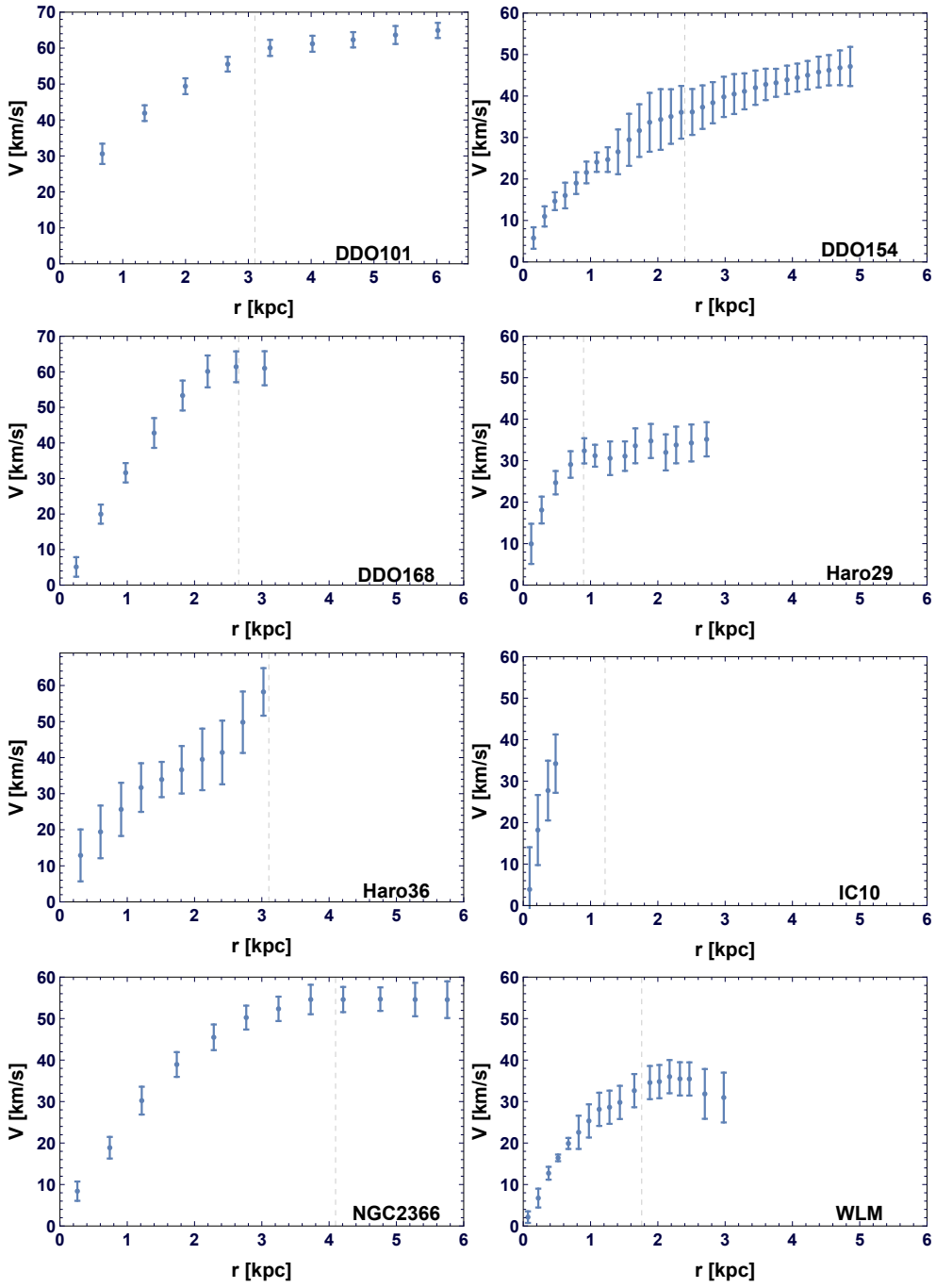


**Figure 4.A.1:** Individual RCs. Here the $R_{opt}$ are indicated by dashed vertical lines.

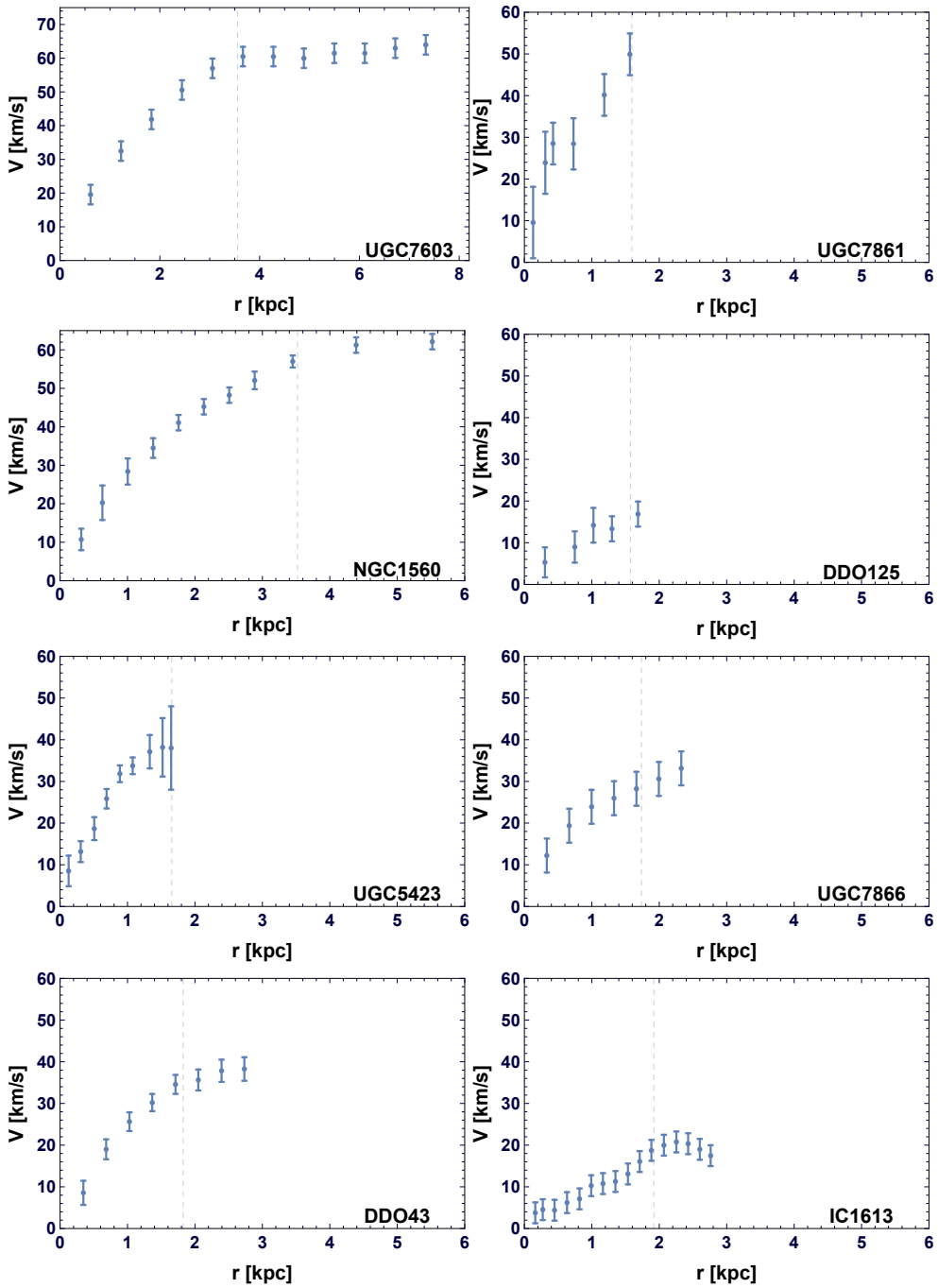


**Figure 4.A.1:** Individual RCs. Here the $R_{opt}$ are indicated by dashed vertical lines.

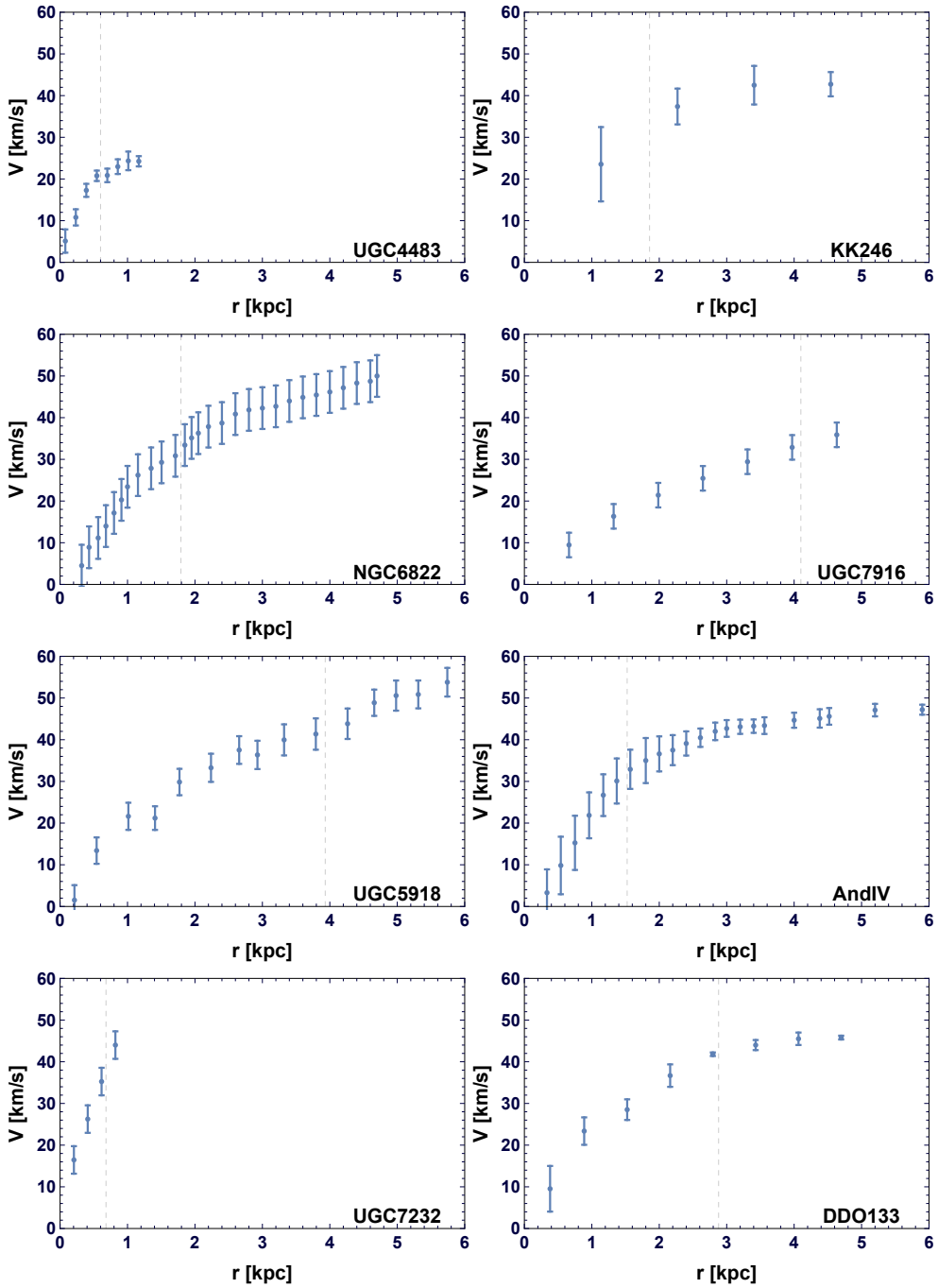


**Figure 4.A.1:** Individual RCs. Here the $R_{opt}$ are indicated by dashed vertical lines.

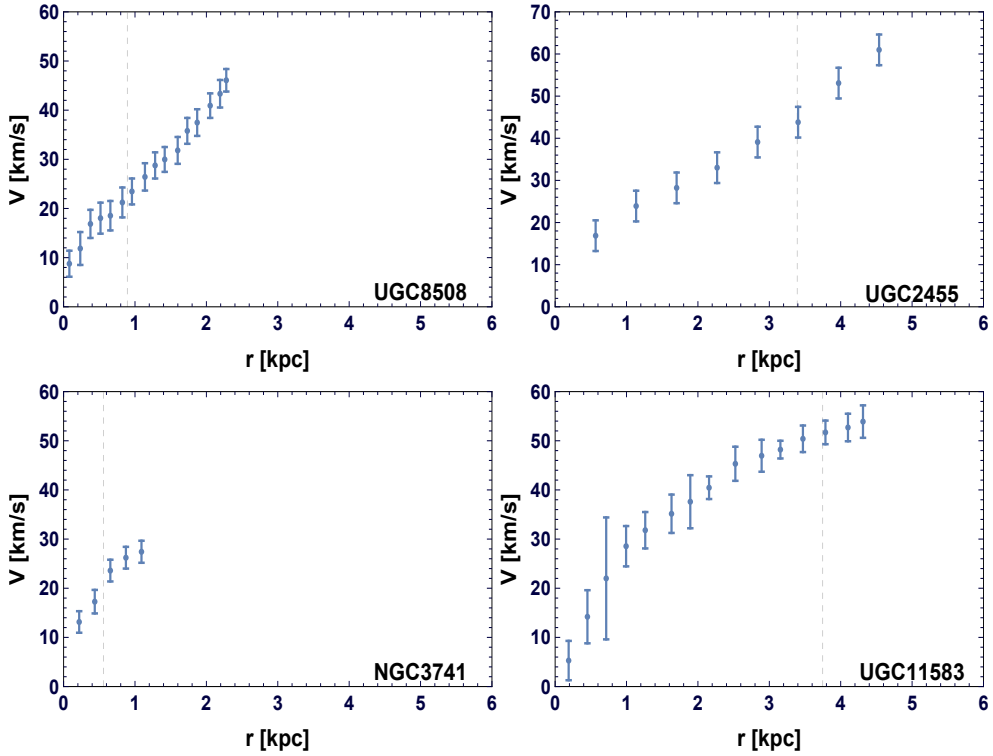


**Figure 4.A.1:** Individual RCs. Here the $R_{opt}$ are indicated by dashed vertical lines.

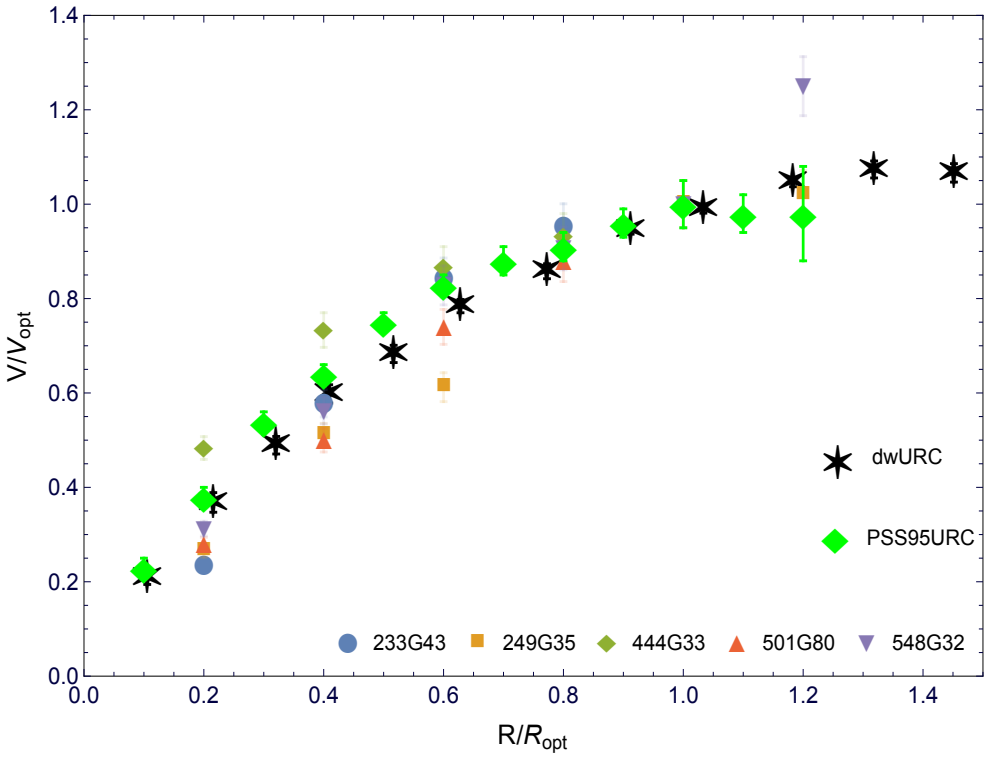


**Figure 4.B.1:** Black stars indicate the synthetic RC of the current paper. Green diamonds indicate the synthetic RC of the last bin in PSS. The individual double normalized RCs of PS95 are shown by different symbols.

# Chapter 5

# Conclusions and future perspectives

In this Chapter we summarize the main results obtained and reported in this thesis, and discuss prospects for future research. A more detailed discussion of our work can be found at the end of every previous Chapter starting from Chapter 2.

In this PhD Thesis we investigated the structure and dynamics of galactic dark matter (DM) halos, encouraged by the complex scenario emerging about their mass profile. In fact, while the standard hierarchical clustering ($\Lambda$)CDM scenario leads naturally to the NFW profile, the latter is challenged by observations. These include

- the much larger predicted number of satellite halos in Milky-Way type galaxies than observed (missing satellite problem, Klypin et al., 1999; Moore et al., 1999),
- the discrepancy between the predicted sharp increasing of DM halo density profile (cusp) towards its center and the observations that indicate a constant-density core (core-cusp problem, Dubinski and Carlberg, 1991; Navarro et al., 1996b, 1997; de Blok et al., 1996; McGaugh and de Blok, 1998),
- the majority of the most massive predicted subhalos of the Milky Way are too dense to host any of its observed bright satellites (too big to fail TBTF, Boylan-Kolchin et al., 2011).

In view of all these galactic and sub-galactic challenges of the standard ($\Lambda$)CDM model and due to the fact that the only evidence of DM is of gravitational origins, it is reasonable to imagine that what we observe in galaxies is not a new kind of matter

but a deviation of the law of gravitation with respect to Newtonian Gravity and General Relativity. Therefore, in this Thesis we test whether a well known modified theories of gravity, without DM, can be applied to the observed rotation curves (RCs) in order to account for their inner behaviour. In particular, we analyzed the high quality and very extended RCs of two objects, the Dwarf Orion galaxy and the spiral galaxy NGC 3198, in the framework of $R^n$ gravity. The latter is the recently proposed theory of the modification of the usual Newtonian gravitational potential generated by matter as an effect of power-law forth order theories of gravity (Capozziello et al., 2007). We found that in these two galaxies the no DM power-law f(R) case fits the RCs much better than ($\Lambda$)CDM halo models, encouraging further investigation of this theory.

Next we study one of the greatest challenges for current numerical cosmology - the core-cusp controversy. For this purpose, we derived the mass content of the spiral galaxy NGC 3198 by means of high quality very extended 21 cm kinematical data obtained by Gentile et al. (2013) combining them with the optical RCs of the innermost region of the galaxy presented in Corradi et al. (1991); Daigle et al. (2006). Then we mass modelled the RC of NGC 3198 as consisting of three components, namely the stellar disk, the gaseous disk and the dark halo. However, it is very well known that the mass models of spirals have degeneracies that might prevent an unique mass decomposition. The most important relates to the unknown value of the stellar mass-to-light ratio, that complicates the derivation of the inner DM density slope. Therefore, in some cases where the RC is almost always flattish as in NGC 3198, the latter are well fitted by either a core or a cuspy DM halo, by just adjusting the amount of the stellar matter content. Nevertheless, in the case of the cuspy NFW profile, we found that the resulting best fit parameters are not physical. Furthermore, we used the model independent local DM density analysis, developed by Salucci et al. (2010), in order to discriminate between a core or a cuspy profile even in this difficult case. In fact, the derived DM density profile of NGC 3198 corresponds to a cored distribution of DM. Additionally we also tested whether the baryon modified mass-dependent density profile, which emerges from hydrodynamic simulations (see Di Cintio et al., 2014b) in ($\Lambda$)CDM scenario, fits the derived density profile of NGC 3198 with the adequate and physically sound best fit parameters. Such baryonic ($\Lambda$)CDM halo profile fits the detected halo density very well especially in its cored region and the emerging fit parameters are compatible to those of the cored Burkert profile. However, at the large distances, $\sim$ 25 kpc, the DM halo density derived here results in a clash, i.e. it is significantly overdense than the outcome of the hydrodynamical N-body ($\Lambda$)CDM simulations by Di Cintio et al. (2014b). Similar result was also shown in Gentile et al. (2007c). Therefore, as a future perspective, it will be extremely interesting to test this result with more data in order to improve statistical significance.

In the second part of this Thesis we investigated the dark and luminous matter properties of dwarf disk galaxies in the Local Volume ($\sim$ 11 Mpc, Karachentsev et al., 2013) by means of their kinematical data.

Local dwarf disk dominated galaxies are interesting systems for many reasons. First of all, they are close enough to study their dynamical properties. Second of all, they are the most common type of galaxies (together with dwarf spheroidals) in the Universe. Dwarf disk galaxies can be considered late-type galaxies, at least as concerning the rotation curve and the associated dark matter. Additionally, dwarf low-mass galaxies are characterized by low baryonic fraction, i.e. they are DM dominated at any radius, which is, therefore, ideal for studying the structure of DM haloes. Consequently, dwarf galaxies are a key part of the galaxy formation and evolution.

In this work, we analyzed the kinematical data of a sample of dwarf disk galaxies in order to extend to them the property related to the concept of RCs universality [1] and then, to use it to derive their DM distribution.

We considered 36 Local Volume objects for which we collected both the HI and optical kinematical data. The optical data, by Moiseev (2014), used in our analysis, have never been applied for the mass modelling before. Furthermore, by investigating the galaxies in a limited size volume guarantee us against several luminosity biases that may affect such faint objects. We also would like to stress, that studying the nearest galaxies provides us a direct window to low-mass systems in the high-redshift Universe (Boylan-Kolchin et al., 2016).

Our sample includes low surface brightness dwarf irregular galaxies and blue compact dwarf galaxies; moreover, these objects are spanning $\sim$ 2 decades in luminosity ($\sim 10^6 - 3 \times 10^8 L_\odot$); as results it is found that their RCs, $V(R)$, in physical units, km/s and kpc are very diverse. However, surprisingly, once we normalized them on their optical radii and optical velocities, all our double normalized RCs have become similar to each other, leading to a universal velocity profile. Noticeably, this universal velocity profile is very similar to the first luminosity bin of Persic et al. (1996), that contains 30 normal spiral galaxies with the average I-band magnitude of $\langle M_I \rangle = -18.29$.

Then, we applied to the universal double normalized RC the standard mass modelling by using three different DM density profiles: NFW (Navarro et al., 1996a), Burkert (Burkert, 1995a) and the mass-dependent baryonic halo profile (Di Cintio et al., 2014b). Next, we used the denormalization procedure and found, galaxy by galaxy, the values of

[1] The RCs of spirals are rigidly determined by a single function of total galaxy luminosity and of characteristic radius of the luminous matter distribution. This scenario was set by Persic et al. (1996) and extended to large galactocentric radii by Salucci et al. (2007).

the dark and luminous matter structural parameters. The results of this analysis can be briefly summarized as follows:

- the mass modelling result points to the cored DM distribution in dwarf disk galaxies, where the cuspy NFW profile fails to reproduce the coadded curve. Additionally, these systems are totally DM dominated and their density shows a core size between 2 and 3 disk scale lengths;
- similar to what happened in galaxies of different Hubble type and luminosities (see, e.g., Kormendy and Freeman, 2004; Gentile et al., 2009; Donato et al., 2009a; Plana et al., 2010; Salucci et al., 2012), the core radius $r_0$ and the central density $\rho_0$ of the DM halo emerge related by $r_0\rho_0 \sim 100 M_\odot pc^{-2}$;
- no sharp decline in the baryonic to halo mass relation was found. This result is in contradiction with the general predictions of the ($\Lambda$)CDM abundance matching or semianalytical models of galaxy formation. The latter predict that there are no dwarf galaxies in halos with virial masses below $10^{10} M_\odot$;
- in order to set the relationships between properties of dark and luminous matter, e.g. the disk length scale versus the halo mass or the central density versus core radius, we need to introduce a new quantity, which we call compactness $C$[1].
- differently from what happens in normal spirals the Universal Function that describes the RCs in physical units has two parameters, disk mass $M_D$ and the newly introduced compactness of the stellar component $C$. This accounts for the diversity of the luminosities and morphologies of these galaxies.

The above results point out that the cosmological relationships holding in spirals break down at low-masses. This may indicate that there are some uncounted baryonic effects and/or some additional physics related to the dark matter particle. Besides, in future, we are going to use the above results together with the Local Volume luminosity functions (Karachentsev et al., 2013) in order to construct the corresponding stellar mass and halo mass functions. This will address the too big to fail and the deficit of small DM halos issues in a very advantaged situation.

By means of the above described results on the matter distribution in dwarf disk galaxies we are going to derive the specific angular momentum of the stars in these objects. The understanding of the relation between the specific angular momentum of

[1] $C$ is the ratio between the value of $R_D$ measured from photometry and that *predicted* from the measured galaxy disk mass $M_D$.

the baryons and that of the DM halo in galaxies of different morphologies is an extremely interesting task which might help in analyzing theories of galaxy formation and evolution.

Finally, we forecast big progress on the observational front with upcoming large-area HI interferometric surveys (such as WSRT and ASKAP, and eventually SKA). These data will greatly enlarge the current sample leading to a wide range of results.

In conclusion, by means of Fig. 5.0.1, where it is shown the central surface brightness versus the absolute magnitude in I-band for different type of galaxies, we indicate that the distribution of DM in normal spirals and, most probably, in low surface brightness (LSB) is known and it diverges from ($\Lambda$)CDM predictions. However, for the rest of galaxies we need farther investigations.

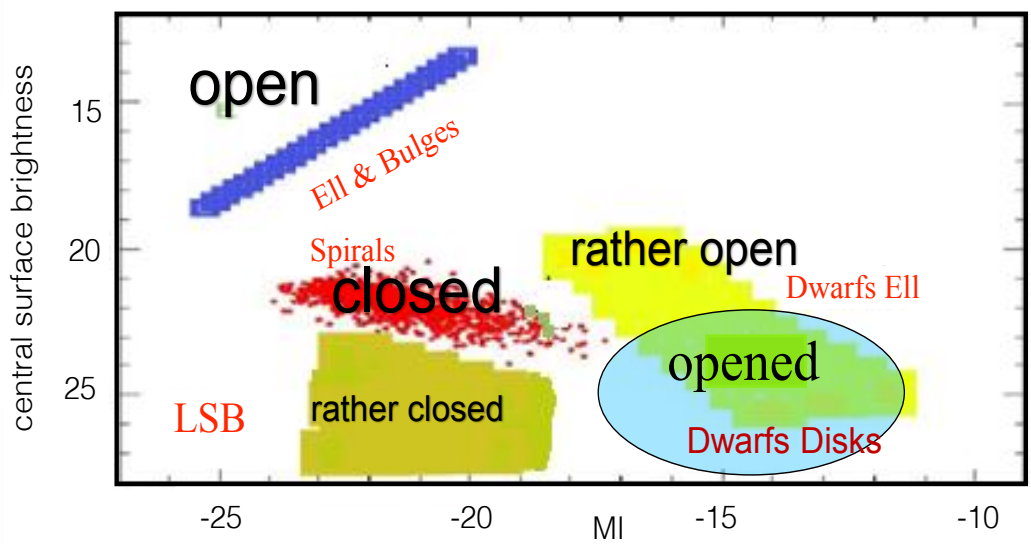


**Figure 5.0.1:** The central surface brightness versus the absolute magnitude in I-band.

# References


Ackermann, M. et al. (2012). Search for Dark Matter Satellites using the FERMI-LAT. *Astrophys. J.*, 747:121. 11

Agnese, R. et al. (2013). Silicon Detector Dark Matter Results from the Final Exposure of CDMS II. *Phys. Rev. Lett.*, 111(25):251301. 10

Agnese, R. et al. (2014). Search for Low-Mass Weakly Interacting Massive Particles with SuperCDMS. *Phys. Rev. Lett.*, 112(24):241302. 10

Akerib, D. S. et al. (2014). First results from the LUX dark matter experiment at the Sanford Underground Research Facility. *Phys. Rev. Lett.*, 112:091303. 10

Allen, S. W., Schmidt, R. W., Fabian, A. C., and Ebeling, H. (2003). Cosmological constraints from the local X-ray luminosity function of the most X-ray-luminous galaxy clusters. *MNRAS*, 342:287–298. 3

Arraki, K. S., Klypin, A., More, S., and Trujillo-Gomez, S. (2014). Effects of baryon removal on the structure of dwarf spheroidal galaxies. *MNRAS*, 438:1466–1482. 17

Athanassoula, E., Bosma, A., and Papaioannou, S. (1987). Halo parameters of spiral galaxies. *Astron. Astrophys.*, 179:23–40. 28

Babcock, H. W. (1939). The rotation of the Andromeda Nebula. *Lick Observatory Bulletin*, 19:41–51. 2

Battaglia, G., Helmi, A., Tolstoy, E., Irwin, M., Hill, V., and Jablonka, P. (2008). The Kinematic Status and Mass Content of the Sculptor Dwarf Spheroidal Galaxy. *The Astrophysical Journal Letters*, 681:L13. 12

Begeman, K. G. (1987). *HI rotation curves of spiral galaxies.* PhD thesis, , Kapteyn Institute, (1987). 28

## REFERENCES


Begeman, K. G., Broeils, A. H., and Sanders, R. H. (1991). Extended rotation curves of spiral galaxies - Dark haloes and modified dynamics. *MNRAS*, 249:523–537. 28

Begum, A. and Chengalur, J. N. (2004). Kinematics of two dwarf galaxies in the NGC 6946 group. *Astron. Astrophys.*, 424:509–517. 54

Bell, E. F. and de Jong, R. S. (2001). Stellar Mass-to-Light Ratios and the Tully-Fisher Relation. *The Astrophysical Journal*, 550:212–229. 62

Bell, E. F., McIntosh, D. H., Katz, N., and Weinberg, M. D. (2003). The Optical and Near-Infrared Properties of Galaxies. I. Luminosity and Stellar Mass Functions. *The Astrophysical Journal Supp. Series*, 149:289–312. 70

Bernabei, R. et al. (2013). Final model independent result of DAMA/LIBRA-phase1. *Eur. Phys. J.*, C73:2648. 10

Binggeli, B. (1994). A Note on the Definition and Nomenclature of Dwarf Galaxies. In Meylan, G. and Prugniel, P., editors, *European Southern Observatory Conference and Workshop Proceedings*, volume 49 of *European Southern Observatory Conference and Workshop Proceedings*, page 13. 52

Binney, J., Gerhard, O., and Silk, J. (2001). The dark matter problem in disc galaxies. *MNRAS*, 321:471–474. iv

Blumenthal, G. R., Faber, S. M., Primack, J. R., and Rees, M. J. (1984). Formation of galaxies and large-scale structure with cold dark matter. *Nature*, 311:517–525. 8

Bode, P., Ostriker, J. P., and Turok, N. (2001). Halo Formation in Warm Dark Matter Models. *The Astrophysical Journal*, 556:93–107. 9

Bœhm, C., Fayet, P., and Schaeffer, R. (2001). Constraining dark matter candidates from structure formation. *Physics Letters B*, 518:8–14. 9

Boehm, C., Mathis, H., Devriendt, J., and Silk, J. (2005). Non-linear evolution of suppressed dark matter primordial power spectra. *MNRAS*, 360:282–287. 9

Bœhm, C., Riazuelo, A., Hansen, S. H., and Schaeffer, R. (2002). Interacting dark matter disguised as warm dark matter. *Phys. Rev. D*, 66(8):083505. 9

Bœhm, C., Schewtschenko, J. A., Wilkinson, R. J., Baugh, C. M., and Pascoli, S. (2014). Using the Milky Way satellites to study interactions between cold dark matter and radiation. *MNRAS*, 445:L31–L35. 9

Bosma, A. (1978). *The distribution and kinematics of neutral hydrogen in spiral galaxies of various morphological types*. PhD thesis, PhD Thesis, Groningen Univ., (1978). 2, 28

Bosma, A. (1981a). 21-cm line studies of spiral galaxies. I - Observations of the galaxies NGC 5033, 3198, 5055, 2841, and 7331. II - The distribution and kinematics of neutral hydrogen in spiral galaxies of various morphological types. *Astronomic. J.*, 86:1791–1846. 2, 28

Bosma, A. (1981b). 21-cm line studies of spiral galaxies. II. The distribution and kinematics of neutral hydrogen in spiral galaxies of various morphological types. *Astronomic. J.*, 86:1825–1846. 2

Bosma, A. (2004). Dark Matter in Galaxies: Observational overview. In Ryder, S., Pisano, D., Walker, M., and Freeman, K., editors, *Dark Matter in Galaxies*, volume 220 of *IAU Symposium*, page 39. 50

Bosma, A. and van der Kruit, P. C. (1979). The local mass-to-light ratio in spiral galaxies. *Astron. Astrophys.*, 79:281–286. 28

Bottema, R. (1988). The stellar kinematics of the spiral galaxies NGC 3198 and NGC 3938. *Astron. Astrophys.*, 197:105–122. 28, 29

Boylan-Kolchin, M., Bullock, J. S., and Kaplinghat, M. (2011). Too big to fail? The puzzling darkness of massive Milky Way subhaloes. *MNRAS*, 415:L40–L44. 15, 85

Boylan-Kolchin, M., Bullock, J. S., and Kaplinghat, M. (2012). The Milky Way's bright satellites as an apparent failure of ΛCDM. *MNRAS*, 422:1203–1218. 15, 16, 50

Boylan-Kolchin, M., Weisz, D. R., Bullock, J. S., and Cooper, M. C. (2016). The Local Group: The Ultimate Deep Field. *ArXiv e-prints*. 51, 87

Bozorgnia, N., Calore, F., Schaller, M., Lovell, M., Bertone, G., Frenk, C. S., Crain, R. A., Navarro, J. F., Schaye, J., and Theuns, T. (2016). Simulated Milky Way analogues: implications for dark matter direct searches. *JCAP*, 1605(05):024. 11

Bringmann, T., Tveit Ihle, H., Kersten, J., and Walia, P. (2016). Suppressing structure formation at dwarf galaxy scales and below: late kinetic decoupling as a compelling alternative to warm dark matter. *ArXiv e-prints*. 9

## REFERENCES


Brook, C. B., Stinson, G., Gibson, B. K., Wadsley, J., and Quinn, T. (2012a). MaGICC discs: matching observed galaxy relationships over a wide stellar mass range. *MNRAS*, 424:1275–1283. 44

Brook, C. B., Stinson, G. S., Gibson, B. K., Kawata, D., House, E. L., Miranda, M. S., Macciò, A. V., Pilkington, K., Roškar, R., Wadsley, J., and Quinn, T. R. (2012b). Thin disc, thick disc and halo in a simulated galaxy. *MNRAS*, 426:690–700. 65

Buckley, M. R., Charles, E., Gaskins, J. M., Brooks, A. M., Drlica-Wagner, A., Martin, P., and Zhao, G. (2015). Search for gamma-ray emission from dark matter annihilation in the large magellanic cloud with the fermi large area telescope. *Phys. Rev. D*, 91(10):102001. 11

Bullock, J. S., Kolatt, T. S., Sigad, Y., Somerville, R. S., Kravtsov, A. V., Klypin, A. A., Primack, J. R., and Dekel, A. (2001). Profiles of dark haloes: evolution, scatter and environment. *MNRAS*, 321:559–575. 34

Burkert, A. (1995a). The Structure of Dark Matter Halos in Dwarf Galaxies. *The Astrophysical Journal Letters*, 447:L25. 13, 63, 87

Burkert, A. (1995b). The Structure of Dark Matter Halos in Dwarf Galaxies. *The Astrophysical Journal Letters*, 447:L25. 33

Burkert, A. (2015). The Structure and Dark Halo Core Properties of Dwarf Spheroidal Galaxies. *The Astrophysical Journal*, 808:158. 71

Calore, F., Bozorgnia, N., Lovell, M., Bertone, G., Schaller, M., Frenk, C. S., Crain, R. A., Schaye, J., Theuns, T., and Trayford, J. W. (2015). Simulated Milky Way analogues: implications for dark matter indirect searches. *JCAP*, 1512(12):053. 11

Capozziello, S., Cardone, V. F., Carloni, S., and Troisi, A. (2004). Can higher order curvature theories explain rotation curves of galaxies? *Physics Letters A*, 326:292–296. 21

Capozziello, S., Cardone, V. F., and Troisi, A. (2006). Dark energy and dark matter as curvature effects? *JCAP*, 8:001. 8, 21

Capozziello, S., Cardone, V. F., and Troisi, A. (2007). Low surface brightness galaxy rotation curves in the low energy limit of $R^n$ gravity: no need for dark matter? *MNRAS*, 375:1423–1440. iv, 4, 7, 86

Capozziello, S. and de Laurentis, M. (2011). Extended Theories of Gravity. *Phys. Rep.*, 509:167–321. 7, 21

Capozziello, S. and De Laurentis, M. (2012). The dark matter problem from f(R) gravity viewpoint. *Annalen der Physik*, 524:545–578. 25

Caputo, R., Buckley, M. R., Martin, P., Charles, E., Brooks, A. M., Drlica-Wagner, A., Gaskins, J., and Wood, M. (2016). Search for gamma-ray emission from dark matter annihilation in the Small Magellanic Cloud with the Fermi Large Area Telescope. *Phys. Rev. D*, 93(6):062004. 11

Carroll, S. M., Duvvuri, V., Trodden, M., and Turner, M. S. (2004). Is cosmic speed-up due to new gravitational physics? *Phys. Rev. D*, 70(4):043528. 21

Chan, T. K., Kereš, D., Oñorbe, J., Hopkins, P. F., Muratov, A. L., Faucher-Giguère, C.-A., and Quataert, E. (2015). The impact of baryonic physics on the structure of dark matter haloes: the view from the FIRE cosmological simulations. *MNRAS*, 454:2981–3001. 76

Cheriguène, M. F. (1975). A Kinematic Study of Several Barred Spirals. In Weliachew, L., editor, *La Dynamique des galaxies spirales*, page 439. 28, 29

Clowe, D., Bradač, M., Gonzalez, A. H., Markevitch, M., Randall, S. W., Jones, C., and Zaritsky, D. (2006). A Direct Empirical Proof of the Existence of Dark Matter. *The Astrophysical Journal Letters*, 648:L109–L113. 6

Colín, P., Valenzuela, O., and Avila-Reese, V. (2008). On the Structure of Dark Matter Halos at the Damping Scale of the Power Spectrum with and without Relict Velocities. *The Astrophysical Journal*, 673:203–214. 9

Collins, M. L. M., Chapman, S. C., Rich, R. M., Ibata, R. A., Martin, N. F., Irwin, M. J., Bate, N. F., Lewis, G. F., Peñarrubia, J., Arimoto, N., Casey, C. M., Ferguson, A. M. N., Koch, A., McConnachie, A. W., and Tanvir, N. (2014). The Masses of Local Group Dwarf Spheroidal Galaxies: The Death of the Universal Mass Profile. *The Astrophysical Journal*, 783:7. 16

Corradi, R. L. M., Boulesteix, J., Bosma, A., Amram, P., and Capaccioli, M. (1991). H-alpha morphology and kinematics of the spiral galaxy NGC 3198. *Astron. Astrophys.*, 244:27–36. 28, 29, 30, 31, 86

## REFERENCES


Daigle, O., Carignan, C., Amram, P., Hernandez, O., Chemin, L., Balkowski, C., and Kennicutt, R. (2006). H$\alpha$kinematics of the SINGS nearby galaxies survey - I*. *MNRAS*, 367:469–512. 28, 29, 30, 31, 86

Dalcanton, J. J. and Stilp, A. M. (2010). Pressure Support in Galaxy Disks: Impact on Rotation Curves and Dark Matter Density Profiles. *The Astrophysical Journal*, 721:547–561. 53

Dawson, W. A., Wittman, D., Jee, M. J., Gee, P., Hughes, J. P., Tyson, J. A., Schmidt, S., Thorman, P., Bradač, M., Miyazaki, S., Lemaux, B., Utsumi, Y., and Margoniner, V. E. (2012). Discovery of a Dissociative Galaxy Cluster Merger with Large Physical Separation. *The Astrophysical Journal Letters*, 747:L42. 9

Daylan, T., Finkbeiner, D. P., Hooper, D., Linden, T., Portillo, S. K. N., Rodd, N. L., and Slatyer, T. R. (2016). The characterization of the gamma-ray signal from the central Milky Way: A case for annihilating dark matter. *Physics of the Dark Universe*, 12:1–23. 11

de Blok, W. J. G. and Bosma, A. (2002a). High-resolution rotation curves of low surface brightness galaxies. *Astron. Astrophys.*, 385:816–846. 12, 50

de Blok, W. J. G. and Bosma, A. (2002b). High-resolution rotation curves of low surface brightness galaxies. *Astron. Astrophys.*, 385:816–846. 28

de Blok, W. J. G., McGaugh, S. S., Bosma, A., and Rubin, V. C. (2001). Mass Density Profiles of Low Surface Brightness Galaxies. *The Astrophysical Journal Letters*, 552:L23–L26. 12, 13

de Blok, W. J. G., McGaugh, S. S., and van der Hulst, J. M. (1996). HI observations of low surface brightness galaxies: probing low-density galaxies. *MNRAS*, 283:18–54. 85

de Blok, W. J. G., Walter, F., Brinks, E., Trachternach, C., Oh, S.-H., and Kennicutt, Jr., R. C. (2008). High-Resolution Rotation Curves and Galaxy Mass Models from THINGS. *Astronomic. J.*, 136:2648–2719. 28, 31, 32, 34, 38

de Vega, H. J., Moreno, O., Moya de Guerra, E., Ramón Medrano, M., and Sánchez, N. G. (2013). Role of sterile neutrino warm dark matter in rhenium and tritium beta decays. *Nuclear Physics B*, 866:177–195. 50

de Vega, H. J., Salucci, P., and Sanchez, N. G. (2014a). Observational rotation curves and density profiles versus the Thomas-Fermi galaxy structure theory. *MNRAS*, 442:2717–2727. iv, 9, 43

de Vega, H. J., Salucci, P., and Sanchez, N. G. (2014b). Observational rotation curves and density profiles versus the Thomas-Fermi galaxy structure theory. *MNRAS*, 442:2717–2727. 50

de Vega, H. J. and Sanchez, N. G. (2013). Dark matter in galaxies: the dark matter particle mass is about 7 keV. *ArXiv e-prints*. 50

Destri, C., de Vega, H. J., and Sanchez, N. G. (2013). Fermionic warm dark matter produces galaxy cores in the observed scales because of quantum mechanics. *New Astronomy*, 22:39–50. 9

Di Cintio, A., Brook, C. B., Dutton, A. A., Macciò, A. V., Stinson, G. S., and Knebe, A. (2014a). A mass-dependent density profile for dark matter haloes including the influence of galaxy formation. *MNRAS*, 441:2986–2995. 43, 44, 45, 46, 47

Di Cintio, A., Brook, C. B., Macciò, A. V., Stinson, G. S., Knebe, A., Dutton, A. A., and Wadsley, J. (2014b). The dependence of dark matter profiles on the stellar-to-halo mass ratio: a prediction for cusps versus cores. *MNRAS*, 437:415–423. 17, 19, 27, 50, 64, 65, 76, 86, 87

Donato, F., Gentile, G., Salucci, P., Frigerio Martins, C., Wilkinson, M. I., Gilmore, G., Grebel, E. K., Koch, A., and Wyse, R. (2009a). A constant dark matter halo surface density in galaxies. *MNRAS*, 397:1169–1176. 22, 50, 71, 88

Donato, F., Gentile, G., Salucci, P., Frigerio Martins, C., Wilkinson, M. I., Gilmore, G., Grebel, E. K., Koch, A., and Wyse, R. (2009b). A constant dark matter halo surface density in galaxies. *MNRAS*, 397:1169–1176. 43

Doroshkevich, A. G., Zeldovich, Y. B., Syunyaev, R. A., and Khlopov, M. Y. (1980). Astrophysical implications of the neutrino rest mass. II - The density-perturbation spectrum and small-scale fluctuations in the microwave background. III - Nonlinear growth of perturbations and the missing mass. *Pisma v Astronomicheskii Zhurnal*, 6:457–469. 8

Drlica-Wagner, A. et al. (2015). Search for Gamma-Ray Emission from DES Dwarf Spheroidal Galaxy Candidates with Fermi-LAT Data. *Astrophys. J.*, 809(1):L4. 11

## REFERENCES


Dubinski, J. and Carlberg, R. G. (1991). The structure of cold dark matter halos. *The Astrophysical Journal*, 378:496–503. 12, 85

Dvorkin, C., Blum, K., and Kamionkowski, M. (2014). Constraining dark matter-baryon scattering with linear cosmology. *Phys. Rev. D*, 89(2):023519. 9

Elbert, O. D., Bullock, J. S., Garrison-Kimmel, S., Rocha, M., Oñorbe, J., and Peter, A. H. G. (2015). Core formation in dwarf haloes with self-interacting dark matter: no fine-tuning necessary. *MNRAS*, 453:29–37. 50

Epinat, B., Amram, P., Marcelin, M., Balkowski, C., Daigle, O., Hernandez, O., Chemin, L., Carignan, C., Gach, J.-L., and Balard, P. (2008). GHASP: an H$\alpha$ kinematic survey of spiral and irregular galaxies - VI. New H$\alpha$ data cubes for 108 galaxies. *MNRAS*, 388:500–550. 54

Evoli, C., Salucci, P., Lapi, A., and Danese, L. (2011). The H I Content of Local Late-type Galaxies. *The Astrophysical Journal*, 743:45. 68

Ferrero, I., Abadi, M. G., Navarro, J. F., Sales, L. V., and Gurovich, S. (2012). The dark matter haloes of dwarf galaxies: a challenge for the $\Lambda$ cold dark matter paradigm? *MNRAS*, 425:2817–2823. 14, 15, 16, 17, 50, 72, 76

Fields, B. and Sarkar, S. (2006). Big-Bang nucleosynthesis (Particle Data Group mini-review). *ArXiv Astrophysics e-prints*. 3

Freedman, W. L., Madore, B. F., Gibson, B. K., Ferrarese, L., Kelson, D. D., Sakai, S., Mould, J. R., Kennicutt, Jr., R. C., Ford, H. C., Graham, J. A., Huchra, J. P., Hughes, S. M. G., Illingworth, G. D., Macri, L. M., and Stetson, P. B. (2001). Final Results from the Hubble Space Telescope Key Project to Measure the Hubble Constant. *The Astrophysical Journal*, 553:47–72. 28

Freeman, K. C. (1970). On the Disks of Spiral and so Galaxies. *The Astrophysical Journal*, 160:811. 25, 38, 62

Frigerio Martins, C. and Salucci, P. (2007). Analysis of rotation curves in the framework of R$^n$ gravity. *MNRAS*, 381:1103–1108. 8, 21, 23

Frusciante, N., Salucci, P., Vernieri, D., Cannon, J. M., and Elson, E. C. (2012). The distribution of mass in the Orion dwarf Galaxy. *MNRAS*, 426:751–757. 22

Fukugita, M., Shimasaku, K., and Ichikawa, T. (1995). Galaxy Colors in Various Photometric Band Systems. *PASP*, 107:945. 52

Garrison-Kimmel, S., Boylan-Kolchin, M., Bullock, J. S., and Kirby, E. N. (2014a). Too big to fail in the Local Group. *MNRAS*, 444:222–236. 50

Garrison-Kimmel, S., Boylan-Kolchin, M., Bullock, J. S., and Lee, K. (2014b). ELVIS: Exploring the Local Volume in Simulations. *MNRAS*, 438:2578–2596. 16

Garzilli, A., Boyarsky, A., and Ruchayskiy, O. (2015). Cutoff in the Lyman {\alpha} forest power spectrum: warm IGM or warm dark matter? *ArXiv e-prints*. 9

Gentile, G. (2008). MOND and the Universal Rotation Curve: Similar Phenomenologies. *The Astrophysical Journal*, 684:1018–1025. 28, 30

Gentile, G., Angus, G. W., Famaey, B., Oh, S.-H., and de Blok, W. J. G. (2012). Isolated and non-isolated dwarfs in terms of modified Newtonian dynamics. *Astron. Astrophys.*, 543:A47. 53, 54, 62, 63

Gentile, G., Baes, M., Famaey, B., and van Acoleyen, K. (2010). Mass models from high-resolution HI data of the dwarf galaxy NGC 1560. *MNRAS*, 406:2493–2503. 53, 54, 62, 63

Gentile, G., Burkert, A., Salucci, P., Klein, U., and Walter, F. (2005). The Dwarf Galaxy DDO 47 as a Dark Matter Laboratory: Testing Cusps Hiding in Triaxial Halos. *The Astrophysical Journal Letters*, 634:L145–L148. 12, 28, 47, 50

Gentile, G., Famaey, B., Combes, F., Kroupa, P., Zhao, H. S., and Tiret, O. (2007a). Tidal dwarf galaxies as a test of fundamental physics. *Astron. Astrophys.*, 472:L25–L28. 4

Gentile, G., Famaey, B., Zhao, H., and Salucci, P. (2009). Universality of galactic surface densities within one dark halo scale-length. *Nature*, 461:627–628. 71, 88

Gentile, G., Józsa, G. I. G., Serra, P., Heald, G. H., de Blok, W. J. G., Fraternali, F., Patterson, M. T., Walterbos, R. A. M., and Oosterloo, T. (2013). HALOGAS: Extraplanar gas in NGC 3198. *Astron. Astrophys.*, 554:A125. 22, 28, 29, 30, 31, 32, 38, 47, 86

Gentile, G., Salucci, P., Klein, U., and Granato, G. L. (2007b). NGC 3741: the dark halo profile from the most extended rotation curve. *MNRAS*, 375:199–212. 4

Gentile, G., Salucci, P., Klein, U., Vergani, D., and Kalberla, P. (2004). The cored distribution of dark matter in spiral galaxies. *MNRAS*, 351:903–922. 13, 28, 36, 50

Gentile, G., Tonini, C., and Salucci, P. (2007c). ΛCDM halo density profiles: where do actual halos converge to NFW ones? *Astron. Astrophys.*, 467:925–931. 48, 50, 54, 86

Gilmore, G., Wilkinson, M. I., Wyse, R. F. G., Kleyna, J. T., Koch, A., Evans, N. W., and Grebel, E. K. (2007). The Observed Properties of Dark Matter on Small Spatial Scales. *The Astrophysical Journal*, 663:948–959. 12, 50

Gnedin, O. Y., Kravtsov, A. V., Klypin, A. A., and Nagai, D. (2004). Response of Dark Matter Halos to Condensation of Baryons: Cosmological Simulations and Improved Adiabatic Contraction Model. *The Astrophysical Journal*, 616:16–26. 43

Gnedin, O. Y. and Zhao, H. (2002). Maximum feedback and dark matter profiles of dwarf galaxies. *MNRAS*, 333:299–306. 17

Goodman, M. W. and Witten, E. (1985). Detectability of Certain Dark Matter Candidates. *Phys. Rev.*, D31:3059. 10

Governato, F., Brook, C., Mayer, L., Brooks, A., Rhee, G., Wadsley, J., Jonsson, P., Willman, B., Stinson, G., Quinn, T., and Madau, P. (2010). Bulgeless dwarf galaxies and dark matter cores from supernova-driven outflows. *Nature*, 463:203–206. iv, 17

Governato, F., Zolotov, A., Pontzen, A., Christensen, C., Oh, S. H., Brooks, A. M., Quinn, T., Shen, S., and Wadsley, J. (2012). Cuspy no more: how outflows affect the central dark matter and baryon distribution in Λ cold dark matter galaxies. *MNRAS*, 422:1231–1240. 17, 18

Guo, Q., White, S., Li, C., and Boylan-Kolchin, M. (2010). How do galaxies populate dark matter haloes? *MNRAS*, 404:1111–1120. 16

Heald, G., Józsa, G., Serra, P., Zschaechner, L., Rand, R., Fraternali, F., Oosterloo, T., Walterbos, R., Jütte, E., and Gentile, G. (2011). The Westerbork Hydrogen Accretion in LOcal GAlaxieS (HALOGAS) survey. I. Survey description and pilot observations. *Astron. Astrophys.*, 526:A118. 29

Herrmann, K. A., Hunter, D. A., and Elmegreen, B. G. (2013). Surface Brightness Profiles of Dwarf Galaxies. I. Profiles and Statistics. *Astronomic. J.*, 146:104. 54

Holmberg, E. (1937). A study of double and multiple galaxies. *Annals of the Observatory of Lund*, 6. 2

Hunter, D. A. and Elmegreen, B. G. (2004). Star Formation Properties of a Large Sample of Irregular Galaxies. *Astronomic. J.*, 128:2170–2205. 54

Hunter, D. A., Elmegreen, B. G., Oh, S.-H., Anderson, E., Nordgren, T. E., Massey, P., Wilsey, N., and Riabokin, M. (2011). The Outer Disks of Dwarf Irregular Galaxies. *Astronomic. J.*, 142:121. 54

Hunter, D. A., Ficut-Vicas, D., Ashley, T., Brinks, E., Cigan, P., Elmegreen, B. G., Heesen, V., Herrmann, K. A., Johnson, M., Oh, S.-H., Rupen, M. P., Schruba, A., Simpson, C. E., Walter, F., Westpfahl, D. J., Young, L. M., and Zhang, H.-X. (2012). Little Things. *Astronomic. J.*, 144:134. 54

Hunter, D. A., Rubin, V. C., and Gallagher, III, J. S. (1986). Optical rotation velocities and images of the spiral galaxy NGC 3198. *Astronomic. J.*, 91:1086–1090. 28, 29

Jarrett, T. H., Chester, T., Cutri, R., Schneider, S. E., and Huchra, J. P. (2003). The 2MASS Large Galaxy Atlas. *Astronomic. J.*, 125:525–554. 52

Jeans, J. H. (1922). The motions of stars in a Kapteyn universe. *MNRAS*, 82:122–132. 1

Jee, M. J., Mahdavi, A., Hoekstra, H., Babul, A., Dalcanton, J. J., Carroll, P., and Capak, P. (2012). A Study of the Dark Core in A520 with the Hubble Space Telescope: The Mystery Deepens. *The Astrophysical Journal*, 747:96. 9

Jungman, G., Kamionkowski, M., and Griest, K. (1996). Supersymmetric dark matter. *Phys. Rep.*, 267:195–373. 3

Kahlhoefer, F., Schmidt-Hoberg, K., Frandsen, M. T., and Sarkar, S. (2014). Colliding clusters and dark matter self-interactions. *Mon. Not. Roy. Astron. Soc.*, 437(3):2865–2881. 9

Kapteyn, J. C. (1922). First Attempt at a Theory of the Arrangement and Motion of the Sidereal System. *The Astrophysical Journal*, 55:302. 1

Karachentsev, I. D., Chengalur, J. N., Tully, R. B., Makarova, L. N., Sharina, M. E., Begum, A., and Rizzi, L. (2016). Andromeda IV, a solitary gas-rich dwarf galaxy. *Astronomische Nachrichten*, 337:306. 53, 54

Karachentsev, I. D., Makarov, D. I., and Kaisina, E. I. (2013). Updated Nearby Galaxy Catalog. *Astronomic. J.*, 145:101. v, 51, 52, 54, 87, 88

Katz, H., McGaugh, S. S., Sellwood, J. A., and de Blok, W. J. G. (2014). The formation of spiral galaxies: adiabatic compression with Young's algorithm and the relation of dark matter haloes to their primordial antecedents. *MNRAS*, 439:1897–1908. 43

Kent, S. M. (1986). Dark matter in spiral galaxies. I - Galaxies with optical rotation curves. *Astronomic. J.*, 91:1301–1327. 28

Kent, S. M. (1987). Dark matter in spiral galaxies. II - Galaxies with H I rotation curves. *Astronomic. J.*, 93:816–832. 28, 29

Kirby, E. N., Bullock, J. S., Boylan-Kolchin, M., Kaplinghat, M., and Cohen, J. G. (2014). The dynamics of isolated Local Group galaxies. *MNRAS*, 439:1015–1027. 16

Klypin, A., Karachentsev, I., Makarov, D., and Nasonova, O. (2015). Abundance of field galaxies. *MNRAS*, 454:1798–1810. 14, 15, 50

Klypin, A., Kravtsov, A. V., Valenzuela, O., and Prada, F. (1999). Where Are the Missing Galactic Satellites? *The Astrophysical Journal*, 522:82–92. 14, 50, 85

Klypin, A. A., Trujillo-Gomez, S., and Primack, J. (2011). Dark Matter Halos in the Standard Cosmological Model: Results from the Bolshoi Simulation. *The Astrophysical Journal*, 740:102. 34

Koch, A., Wilkinson, M. I., Kleyna, J. T., Gilmore, G. F., Grebel, E. K., Mackey, A. D., Evans, N. W., and Wyse, R. F. G. (2007). Stellar Kinematics and Metallicities in the Leo I Dwarf Spheroidal Galaxy-Wide-Field Implications for Galactic Evolution. *The Astrophysical Journal*, 657:241–261. 12

Komatsu, E., Smith, K. M., Dunkley, J., Bennett, C. L., Gold, B., Hinshaw, G., Jarosik, N., Larson, D., Nolta, M. R., Page, L., Spergel, D. N., Halpern, M., Hill, R. S., Kogut, A., Limon, M., Meyer, S. S., Odegard, N., Tucker, G. S., Weiland, J. L., Wollack, E., and Wright, E. L. (2011). Seven-year Wilkinson Microwave Anisotropy Probe (WMAP) Observations: Cosmological Interpretation. *The Astrophysical Journal Supp. Series*, 192:18. 4

Kormendy, J. (1985). Families of ellipsoidal stellar systems and the formation of dwarf elliptical galaxies. *The Astrophysical Journal*, 295:73–79. 52

Kormendy, J. and Freeman, K. C. (2004). Scaling Laws for Dark Matter Halos in Late-Type and Dwarf Spheroidal Galaxies. In Ryder, S., Pisano, D., Walker, M., and Freeman, K., editors, *Dark Matter in Galaxies*, volume 220 of *IAU Symposium*, page 377. 71, 88

Kuijken, K. and Gilmore, G. (1989). The Mass Distribution in the Galactic Disc - Part III - the Local Volume Mass Density. *MNRAS*, 239:651–664. 1

Kuzio de Naray, R., Martinez, G. D., Bullock, J. S., and Kaplinghat, M. (2010). The Case Against Warm or Self-Interacting Dark Matter as Explanations for Cores in Low Surface Brightness Galaxies. *The Astrophysical Journal Letters*, 710:L161–L166. 9

Lelli, F., McGaugh, S. S., and Schombert, J. M. (2016). SPARC: Mass Models for 175 Disk Galaxies with Spitzer Photometry and Accurate Rotation Curves. *ArXiv e-prints*. 70, 71

Lelli, F., Verheijen, M., and Fraternali, F. (2014). Dynamics of starbursting dwarf galaxies. III. A H I study of 18 nearby objects. *Astron. Astrophys.*, 566:A71. 53, 54

Lelli, F., Verheijen, M., Fraternali, F., and Sancisi, R. (2012). Dynamics of starbursting dwarf galaxies. II. UGC 4483. *Astron. Astrophys.*, 544:A145. 53

Lovell, M. R., Frenk, C. S., Eke, V. R., Jenkins, A., Gao, L., and Theuns, T. (2014). The properties of warm dark matter haloes. *MNRAS*, 439:300–317. iv, 9, 50

Lubini, M., Tortora, C., Näf, J., Jetzer, P., and Capozziello, S. (2011). Probing the dark matter issue in f( R)-gravity via gravitational lensing. *European Physical Journal C*, 71:1834. 8

Macciò, A. V., Paduroiu, S., Anderhalden, D., Schneider, A., and Moore, B. (2012). Cores in warm dark matter haloes: a Catch 22 problem. *MNRAS*, 424:1105–1112. 9

Madau, P., Shen, S., and Governato, F. (2014). Dark Matter Heating and Early Core Formation in Dwarf Galaxies. *The Astrophysical Journal Letters*, 789:L17. 17

Mahdavi, A., Hoekstra, H., Babul, A., Balam, D. D., and Capak, P. L. (2007). A Dark Core in Abell 520. *The Astrophysical Journal*, 668:806–814. 9

Martin, M. C. (1998). Catalogue of HI maps of galaxies. I. *Astron. Astrophys. Supp. Series*, 131:73–75. 54

Mashchenko, S., Couchman, H. M. P., and Wadsley, J. (2006). The removal of cusps from galaxy centres by stellar feedback in the early Universe. *Nature*, 442:539–542. 17, 50

McGaugh, S. (2014). The Third Law of Galactic Rotation. *Galaxies*, 2:601–622. 56

McGaugh, S. S. (2004). The Mass Discrepancy-Acceleration Relation: Disk Mass and the Dark Matter Distribution. *The Astrophysical Journal*, 609:652–666. 4

McGaugh, S. S. (2005). The Baryonic Tully-Fisher Relation of Galaxies with Extended Rotation Curves and the Stellar Mass of Rotating Galaxies. *The Astrophysical Journal*, 632:859–871. 4

McGaugh, S. S., Barker, M. K., and de Blok, W. J. G. (2003). A Limit on the Cosmological Mass Density and Power Spectrum from the Rotation Curves of Low Surface Brightness Galaxies. *The Astrophysical Journal*, 584:566–576. 36

McGaugh, S. S. and de Blok, W. J. G. (1998). Testing the Dark Matter Hypothesis with Low Surface Brightness Galaxies and Other Evidence. *The Astrophysical Journal*, 499:41–65. 85

McGaugh, S. S., Rubin, V. C., and de Blok, W. J. G. (2001). High-Resolution Rotation Curves of Low Surface Brightness Galaxies. I. Data. *Astronomic. J.*, 122:2381–2395. 12

McGaugh, S. S. and Schombert, J. M. (2015). Weighing Galaxy Disks With the Baryonic Tully-Fisher Relation. *The Astrophysical Journal*, 802:18. 70

Memola, E., Salucci, P., and Babić, A. (2011). Dark matter halos around isolated ellipticals. *Astron. Astrophys.*, 534:A50. 36

Milgrom, M. (1983). A modification of the Newtonian dynamics as a possible alternative to the hidden mass hypothesis. *The Astrophysical Journal*, 270:365–370. iv, 4, 5, 21

Milgrom, M. and Sanders, R. H. (2003). Modified Newtonian Dynamics and the "Dearth of Dark Matter in Ordinary Elliptical Galaxies". *The Astrophysical Journal Letters*, 599:L25–L28. 4

Mo, H. J. and Mao, S. (2004). Galaxy formation in pre-processed dark haloes. *MNRAS*, 353:829–840. 17

Moiseev, A. V. (2014). Ionized gas rotation curves in nearby dwarf galaxies. *Astrophysical Bulletin*, 69:1–20. 54, 87

Moore, B., Ghigna, S., Governato, F., Lake, G., Quinn, T., Stadel, J., and Tozzi, P. (1999). Dark Matter Substructure within Galactic Halos. *The Astrophysical Journal Letters*, 524:L19–L22. 14, 50, 85

Moster, B. P., Naab, T., and White, S. D. M. (2013). Galactic star formation and accretion histories from matching galaxies to dark matter haloes. *MNRAS*, 428:3121–3138. 16

Navarro, J. F., Eke, V. R., and Frenk, C. S. (1996a). The cores of dwarf galaxy haloes. *MNRAS*, 283:L72–L78. 2, 17, 50, 87

Navarro, J. F., Frenk, C. S., and White, S. D. M. (1996b). The Structure of Cold Dark Matter Halos. *ApJ*, 462:563. 12, 28, 33, 63, 85

Navarro, J. F., Frenk, C. S., and White, S. D. M. (1997). A Universal Density Profile from Hierarchical Clustering. *The Astrophysical Journal*, 490:493–508. 12, 85

Newman, A. B., Treu, T., Ellis, R. S., and Sand, D. J. (2013a). The Density Profiles of Massive, Relaxed Galaxy Clusters. II. Separating Luminous and Dark Matter in Cluster Cores. *The Astrophysical Journal*, 765:25. 14

Newman, A. B., Treu, T., Ellis, R. S., Sand, D. J., Nipoti, C., Richard, J., and Jullo, E. (2013b). The Density Profiles of Massive, Relaxed Galaxy Clusters. I. The Total Density Over Three Decades in Radius. *The Astrophysical Journal*, 765:24. 14

Nojiri, S. and Odintsov, S. D. (2011). Unified cosmic history in modified gravity: From F(R) theory to Lorentz non-invariant models. *Phys. Rep.*, 505:59–144. 21

Nojiri, S. and Oodintsiv, S. D. (2007). Introduction to modified gravity and gravitational alternative for dark energy. *International Journal of Geometric Methods in Modern Physics*, 04(01):115–145. 7

Noordermeer, E., van der Hulst, J. M., Sancisi, R., Swaters, R. S., and van Albada, T. S. (2007). The mass distribution in early-type disc galaxies: declining rotation curves and correlations with optical properties. *MNRAS*, 376:1513–1546. 3, 51

Oñorbe, J., Boylan-Kolchin, M., Bullock, J. S., Hopkins, P. F., Kereš, D., Faucher-Giguère, C.-A., Quataert, E., and Murray, N. (2015). Forged in FIRE: cusps, cores and baryons in low-mass dwarf galaxies. *MNRAS*, 454:2092–2106. 76

Ogiya, G. and Burkert, A. (2015). Re-examining the too-big-to-fail problem for dark matter haloes with central density cores. *MNRAS*, 446:2363–2369. 17

Oh, S.-H., de Blok, W. J. G., Brinks, E., Walter, F., and Kennicutt, Jr., R. C. (2011). Dark and Luminous Matter in THINGS Dwarf Galaxies. *Astronomic. J.*, 141:193. 50, 53, 76

Oh, S.-H., Hunter, D. A., Brinks, E., Elmegreen, B. G., Schruba, A., Walter, F., Rupen, M. P., Young, L. M., Simpson, C. E., Johnson, M. C., Herrmann, K. A., Ficut-Vicas, D., Cigan, P., Heesen, V., Ashley, T., and Zhang, H.-X. (2015). High-resolution Mass Models of Dwarf Galaxies from LITTLE THINGS. *Astronomic. J.*, 149:180. 12, 13, 53, 54, 55, 62, 63, 76

Oman, K. A., Navarro, J. F., Fattahi, A., Frenk, C. S., Sawala, T., White, S. D. M., Bower, R., Crain, R. A., Furlong, M., Schaller, M., Schaye, J., and Theuns, T. (2015). The unexpected diversity of dwarf galaxy rotation curves. *MNRAS*, 452:3650–3665. 55

Oman, K. A., Navarro, J. F., Sales, L. V., Fattahi, A., Frenk, C. S., Sawala, T., Schaller, M., and White, S. D. M. (2016). Missing dark matter in dwarf galaxies? *ArXiv e-prints*. 76

Oort, J. H. (1932). The force exerted by the stellar system in the direction perpendicular to the galactic plane and some related problems. *Bull. Astron. Inst. Netherlands*, 6:249. 1

Öpik, E. (1915). . *Bull. de la Soc. Astr. de Russie*, 21:150. 1

Opik, E. V., Salucci, P., and Gentile, G. (2015). The dark matter distribution in the spiral NGC 3198 out to 0.22 $R_{vir}$. *Astron. Astrophys.*, 578:A13. 22

Ostriker, J. P. and Peebles, P. J. E. (1973). A Numerical Study of the Stability of Flattened Galaxies: or, can Cold Galaxies Survive? *The Astrophysical Journal*, 186:467–480. 2

Pace, A. B. (2016). Comparing rotation curve observations to hydrodynamic {\Lambda}CDM simulations of galaxies. *ArXiv e-prints*. 76

Page, T. (1952). Radial Velocities and Masses of Double Galaxies. *The Astrophysical Journal*, 116:63. 2

Page, T. (1959). Masses of the double galaxies. *Astronomic. J.*, 64:53. 2

Page, T. (1960). Average Masses and Mass-Luminosity Ratios of the Double Galaxies. *The Astrophysical Journal*, 132:910–912. 2

Palunas, P. and Williams, T. B. (2000). Maximum Disk Mass Models for Spiral Galaxies. *Astronomic. J.*, 120:2884–2903. 28

Papastergis, E., Giovanelli, R., Haynes, M. P., and Shankar, F. (2015). Is there a "too big to fail" problem in the field? *Astron. Astrophys.*, 574:A113. 16, 17, 50

Papastergis, E., Martin, A. M., Giovanelli, R., and Haynes, M. P. (2011). The Velocity Width Function of Galaxies from the 40% ALFALFA Survey: Shedding Light on the Cold Dark Matter Overabundance Problem. *The Astrophysical Journal*, 739:38. 14, 50

Parodi, B. R., Barazza, F. D., and Binggeli, B. (2002). Structure and stellar content of dwarf galaxies. VII. B and R photometry of 25 southern field dwarfs and a disk parameter analysis of the complete sample of nearby irregulars. *Astron. Astrophys.*, 388:29–49. 54

Perlmutter, S., Aldering, G., Goldhaber, G., Knop, R. A., Nugent, P., Castro, P. G., Deustua, S., Fabbro, S., Goobar, A., Groom, D. E., Hook, I. M., Kim, A. G., Kim, M. Y., Lee, J. C., Nunes, N. J., Pain, R., Pennypacker, C. R., Quimby, R., Lidman, C., Ellis, R. S., Irwin, M., McMahon, R. G., Ruiz-Lapuente, P., Walton, N., Schaefer, B., Boyle, B. J., Filippenko, A. V., Matheson, T., Fruchter, A. S., Panagia, N., Newberg, H. J. M., Couch, W. J., and Project, T. S. C. (1999). Measurements of $\Omega$ and $\Lambda$ from 42 High-Redshift Supernovae. *The Astrophysical Journal*, 517:565–586. 4

Persic, M. and Salucci, P. (1988). Dark and visible matter in spiral galaxies. *MNRAS*, 234:131–154. 28

Persic, M. and Salucci, P. (1991). The universal galaxy rotation curve. *The Astrophysical Journal*, 368:60–65. 3, 51

Persic, M. and Salucci, P. (1995). Rotation Curves of 967 Spiral Galaxies. *The Astrophysical Journal Supp. Series*, 99:501. 61, 77

Persic, M., Salucci, P., and Stel, F. (1996). The universal rotation curve of spiral galaxies - I. The dark matter connection. *MNRAS*, 281:27–47. v, 3, 13, 22, 49, 51, 87

Peter, A. H. G., Rocha, M., Bullock, J. S., and Kaplinghat, M. (2013). Cosmological simulations with self-interacting dark matter - II. Halo shapes versus observations. *MNRAS*, 430:105–120. 9

Pineda, J. C. B., Hayward, C. C., Springel, V., and Mendes de Oliveira, C. (2016). Rotation curve fitting and its fatal attraction to cores in realistically simulated galaxy observations. *ArXiv e-prints*. 76

Plana, H., Amram, P., Mendes de Oliveira, C., and Balkowski, C. (2010). Mass Distribution in Hickson Compact Groups of Galaxies. *Astronomic. J.*, 139:1–16. 71, 88

Pontzen, A. and Governato, F. (2012). How supernova feedback turns dark matter cusps into cores. *MNRAS*, 421:3464–3471. iv, 17, 50, 64

Pontzen, A. and Governato, F. (2014). Cold dark matter heats up. *Nature*, 506:171–178. 50, 64

Read, J. I. and Gilmore, G. (2005). Mass loss from dwarf spheroidal galaxies: the origins of shallow dark matter cores and exponential surface brightness profiles. *MNRAS*, 356:107–124. 17, 50

Read, J. I., Wilkinson, M. I., Evans, N. W., Gilmore, G., and Kleyna, J. T. (2006). The importance of tides for the Local Group dwarf spheroidals. *MNRAS*, 367:387–399. 17

Refregier, A. (2003). Weak Gravitational Lensing by Large-Scale Structure. *Annu. Rev. Astron. Astrophys.*, 41:645–668. 3

Riess, A. G., Filippenko, A. V., Challis, P., Clocchiatti, A., Diercks, A., Garnavich, P. M., Gilliland, R. L., Hogan, C. J., Jha, S., Kirshner, R. P., Leibundgut, B., Phillips, M. M., Reiss, D., Schmidt, B. P., Schommer, R. A., Smith, R. C., Spyromilio, J., Stubbs, C., Suntzeff, N. B., and Tonry, J. (1998). Observational Evidence from Supernovae for an Accelerating Universe and a Cosmological Constant. *Astronomic. J.*, 116:1009–1038. 3

Roberts, M. S. (1966). A High-Resolution 21-CM Hydrogen-Line Survey of the Andromeda Nebula. *The Astrophysical Journal*, 144:639. 2, 3

Roberts, M. S. and Rots, A. H. (1973). Comparison of Rotation Curves of Different Galaxy Types. *Astron. Astrophys.*, 26:483–485. 2

Robertson, A., Massey, R., and Eke, V. (2016). What does the Bullet Cluster tell us about Self-Interacting Dark Matter? *ArXiv e-prints*. 9

Rocha, M., Peter, A. H. G., Bullock, J. S., Kaplinghat, M., Garrison-Kimmel, S., Oñorbe, J., and Moustakas, L. A. (2013). Cosmological simulations with self-interacting dark matter - I. Constant-density cores and substructure. *MNRAS*, 430:81–104. 9

Rubin, V. C. (1983). The rotation of spiral galaxies. *Science*, 220:1339–1344. 21

Rubin, V. C., Burstein, D., Ford, Jr., W. K., and Thonnard, N. (1985). Rotation velocities of 16 SA galaxies and a comparison of Sa, Sb, and SC rotation properties. *The Astrophysical Journal*, 289:81–98. 3, 51

Rubin, V. C. and Ford, Jr., W. K. (1970). Rotation of the Andromeda Nebula from a Spectroscopic Survey of Emission Regions. *The Astrophysical Journal*, 159:379. 2, 3

Rubin, V. C., Ford, W. K. J., and . Thonnard, N. (1980). Rotational properties of 21 SC galaxies with a large range of luminosities and radii, from NGC 4605 /R = 4kpc/ to UGC 2885 /R = 122 kpc/. *The Astrophysical Journal*, 238:471–487. 2, 28

Salucci, P. (2001). The constant-density region of the dark haloes of spiral galaxies. *MNRAS*, 320:L1–L5. 12, 50

Salucci, P. and Burkert, A. (2000a). Dark Matter Scaling Relations. *The Astrophysical Journal Letters*, 537:L9–L12. 28, 33

Salucci, P. and Burkert, A. (2000b). Dark Matter Scaling Relations. *The Astrophysical Journal Letters*, 537:L9–L12. 63

Salucci, P., Frigerio Martins, C., and Karukes, E. (2014). $R^n$ gravity is kicking and alive: The cases of Orion and NGC 3198. *International Journal of Modern Physics D*, 23:42005. 47

Salucci, P., Lapi, A., Tonini, C., Gentile, G., Yegorova, I., and Klein, U. (2007). The universal rotation curve of spiral galaxies - II. The dark matter distribution out to the virial radius. *MNRAS*, 378:41–47. 3, 33, 51, 61, 67, 72, 87

Salucci, P., Nesti, F., Gentile, G., and Frigerio Martins, C. (2010). The dark matter density at the Sun's location. *Astron. Astrophys.*, 523:A83. v, 36, 37, 38, 41, 43, 47, 86

Salucci, P. and Persic, M. (1997). Dark Halos around Galaxies. In Persic, M. and Salucci, P., editors, *Dark and Visible Matter in Galaxies and Cosmological Implications*, volume 117 of *Astronomical Society of the Pacific Conference Series*, page 1. 3, 51, 56

Salucci, P. and Persic, M. (1999). Maximal halos in high-luminosity spiral galaxies. *Astron. Astrophys.*, 351:442–446. 22, 28

Salucci, P., Wilkinson, M. I., Walker, M. G., Gilmore, G. F., Grebel, E. K., Koch, A., Frigerio Martins, C., and Wyse, R. F. G. (2012). Dwarf spheroidal galaxy kinematics and spiral galaxy scaling laws. *MNRAS*, 420:2034–2041. 71, 88

Salucci, P., Yegorova, I. A., and Drory, N. (2008). The disc mass of spiral galaxies. *MNRAS*, 388:159–164. 70

Sand, D. J., Treu, T., and Ellis, R. S. (2002). The Dark Matter Density Profile of the Lensing Cluster MS 2137-23: A Test of the Cold Dark Matter Paradigm. *The Astrophysical Journal Letters*, 574:L129–L133. 14

Sand, D. J., Treu, T., Smith, G. P., and Ellis, R. S. (2004). The Dark Matter Distribution in the Central Regions of Galaxy Clusters: Implications for Cold Dark Matter. *The Astrophysical Journal*, 604:88–107. 14

Sanders, R. H. and McGaugh, S. S. (2002). Modified Newtonian Dynamics as an Alternative to Dark Matter. *Annu. Rev. Astron. Astrophys.*, 40:263–317. 4

Sanders, R. H. and Noordermeer, E. (2007). Confrontation of MOdified Newtonian Dynamics with the rotation curves of early-type disc galaxies. *MNRAS*, 379:702–710. 4

Schewtschenko, J. A., Baugh, C. M., Wilkinson, R. J., Bœhm, C., Pascoli, S., and Sawala, T. (2016). Dark matter-radiation interactions: the structure of Milky Way satellite galaxies. *MNRAS*. 9

Sharina, M. E., Karachentsev, I. D., Dolphin, A. E., Karachentseva, V. E., Tully, R. B., Karataeva, G. M., Makarov, D. I., Makarova, L. N., Sakai, S., Shaya, E. J., Nikolaev, E. Y., and Kuznetsov, A. N. (2008). Photometric properties of the Local Volume dwarf galaxies. *MNRAS*, 384:1544–1562. 54

Simard, L., Trevor Mendel, J., Patton, D. R., Ellison, S. L., and McConnachie, A. W. (2011). VizieR Online Data Catalog: Bulge+disk decompositions of SDSS galaxies (Simard+, 2011). *VizieR Online Data Catalog*, 219. 54

Simon, J. D., Bolatto, A. D., Leroy, A., Blitz, L., and Gates, E. L. (2005). High-Resolution Measurements of the Halos of Four Dark Matter-Dominated Galaxies: Deviations from a Universal Density Profile. *The Astrophysical Journal*, 621:757–776. 50

Skordis, C. (2008). Generalizing tensor-vector-scalar cosmology. *Phys. Rev. D*, 77(12):123502. 6

Smith, S. (1936). The Mass of the Virgo Cluster. *The Astrophysical Journal*, 83:23. 2

Sotiriou, T. P. and Faraoni, V. (2010). f(R) theories of gravity. *Reviews of Modern Physics*, 82:451–497. 21

Spergel, D. N. and Steinhardt, P. J. (2000). Observational Evidence for Self-Interacting Cold Dark Matter. *Physical Review Letters*, 84:3760–3763. iv, 9

Springel, V. (2005). The cosmological simulation code GADGET-2. *MNRAS*, 364:1105–1134. 28

Springel, V., Wang, J., Vogelsberger, M., Ludlow, A., Jenkins, A., Helmi, A., Navarro, J. F., Frenk, C. S., and White, S. D. M. (2008). The Aquarius Project: the subhaloes of galactic haloes. *MNRAS*, 391:1685–1711. 15

Stinson, G. S., Brook, C., Macciò, A. V., Wadsley, J., Quinn, T. R., and Couchman, H. M. P. (2013a). Making Galaxies In a Cosmological Context: the need for early stellar feedback. *MNRAS*, 428:129–140. 44

Stinson, G. S., Brook, C., Macciò, A. V., Wadsley, J., Quinn, T. R., and Couchman, H. M. P. (2013b). Making Galaxies In a Cosmological Context: the need for early stellar feedback. *MNRAS*, 428:129–140. 65

Swaters, R. A., Sancisi, R., van Albada, T. S., and van der Hulst, J. M. (2009). The rotation curves shapes of late-type dwarf galaxies. *Astron. Astrophys.*, 493:871–892. 53, 54

Tollerud, E. J., Boylan-Kolchin, M., and Bullock, J. S. (2014). M31 satellite masses compared to ΛCDM subhaloes. *MNRAS*, 440:3511–3519. 16

Tolstoy, E., Hill, V., and Tosi, M. (2009). Star-Formation Histories, Abundances, and Kinematics of Dwarf Galaxies in the Local Group. *Annu. Rev. Astron. Astrophys.*, 47:371–425. 52

Tonini, C., Lapi, A., Shankar, F., and Salucci, P. (2006). Measuring the Spin of Spiral Galaxies. *The Astrophysical Journal Letters*, 638:L13–L16. 62, 63

Tyson, J. A., Kochanski, G. P., and Dell'Antonio, I. P. (1998). Detailed Mass Map of CL 0024+1654 from Strong Lensing. *The Astrophysical Journal Letters*, 498:L107–L110. 3

van Albada, T. S., Bahcall, J. N., Begeman, K., and Sancisi, R. (1985). Distribution of dark matter in the spiral galaxy NGC 3198. *The Astrophysical Journal*, 295:305–313. 22, 28

van den Aarssen, L. G., Bringmann, T., and Pfrommer, C. (2012). Is Dark Matter with Long-Range Interactions a Solution to All Small-Scale Problems of Λ Cold Dark Matter Cosmology? *Physical Review Letters*, 109(23):231301. 9

van den Bosch, F. C., Robertson, B. E., Dalcanton, J. J., and de Blok, W. J. G. (2000). Constraints on the Structure of Dark Matter Halos from the Rotation Curves of Low Surface Brightness Galaxies. *Astronomic. J.*, 119:1579–1591. 12

van den Bosch, F. C. and Swaters, R. A. (2001). Dwarf galaxy rotation curves and the core problem of dark matter haloes. *MNRAS*, 325:1017–1038. 12

van Zee, L. (2001). The Evolutionary Status of Isolated Dwarf Irregular Galaxies. II. Star Formation Histories and Gas Depletion. *Astronomic. J.*, 121:2003–2019. 54

Verheijen, M. and de Blok, E. (1999). The HSB/LSB Galaxies NGC 2403 and UGC 128. *Ap&SS*, 269:673–674. 56

Verheijen, M. A. W. (2001). The Ursa Major Cluster of Galaxies. V. H I Rotation Curve Shapes and the Tully-Fisher Relations. *The Astrophysical Journal*, 563:694–715. 12

Viñas, J., Salvador-Solé, E., and Manrique, A. (2012). Typical density profile for warm dark matter haloes. *MNRAS*, 424:L6–L10. 9

Vogelsberger, M., Zavala, J., and Loeb, A. (2012). Subhaloes in self-interacting galactic dark matter haloes. *MNRAS*, 423:3740–3752. 9

Vogelsberger, M., Zavala, J., Simpson, C., and Jenkins, A. (2014). Dwarf galaxies in CDM and SIDM with baryons: observational probes of the nature of dark matter. *MNRAS*, 444:3684–3698. 50

Wechsler, R. H., Bullock, J. S., Primack, J. R., Kravtsov, A. V., and Dekel, A. (2002). Concentrations of Dark Halos from Their Assembly Histories. *The Astrophysical Journal*, 568:52–70. 34

Weinberg, D. H., Bullock, J. S., Governato, F., Kuzio de Naray, R., and Peter, A. H. G. (2013). Cold dark matter: controversies on small scales. *ArXiv e-prints*. 12, 50

Weldrake, D. T. F., de Blok, W. J. G., and Walter, F. (2003). A high-resolution rotation curve of NGC 6822: a test-case for cold dark matter. *MNRAS*, 340:12–28. 53, 54

Wevers, B. M. H. R., van der Kruit, P. C., and Allen, R. J. (1986). The Palomar-Westerbork survey of northern spiral galaxies. *Astron. Astrophys. Supp. Series*, 66:505–513. 28, 29

White, S. D. M. and Negroponte, J. (1982). The gravitational evolution of structure in a scale-free universe. *MNRAS*, 201:401–414. 3

Yegorova, I. A. and Salucci, P. (2007). The radial Tully-Fisher relation for spiral galaxies - I. *MNRAS*, 377:507–515. 51, 55

Yoshino, A. and Yamauchi, C. (2015). Box/peanut and bar structures in edge-on and face-on nearby galaxies in the Sloan Digital Sky Survey - I. Catalogue. *MNRAS*, 446:3749–3767. 54

Zavala, J., Jing, Y. P., Faltenbacher, A., Yepes, G., Hoffman, Y., Gottlöber, S., and Catinella, B. (2009). The Velocity Function in the Local Environment from ΛCDM and ΛWDM Constrained Simulations. *The Astrophysical Journal*, 700:1779–1793. 14, 50

Zavala, J., Vogelsberger, M., and Walker, M. G. (2013). Constraining self-interacting dark matter with the Milky Way's dwarf spheroidals. *MNRAS*, 431:L20–L24. 9

Zeldovich, Ya. B., Klypin, A. A., Khlopov, M. Yu., and Chechetkin, V. M. (1980). Astrophysical constraints on the mass of heavy stable neutral leptons. *Sov. J. Nucl. Phys.*, 31:664–669. [Yad. Fiz.31,1286(1980)]. 8

Zolotov, A., Brooks, A. M., Willman, B., Governato, F., Pontzen, A., Christensen, C., Dekel, A., Quinn, T., Shen, S., and Wadsley, J. (2012). Baryons Matter: Why Luminous Satellite Galaxies have Reduced Central Masses. *The Astrophysical Journal*, 761:71. 17

Zwicky, F. (1933). Die Rotverschiebung von extragalaktischen Nebeln. *Helvetica Physica Acta*, 6:110–127. 1